UNIVERSITÀ DEGLI STUDI DI PADOVA

DIPARTIMENTO DI INGEGNERIA INDUSTRIALE

CORSO DI LAUREA MAGISTRALE IN INGEGNERIA CHIMICA E DEI PROCESSI INDUSTRIALI

Tesi di Laurea Magistrale in
Ingegneria Chimica e dei Processi Industriali

MICROALGAE CULTIVATION IN PBRs: EXPERIMENTAL MEASUREMENTOF MAINTENANCE ENERGY REQUIREMENT AS A FUNCTION OF LIGHT ENERGY

Relatore: Prof. Alberto Bertucco
Correlatrice: Dott.ssa Eleonora Sforza

Laureanda : Silvia Urbani

ANNO ACCADEMICO 2013-2014

Riassunto

Negli ultimi decenni il progressivo esaurimento dei combustibili fossili e il loro impatto sull'ambiente, dato in particolare dalla produzione di gas, come la CO_2, che contribuiscono al riscaldamento globale, ha fatto sì che l'attenzione mondiale si focalizzasse sullo studio e sull'utilizzo di biocarburanti e sull'analisi approfondita delle loro prestazioni (Amaro *at al.*, 2011). In particolare, ciò che attualmente suscita maggior interesse è il biodiesel di "terza generazione", prodotto a partire dalle microalghe. Le microalghe sono organismi unicellulari fotosintetici, la cui crescita, favorita da luce, una fonte di carbonio, come la CO_2, e nutrienti (principalmente nitrati e fosfati), può essere notevolmente più rapida di quella delle piante terrestri. Alcune specie di microalghe sono in grado di accumulare grandi quantità di lipidi, che possono essere estratti ed utilizzati come oli vegetali per la produzione di biodiesel. I vantaggi dell'utilizzo delle microalghe sono legati al fatto che questi organismi, oltre a presentare elevate velocità di crescita, convertono l'energia solare con un'efficienza molto più alta delle piante terrestri, possono crescere in acque di scarico contribuendo al processo di depurazione, possono essere coltivate in territori non sfruttabili per l'agricoltura e sono in grado di fissare la CO_2 proveniente dagli impianti industriali, contribuendo alla mitigazione dell'effetto serra (Martins *et al*., 2010). Tuttavia, la fattibilità tecnica ed economica su scala industriale del processo di produzione di olio da biomassa algale è ancora una questione aperta (Chisti, 2013).

La luce è il fattore che influenza maggiormente la crescita fotosintetica delle microalghe. In particolare, quando non sussistono condizioni in cui l'apporto dei nutrienti è limitato, la crescita fotosintetica è legata unicamente alla disponibilità e penetrabilità della luce all'interno del fotobioreattore. Uno dei termini che limita l'efficienza di fotoconversione delle microalghe è il mantenimento, ovvero la parte di energia consumata per funzioni diverse da quelle legate alla produzione di nuovo materiale cellulare, quali il turnover di componenti cellulari nel normale metabolismo, il mantenimento di gradienti chimici attraverso le membrane, processi metabolici coinvolti nell'acclimatazione e riparazione cellulare in condizioni di stress (Pirt, 1965; Quigg & Beardall, 2003; van Bodegom, 2007). Inoltre il mantenimento risulta essere un parametro chiave nella maggior parte dei modelli cinetici di crescita microalgale (Bernardi *et al.*, 2014; Wu & Merchuk, 2001), inclusi quelli utilizzati nella progettazione di fotobioreattori su scala industriale (Quinn et al., 2011).

Lo scopo di questa Tesi è stato quello di verificare l'effetto della luce sul mantenimento nel caso di *S. obliquus*. Tale specie si adatta bene all'applicazione su scala industriale in quanto presenta un'elevata resistenza ai contaminanti ed è caratterizzata da un contenuto di lipidi di circa il 30%. Per fare ciò sono stati condotti degli esperimenti in continuo in un

fotobioreattore di tipo *flat-plate*, a diverse intensità e regimi di illuminazione. Per ciascuna condizione di luce sono stati utilizzati diversi tempi di permanenza, in modo da studiare diverse velocità di crescita. In condizioni di nutrienti (N e P) non limitanti, per ciascun tempo di residenza sono stati determinati il contenuto di lipidi e pigmenti, la densità cellulare media, l'efficienza fotosintetica e la resa di nutriente/biomassa.

Su tali dati sperimentali sono stati applicati dei modelli volti a determinare la richiesta di energia per il mantenimento di *S. obliquus*. Tutti i modelli di letteratura sono storicamente basati sull'approccio di Pirt (Pirt, 1965) per organismi eterotrofi. Il modello di Pirt si basa sull'assunzione che una parte di substrato, inteso come fonte di energia, è utilizzato dalle cellule per crescere, mentre l'altra parte per i processi di mantenimento.

In letteratura, solo in pochi hanno applicato gli stessi concetti agli organismi fotosintetici, considerando la luce come substrato limitante (Gons & Mur, 1980; Kliphuis *et al.*, 2012). Entrambi gli approcci sono stati preliminarmente testati, ma il modello di Gons & Mur (1980) si è rivelato poco accurato in quanto basato su assunzioni che nel tempo sono state riviste e corrette. Il modello di Kliphuis *et al*. (2012), invece, ha permesso di derivare separatamente il coefficiente di mantenimento m_E e la resa di biomassa/luce Y_G per *S. obliquus*, mettendo in evidenza l'effetto della luce che, alle alte intensità, provoca fenomeni di fotosaturazione e inibizione, con un conseguente aumento della richiesta energetica per il mantenimento e una minore resa di biomassa/luce. Il modello è comunque risultato incompleto perché non permette di misurare una velocità specifica di mantenimento a in termini di giorni^{-1}. A tale scopo, dopo un'analisi di letteratura, i modelli per gli organismi eterotrofi sono stati modificati per essere applicati sui dati di questo lavoro. In particolare, seguendo l'approccio di Van Bodegom (2007), è stata determinata la a per *S. obliquus* che si è dimostrata più elevata a più alte velocità di crescita. Il fatto che il mantenimento aumenti alle elevate velocità di crescita è giustificabile da un turnover cellulare più elevato, dunque da una maggiore richiesta di energia per il mantenimento (Quigg & Beardall, 2003). Questo è stato ulteriormente confermato dai dati sperimentali per *S. obliquus* relativo al contenuto di lipidi e densità cellulare media che diminuiscono all'aumentare della velocità di crescita. All'aumento della velocità di crescita, quindi, le cellule non accumulano materiale di riserva, quali i lipidi, e mostrano dimensioni più piccole essendo in attiva fase di replicazione.

Inoltre, la a è stata trovata più elevata ad alte irradianze. Il probabile significato biologico è che la a, nel caso degli organismi fotosintetici, include non solo i componenti di non crescita, citati prima, ma anche tutti i meccanismi di dissipazione dell'energia a livello dell'apparato fotosintetico. L'effetto saturante, ben evidente sulla resa di biomassa su luce Y_{APP}, che presenta al variare della velocità di crescita due andamenti ben distinti a basse ed elevate intensità di luce, è stato modellato come inibizione da substrato seguendo gli approcci proposti da Chen & Johns (1996) e Minkevich *et al*., (2000) per organismi eterotrofi. I modelli sono stati in grado di riprodurre con buona approssimazione i dati sperimentali.

L’aumento di mantenimento si riflette anche sull’uptake di nutrienti. Infatti valori differenti di consumo di nutrienti, espresso come resa di nutriente/biomassa, sono stati misurati al variare del tempo di residenza e dell’intensità di luce, suggerendo che tale parametro dipende dalla velocità di crescita ed è influenzato dalla richiesta di mantenimento. In conclusione,in questo lavoro di tesi è stata misurata quantitativamente la parte di dispendio energetico degli organismi fotosintetici al variare dell’intensità di luce. I parametri del mantenimento sono quindi stati descritti mediante relazioni matematiche che possono essere integrate nei modelli di crescita in funzione della luce.

Abstract

Most relevant factors influencing microalgal growth are light availability and utilization. The concept of maintenance energy is essential to understand the energy requirements for cell growth and is also a key parameter of most mathematical growth models, including those used for large scale design. In this work continuous experiments were carried out in laboratory-scale flat-plate photobioreactors (PBRs), in order to investigate the effect of light intensity and irradiation regime on *S.obliquus* maintenance energy requirement Energy balances were applied to measure the maintenance term as a function of irradiation, under both continuous and simulated seasonal irradiation at middle-latitudes. It was found that light strongly influenced the maintenance, which resulted higher under higher irradiances as a result of photoinhibition effect, which was correlated to a substrate inhibition model. In addition, at non limiting nutrient (N and P) conditions, for each resident time lipid and pigment content, photosynthetic efficiency and nutrient/biomass yields were measured. It was observed that these factors depended both on growth rate and irradiance. Particularly, it was found that the nutrient uptake was strongly linked to the energetic losses due to the maintenance**.**

Contents

Introduction

Biofuels derived from microalgae via photosynthesis have been proposed as potentially superior to crop derived fuels and likely to become essential in order to supply the demand of liquid fuels which is expected to grow quite fast in the next few decades (Borowitzka & Moheimani, 2010; Chisti, 2013) On the other hand, whether they can be produced inexpensively in a sufficient quantity to significantly replace petroleum derived transport fuels, is still an open issue (Chisti, 2013). In fact, many factors still limit the feasibility of a competitive large-scale cultivation system: a low photosynthetic efficiency, a negative value of total energy balance and a lack of a strong experience in the field, as few pilot units are currently in operation throughout the world. In this context, a deeper knowledge of the energy balance of microalgal growth in a PBR plays a crucial role both to better understand the energetic constraints of photosynthesis and to optimize the efficiency of the production process. In fact, the factor with a seminal influence on productivity is light availability, because light energy fully supports autotrophic algal growth.

One of the terms limiting photoconversion is the maintenance energy, which includes the additional energy needed to the turnover of cellular components in the normal metabolism, the maintenance of chemical gradients across membranes and metabolic processes involved in acclimation, as well as the cell repair under stress (Pirt, 1965; Quigg & Beardall, 2003; van Bodegom, 2007). It is essential to understand the energy requirements for cell growth because the maintenance term is also a key parameter of most mathematical growth models (Bernardi *et al.*, 2014; Wu & Merchuk, 2001), including those used for large scale PBR design (Quinn et al., 2011). Several models were applied to measure and characterize the energy requirement of microbial growth as a function of substrate concentration (Minkevich *et al.*, 2000; Pirt, 1965 1965; van Bodegom, 2007). On the other hand, little is known about the experimental quantification of algal maintenance requirement. Only few authors tried to apply the same concepts to photosynthetic organisms, considering the light as a limiting substrate (Gons & Mur, 1980; Kliphuis *et al.*, 2012; Zijffers *et al.*, 2010). However, the effect of saturating light on energy parameters for photosynthetic organisms has not been investigated yet. Instead, this is fundamental in order to understand the possible energy loss in an actual outdoor PBR, where algae are inevitably exposed to variable incident light due to diurnal and seasonal differences in irradiation, which can strongly influence the efficiency of energetic pathways and, eventually, the overall biomass productivity.

Chapter 1

Biofuels from microalgae:state of the art

This chapter addresses the topic of the thesis and reviews the literature on algal biology and cultivation and PBR design. This chapter also reports advances achieved in the last years and the future trends in research and from an industrial perspective.

1.1 Biofuels: an overview

Global warming, as well as the recognition that fossil fuel supplies are finite and expected to decline over the next few decades, combined with an ever increasing global demand for energy, have led to substantial interest and research activity in developing renewable biologically produced fuels, especially ethanol and biodiesel (Borowitzka & Moheimani, 2010). Liquid biofuels are classified into three generations based on the substrate raw materials and the processing or production technology. First generation liquid biofuels were produced from food crops such as corn, sugarcane, wheat, maize and vegetable oils; because of the use of food crops for fuel production, first generation liquid biofuels were criticized for conflicting with the food supply and increasing the costs of food crops. It paved the way for second generation liquid biofuels, which were manufactured using non-edible oils such as *Jatropha curcas L.* The advantages of using jatropha oil are that jatropha trees can grow easily on non-arable or wasteland and the existing biodiesel plants does not require major modification on the equipments and process flow, mainly because the oil has similar properties to edible oils. However, jatropha oil contains higher concentration of free fatty acid (FFA), that may require an additional pre-treatment step. In addition, the cultivation of that species requires regular irrigation, heavy fertilization and good management practices, which are necessary to ensure high oil yield (Lam & Lee, 2012). Due to these weakness, the research for a more sustainable biodiesel feedstock continues and now focuses on microalgae. Potentially, microalgae can provide fuels in several distinct forms: algal biomass for combustion, algal crude oil for direct combustion, or for use in production of other transportation fuels such as diesel, gasoline and jet fuel (kerosene), biogas via anaerobic digestion of the biomass, biohydrogen, bioethanol via fermentation of carbohydrates derived

from algae and biodiesel produced directly through algal photosynthesis. In Fig.1.1 the main microalgal biomass transformation processes for biofuel productions are summarized.

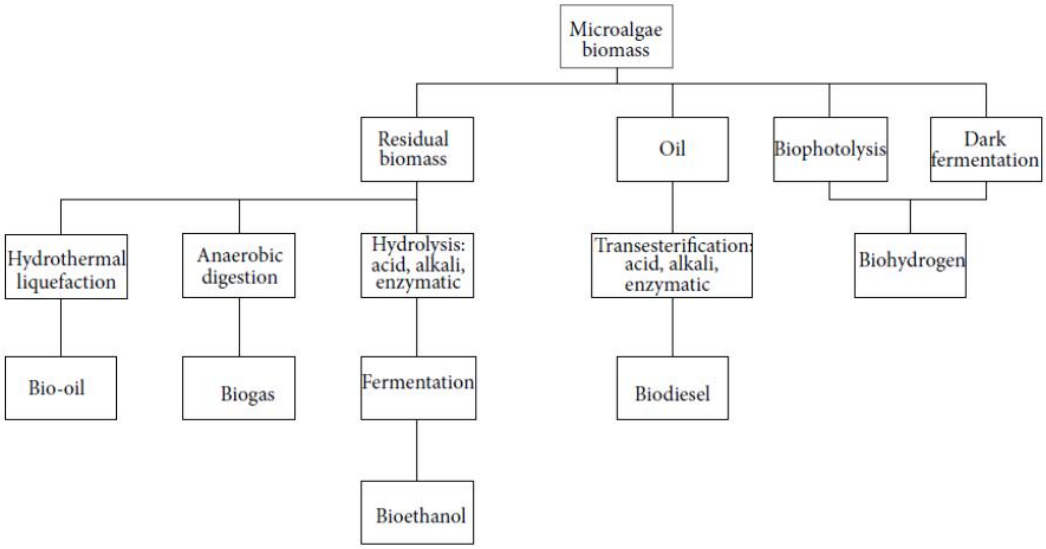

Figura 1.1 - ***Principal microalgal biomass transformation processes for biofuel production*** **(Abishek *et al.*, 2014).**

A significant number of startup companies are making attempts to commercialize algal fuels. Table 1.1 shows a list of the companies which are actively participating in their development.

Table 1.1 – ***List of startup companies attempting to commercialize algal fuels (Bahadar & Khan, 2013).***

S.N.	Company/location	Country	Website
01	Algenol Biofuels, Bonita Springs, FL, Fort Meyers	USA	www.algenolbiofuels.comhttpp
02	Aquaflow Bionomics, Nelson	New Zealand	www.aquaflowgroup.com
03	Aurora Algae Inc., Hayward CA	USA	www.aurorainc.com
04	Algae Link Roosendaal	Netherlands	www.algaelink.com
05	Aquatic Energy, LLC, Lake Charles Louisiana	USA	www.aquaticenergy.com
06	ALG Western Oil	South Africa	www.algbf.co.za
07	Alga Fuel, S.A., Sines	Portugal	www.a4f.pt
09	A2BE Carbon Capture, Boulder Colorado	USA	www.algaeatwork.com
10	Bioalgene, Seatle, WA	USA	www.bioalgene.com
11	BFS Biopetróleo, San Vicente del Raaspeig	Spain	www.biopetroleo.com
12	Blue Marble Energy, Seattle, Washington	USA	www.bluemarblebio.com
13	Bionavitas, Inc, Redmond, WA	USA	www.bionavitas.com
14	Bodega Algae, LLC, Boston, MA	USA	www.bodegaalgae.com
15	Cellana, Hawaii	USA	www.cellana.com
16	Circle Biodiesel and Ethanol Corp., San Marcos, CA	USA	www.circlebio.com
17	Community Fuels, Encinitas, CA	USA	www.communityfuels.com
18	Diversified Energy, Gilbert, Arizona	USA	www.diversified-energy.com
19	Eni	Italy	www.eni.com
20	Galp Energia, Lisbon	Portugal	www.galpenergia.com
21	Global Energy Solutions, Vancouver	Canada	www.globalgreensolutionsinc.com
22	Green Fuel Technologies, Cambridge, Massachusetts	USA	(www.greenfuelonline.com)
23	Green Shift Corp, New York	USA	www.greenshift.com
24	HR Biopetroleum, Hawaii	USA	www.hrbiopetroleum.com
25	Ingrepo B.V, Zutphen	Netherlands	www.ingrepro.nl
26	International Energy, Vancouver	Canada	www.internationalenergyinc.com
27	Inventure Chemical, Seattle	USA	www.inventurechem.com
28	LiveFuels, Inc., San Carlos, CA	USA	www.livefuels.com
29	Mighty Algae Biofuels, CA	USA	
30	Neste Oil, Helsinki	Finland	www.nesteoil.com
31	Origin Oil Inc., Los-Angeles, California	USA	www.originoil.com
32	OilFox S.A	Argentina	www.oilfox.com.ar
33	Parabel Inc. formerly PetroAlgae Inc., Melbourne, FL	USA	www.parabel.com
34	PhycoBiosciences, Chandler, AZ	USA	www.phyco.net
35	PetroSun, Scottsdale, Arizona	USA	
36	Sapphire Energy, San Diego	USA	www.sapphireenergy.com
37	SolenaFuels, WA	USA	www.solenafuels.com
38	Solix Biofuels, Fort Collins, Colorado	USA	www.solixbiofuels.com
39	Solazyme, Inc., San Francisco	USA	www.solazyme.com
40	Seambiotic, Ashkelon	Israel	www.seambiotic.com
41	Sartec Anoka, Minnesota	USA	www.xlrenewables.com/
42	Solarvest BioEnergy	Canada	www.xlrenewables.com
43	XL Renewables, Phoenix, Arizona	USA	www.xlrenewables.com

Most of these companies are focused on oils produced via the photosynthetic route (Chisti, 2013).

1.2 Advantages of using microalgae for biodiesel production

Many research reports and articles described advantages of using microalgae for biodiesel production in comparison with the other available feedstocks, previously mentioned.

Microalgae can grow about 10–50 times faster than terrestrial plants, thus achieving a much higher CO_2 fixation rate (Lam & Lee, 2012) and they require much less land area than other biodiesel feedstocks of agricultural origin, up to 49 or 132 times less when compared to rapeseed or soybean crops, for a 30% (w/w) of oil content in algae biomass (Chisti, 2007). Therefore, the competition for arable soil with other crops, in particular for human consumption, is greatly reduced.

Besides, oil content of microalgae is on the average higher with respect to terrestrial plants used for the production of first and second generation biofuels (Table 1.2).

Table 1.2 - *Comparison of microalgae with other biodiesel feedstock (Martins et al., 2010).*

Plant source	Seed oil content (% oil by wt in biomass)	Oil yield (L oil/ha year)	Land use (m^2 year/kg biodiesel)	Biodiesel productivity (kg biodiesel/ha year)
Corn/Maize (*Zea mays* L.)	44	172	66	152
Hemp (*Cannabis sativa* L.)	33	363	31	321
Soybean (*Glycine max* L.)	18	636	18	562
Jatropha (*Jatropha curcas* L.)	28	741	15	656
Camelina (*Camelina sativa* L.)	42	915	12	809
Canola/Rapeseed (*Brassica napus* L.)	41	974	12	862
Sunflower (*Helianthus annuus* L.)	40	1070	11	946
Castor (*Ricinus communis*)	48	1307	9	1156
Palm oil (*Elaeis guineensis*)	36	5366	2	4747
Microalgae (low oil content)	30	58,700	0.2	51,927
Microalgae (medium oil content)	50	97,800	0.1	86,515
Microalgae (high oil content)	70	136,900	0.1	121,104

Additionally, different microalgae species can be adapted to live in a variety of environmental conditions. Thus, it is possible to find species best suited to local environments or specific growth characteristics. The same is not possible to do with other current biodiesel feedstocks (e.g. soybean, rapeseed, sunflower and palm oil) (Martins *et al*., 2010), which can be grown in areas unsuitable for agricultural purposes (e.g. arid areas where the annual insolation is high); in addition seawater or saline groundwater rather than freshwater can be used to cultivate algae reducing competition for a valuable limited resource such as freshwater (Borowitzka & Moheimani, 2010).

Algae biodiesel contains no sulfur and performs as well as petroleum diesel, while reducing emissions of particulate matter, CO, hydrocarbons, and NOx (Martins *et al*., 2010).

The utilization of microalgae for biofuels production can also serve other purposes. Some possibilities currently being considered are listed below:

- Removal of CO_2 from industrial flue gases by algae bio-fixation, reducing the GHG emissions of a company or process while producing biodiesel (Lam & Lee, 2012);
- Wastewater treatment by removal of NH_4^+, NO_3^-, PO_4^{3-},making algae to grow using these water contaminants as nutrients (Lam & Lee, 2012);

- After oil extraction the resulting algae biomass can be processed into ethanol, methane, livestock feed, used as organic fertilizer due to its high N:P ratio, or simply burned for energy cogeneration (electricity and heat) (Martins *et al*., 2010).

However, although fuels oils derived from microalgae via photosynthetis have been advanced as potentially superior to crop derived fuels, there is still a big question mark surrounding the sustainability of the industry for long term operation (Lam & Lee, 2012). Translating laboratory and pilot scale findings to full scale commercial application still appears to be a hurdle with few credible reports of success. Some of the imperatives that need to be optimised for large scale application include strain selection and seed culture preparation, biomass and lipid yield optimization, bioreactor configuration, physico-chemical parameters and, most important, harvesting and extraction of the lipid from the biomass (Rawat *et al.*, 2013).

1.3 Biodiesel production

In the context of large scale microalgal cultivation, the process configuration is defined as the combination of economic viability, upstream processing and downstream processing (Rawat *et al.*, 2013). Fig. 1.2 shows a schematic of the algal biodiesel value chain stages, starting with the selection of microalgae species depending on local specific conditions and the design and implementation of a cultivation system for microalgae growth. Then, it follows the biomass harvesting, processing and oil extraction to supply the biodiesel production unit.

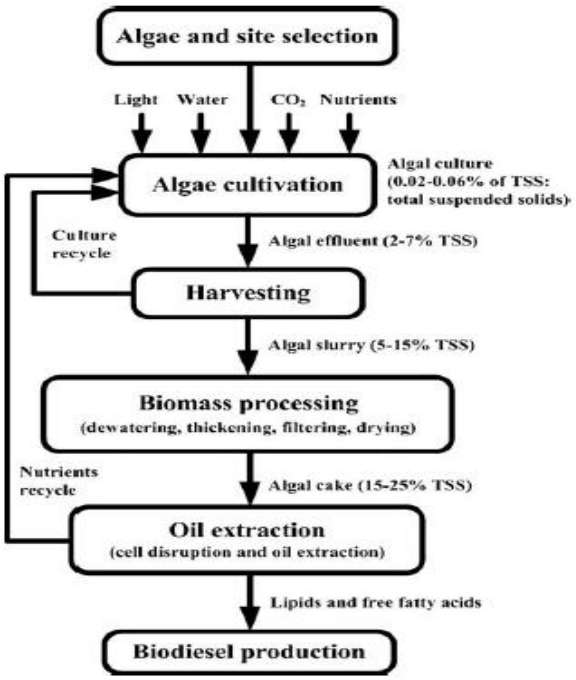

Figure 1.2 – ***Microalgae biodiesel value chain stages (Martins et al., 2010).***

1.3.1 Microalgae cultivation

Microalgae can be cultured using three metabolic pathways :

1. phototrophic;
2. heterotrophic;
3. mixotrophic.

Phototrophic utilizes light as energy source and CO_2 as inorganic carbon source whereas heterotrophic is independent of light and uses organic substrate (e.g. glucose, acetate, glycerol) as both energy and carbon source. For mixotrophic culture, microalgae are able to grow either via phototrophic or heterotrophic pathway, depending on the concentration of organic carbon sources and light intensity. Of these, the most dominant method commonly used for microalgal cultivation is phototrophic cultivation (Martins *et al*., 2010).

A correct design of the culture system is fundamental for the overall process yield and sustainability, since it permits to maximize productivity and quality of microalgal biomass. An effective culture system should consist of the following criteria: (1) effective illumination area, (2) optimal gas–liquid transfer, (3) easy to operate, (4) low contamination probability, (5) low capital and production cost and (6) minimal land area requirement (Xu & Xiong, 2009).

Microalgae can be cultivated in different types of systems, mainly in open raceway ponds or in enclosed PBRs. Open cultures are usually located outdoors and rely on direct light, while closed PBRs can be either indoors or, preferably, outdoors to use free sunlight.

Raceway ponds are the most common cultivation system used. They are made of a closed loop recirculation channel that is typically about 0.25 m wide and 0.4 m deep (Slade & Bauen, 2013) (Fig. 1.3). The channels are shallow to maximize light penetration and CO_2 is sparged at the bottom of the raceway as carbon source. Paddlewheel guarantees mixing and circulation and avoids biomass sedimentation; flow is guided around bends by baffles placed in the flow channel. During daylight, the culture is fed continuously in front of the paddlewheel, where the flow begins. Broth is harvested behind the paddlewheel, on completion of the circulation loop (Chisti, 2007).

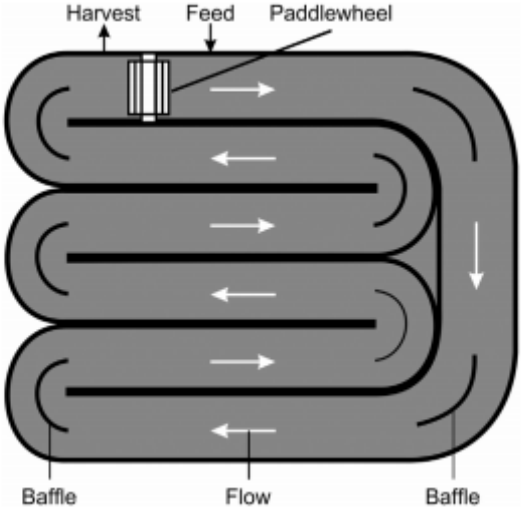

Figure 1.3- ***Schematics of a raceway pond (Bahadar & Bilal Khan, 2013).***

Although raceways are low-cost, they have a low biomass productivity compared with PBRs. In raceways, cooling is achieved by evaporation only and temperature fluctuates within a diurnal cycle and seasonally, leading to a significant evaporative water loss. Evaporative losses result in changes to ionic composition of the media and potentially detrimental effects on culture growth (Rawat *et al*., 2013). Raceways use CO_2 less efficiently than PBRs and they can be easily contaminated by other microorganisms that can compete with the cultivated algal strain. The biomass concentration remains low because raceways are poorly mixed and cannot sustain an optically dark zone. Techniques to enhance CO_2 absorption into the culture media such as aerators or bubbling may improve the overall biomass productivity. Improved mixing can minimize impacts of both CO_2 and light limitation thus improving productivity (Rawat *et al*., 2013). Usage of marginal and non-arable land is a major advantage. Maintenance and cleaning of open systems is easier and less energy intensive than PBRs. In addition, raceways are perceived to be less expensive than closed systems, for both construction and operation.

The limitations of open pond cultures have lead to much research into PBRs, as a method of primarily overcoming contamination and low productivity (Amaro *et al*., 2011). They offer better control over culture conditions and growth parameters (pH, temperature, mixing, CO_2 and O_2), prevent evaporation, reduce CO_2 losses, allow to attain higher microalgae densities or cell (i.e. higher volumetric productivities) due to their high surface area to volume ratio, and offer a safer and more protected environment, preventing contamination or minimizing invasion by competing microorganisms (Martins *et al.*, 2010). In addition, PBRs are more versatile than open opens because they can use sunlight, artificial light and various combinations of light sources thus giving the potential to increase photoperiod and enhance low light intensities given by sunlight variation. The stability of light intensity and photoperiod provided by artificial light has potential to enhance yearly total oil yields by 25-

42% (Amaro *et al*., 2011). PBRs can be designed as tubular or flat panel reactors that are usually made of plastic or glass (Fig. 1.4). In tubular PBRs the tube diameter is limited because light does not penetrate too deeply in the dense culture broth that is necessary for ensuring a high biomass productivity of the system.

Despite their advantages, it is not clear if PBRs could have a significant impact in the near future on any product or process that can be attained in large outdoor raceway ponds. In fact, they suffer from several drawbacks that need to be considered and solved. Their main limitations include: overheating, bio-fouling, oxygen accumulation, difficulty in scaling up, high building and operating costs and cell damage by shear stress.

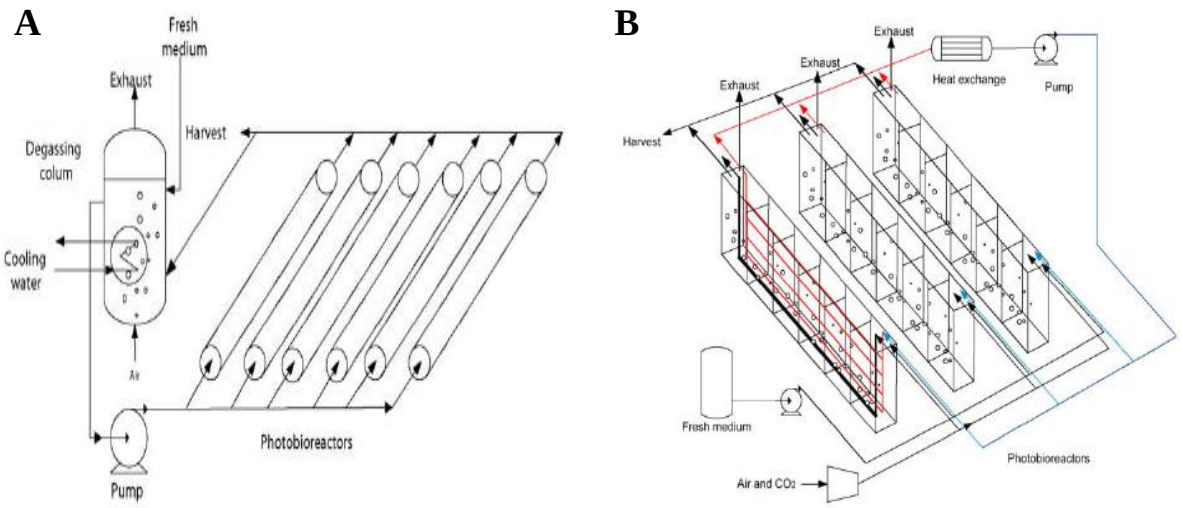

Figure 1.4 - ***Schematic representation of (A) tubular horizontal and (B) flat-panel PBR (Jorquera et al., 2010).***

Considering the advantages and drawbacks of raceways and PBRs, the logical step in cost effective biomass production could be a combination of the technologies (Rawat *et al*., 2013). Hybrid systems for biofuels production utilizes a large scale PBR and open pond sequentially. The first stage of growth is undertaken within a bioreactor to maintain culture purity and achieve high biomass concentrations, while the second stage is undertaken in a raceway pond as this is ideal for nutrient stress (Amaro *et al*., 2011).

1.3.2 Downstream processes

The downstream processes for biodiesel production commences with microalgal biomass harvesting and dewatering, oil extraction and subsequently transesterification of the lipids into biodiesel. The first step is to separate the microalgae from water and to recover their biomass for downstream processing. Currently, there are several methods to harvest microalgae: (1) bulk harvesting – to separate microalgae from suspension, such as natural gravity sedimentation, flocculation and floatation, and (2) thickening – to concentrate the microalgae slurry after bulk harvesting, such as centrifugation and filtration (Lam & Lee,

2012). In Table 1.3 the pros and cons of conventional techniques that are currently used for harvesting microalgae are summarized.

Table 1.3 - ***Summary of pros and cons of techniques that are used for harvesting microalgal biomass (Rawat et al., 2013).***

Technique	Pros	Cons
Filtration	Low cost, water reuse	Slow, membrane fouling and clogging, limited volume, cell damage
Centrifugation	Rapid, easy, efficient	Very high energy input
Gravity sedimentation	Low cost, potential for water recycling	Slow process, product deterioration, separation depends on cell density
Chemical flocculation	Low cost, low cell damage	Biomass toxicity, no water reuse, inefficient, potential to remove lipids, produces large quantity of sludgethat increases the difficulty to dehydrate the biomass
Dissolved air flotation (DAF)	Low cost, easy application at large scale	Needs flocculants, water reuse and product extraction may be negatively affected
Foam fractionation	Small footprint, no addition of chemicals	Low yield due to inefficient floatation
Ozone fractionation	Small footprint, cell disruption required for extraction occurs simultaneously	Ozone generation is expensive, Loss product
Microstrainers	Easy operation, low cost construction, high filtration ratios	Strongly cell concentration dependant, smaller cells may undergo incomplete removal, difficulty and handling solids fluctuations
Bio-flocculation	High efficiency, no damage to cells	No water reuse, higher energy input than other flocculants
Electrolytic flocculation	High efficiency	High energy input (up to 16KWh/kg biomass), increased temp may damage system, fouling of cathodes
Cross-flow membrane	Water reuse, removal of pathogens, protozoa	Membrane fouling, requirement for frequent use
Submerged membrane microfiltration	Low cost, less shear stress, less membrane fouling than conventional cross-flow	Membrane fouling, scale up potentially has problems

Dewatered algae is then dried, milled into fine powder, and pretreated by bead milling, microwaving, chemical lysis, or high-pressure homogenization to increase the mass transfer of lipids during extraction. Pretreatment greatly improves the extraction efficiency by disrupting the cellular structure, releasing lipids into the solvent mixture, and enhancing overall yield (Bahadar & Khan, 2013). Solar drying is assumed to be the best method to dry wet microalgae paste after the harvesting process (Lam & Lee, 2012). However, it is not feasible in temperate countries due to limited sunlight at certain times of the year, so heat generated from fossil fuels is required to dry microalgae biomass continuously to ensure optimum biomass production for each cycle of culture. However, heavy dependency on fossil fuels to dry microalgae biomass will seriously jeopardize commercial viability of microalgae biofuels and thus, new technologies or approaches (e.g. development of efficient dryers) are urgently needed to ensure the sustainability of microalgae biofuel industry (Lam & Lee, 2012).

Lipids can be extracted from the dried algal biomass using different chemical and physical means. Chemical extraction uses organic solvents like hexane or methanol. Other techniques include expeller presses, electromagnetic methods, direct liquefaction, Soxhlet extraction, supercritical fluids (CO_2), ultrasonic waves, and microwave-assisted organic solvent extraction (Halim *et al.*, 2012). In organic solvent extraction, water and solvent are removed using liquid–liquid separation methods, such as evaporation, vacuum distillation, or solvent

adsorption; in supercritical fluid extraction, the mixture is pressure decomposed, converting the solvent and possibly residual water into gases and precipitating the lipids (Bahadar & Khan, 2013).

Extracted lipids are then transesterified into biodiesel. The lipid feedstocks are composed by 90–98% (weight) of triglycerides and small amounts of mono and diglycerides, FFA (1–5%), residual amounts of phospholipids, phosphatides, carotenes, tocopherols, sulphur compounds, and traces of water (Martins *et al.*, 2010). Transesterification is a multiple step reaction, in which tryglicerides are reacted with short chain alcohol (e.g. methanol or ethanol) in the presence of catalyst as shown in Fig. 1.5. Homogeneous base catalyst (e.g. KOH and NaOH) is usually used to accelerate the reaction.

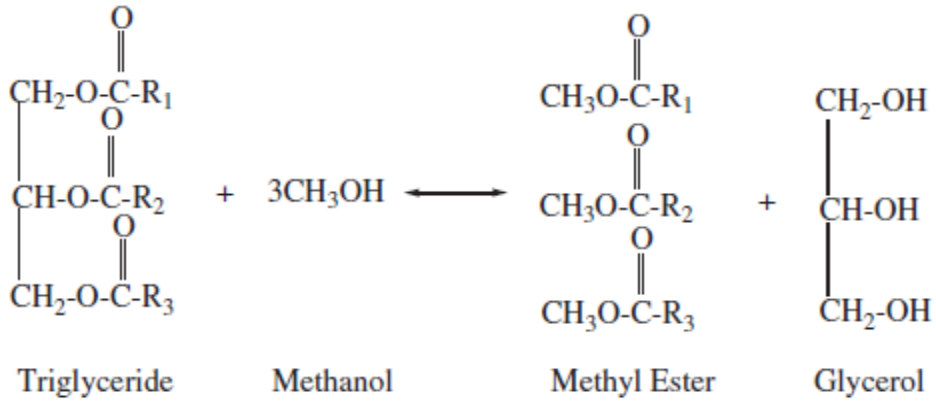

Figure 1.5 - ***Transesterification of triglycerides (overall reaction) (Lam & Lee, 2012).***

Conventional method to produce biodiesel mainly consists of two separate steps: extraction followed by transesterification. In contrast, in-situ transesterification simplifies the process by allowing extraction and transesterification to occur in one single step, in which oil/lipid-bearing biomass is directly contacted with chemical solvent in the presence of the catalyst (Lam & Lee, 2012). Chemical solvent plays two significant roles in this process: (1) as solvent to extract oil/lipid out from biomass and (2) as a reactant to perform transesterification. In-situ transesterification offers several advantages over conventional biodiesel production method such as minimizing the solvent separation step, reducing the processing time and consequently, cutting down the overall biodiesel production cost (Rawat *et al*., 2013).

1.4 Impediments to commercialization and LCA study

Algae have a significant potential compared to other biomass feedstocks to supplement or even replace current transportation fossil fuels use. A life cycle analysis (LCA) on algae production is an effective tool to determine the acceptability of algal biodiesel as replacement

for petroleum and to depict the actual problems and issues facing the microalgae biofuels industry (Dassey *et al*., 2014).

In general, LCA can guide and give a clear idea to researchers and policy makers on revealing the real potential of a particular product that is being evaluated. It can also be used to indicate if the production of a particular product can lead to negative environmental phenomena such as eutrophication, global warming, ozone depletion, human and marine toxicity, land competition, photochemical oxidation, etc; so precautionary steps can be suggested to reduce the negative impacts. In addition, energy balance can be calculated to determine and justify the energy hotspot of all stages within the system boundary of the LCA (Lam & Lee, 2012).

Apparently, there are only a few LCA studies performed on microalgae biofuels due to limited comprehensive data. Therefore, parameters related to microalgae biofuel production such as biomass productivity, lipid content and downstream energy efficiency (harvesting, drying and transesterification) are generally obtained based purely on lab scale experimental data (Lam & Lee, 2012).

Recently, a LCA with parameters of aerial productivity, culturing, CO_2 mitigation, water use, nutrient loading, biomass harvesting, lipid extraction, and energy conversion was explored on algae production in Louisiana (Dassey *et al*., 2014). A 1 acre pond growing algae at a conservative rate of 15 g m^{-2} d^{-1} with 20% lipids was considered and pumping and shipping were omitted from the analysis because they had minimal impact on the overall cost at all levels. In addition, the authors compared their results with the high and low estimates made by other authors. They found that the energy consumed on a daily basis always exceeded the energy extracted from biodiesel and the major costs were due to nutrients, harvesting and lipid extraction. Results are shown in Fig. 1.6. The graph also shows that, of the five major energy consumers, CO_2 was the least influential on total energy consumption.

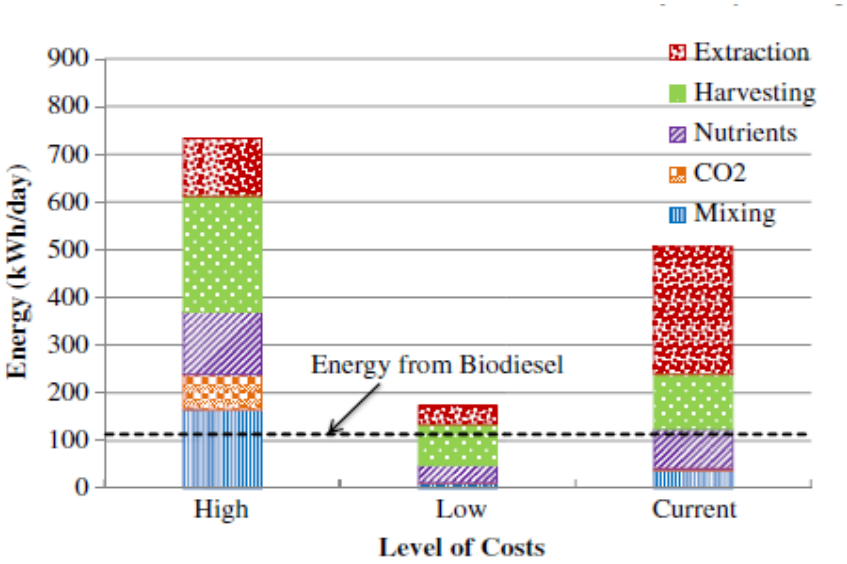

Figure 1.6 - ***Comparison of high, low, and current energy estimates for algal biodiesel production and the e energy extracted as biodiesel (Dassey et al., 2014).***

1.4.1 Availability of CO_2

Carbon dioxide is essential for growing algae. Production of each ton of algal biomass requires at least 1.83 ton of CO_2 (Chisti, 2007). The availability of point sources of CO_2 is a major impediment to the production of algal fuel oils at a meaningful scale. Concentrated sources of CO_2 are mainly the flue gases produced during power generation from combustion of coal; the cement industry is another source of concentrated CO_2 emissions (Chisti, 2013). Additionally, combustion products such as NOx or SOx can be used as nutrients for microalgae, simplifying flue gas scrubbing for combustion systems. A good alternative could be the exploitation of CO_2 from the atmosphere, which contains around 0.039 % of CO_2 by volume, because there would be no need for point CO_2 sources and the carbon footprint of algal fuels would be reduced. However, because of its low concentration, atmospheric CO_2 is not sufficient to support the high microalgal growth rates and productivities needed for full-scale biofuel production (Chisti, 2013).

Many algae and cyanobacteria possess mechanisms for concentrating CO_2 from the culture medium into cell, but CO_2 absorption from the standard atmosphere into the culture medium is not sufficiently fast to grow a large concentration of algae. Therefore, low-energy physical-chemical strategies are needed to cheaply capture and concentrate the CO_2 that is already in the atmosphere, for use in algal culture (Chisti, 2013).

For algae that can be grown in highly alkaline conditions, CO_2 may be supplied in the form of bicarbonate, helping to reduce the cost of supplying CO_2, but it may be not applicable for culturing marine algae as sea salts tend to precipitate once the pH exceeds about 8 (Chisti, 2013).

1.4.2 Supply of N and P nutrients

In addition to CO_2, algal growth requires nitrogen (N) and phosphorous (P) as main nutrients. In order to achieve maximum growth, these elements need to be supplied in sufficient quantity so as not to become limiting. The nutrients are normally from chemical or inorganic fertilizers. Producing 82 million tons of algal biomass will consume 5.4 and 1.1 million tons of N and P, respectively (Chisti, 2013). Lam & Lee (2012) found that culturing of microalgae consumes more chemical fertilizers than all other oil-bearing crops. In Table 1.4 the N-fertilizer consumption for various energy crops and microalgae is shown.

Table 1.4 - N-fertilizer consumption for various energy crops and microalgae (Lam & Lee, 2012).

Biodiesel feedstock	N-fertilizer consumption (kg/kg oil)	Reference
Microalgae (*Haematoccus pluvialis*)	0.37[a]	Razon and Tan, 2011
Microalgae (*Nannochloropsis salina*)	0.29[b]	Batan et al., 2010
Jatropha	0.24[c]	Achten et al., 2010
Rapeseed	0.14[d]	Iriarte et al., 2010
Sunflower	0.12[e]	Iriarte et al., 2010
Palm	0.048[f]	Pleanjai and Gheewala, 2009

[a] 0.032 kg N-fertilizer/kg oil for photobioreactor, 0.34 kg N-fertilizer/kg oil for race-way pond and 100% biodiesel conversion are assumed.
[b] 0.147 kg N-fertilizer/kg dry microalgae and 50% of lipid content are assumed.
[c] 111 kg N-fertilizer/ha, 1695 kg seed/ha and 0.275 kg oil/kg seed are assumed
[d] 68.2 kg N-fertilizer/tonne of seed and seed with 49% of oil content are assumed.
[e] 57.1 kg N-fertilizer/tonne of seed and seed with 49% of oil content are assumed.
[f] 7.79 kg N-fertilizer/tonne of fresh fruit bunch (FFB), 0.163 tonne oil/tonne FFB are assumed.

Existing supply of N and P fertilizers for agriculture is insufficient to provide for any significant scale production of algal biomass for oil extractions (Chisti, 2013). In addition, the production of fertilizers uses much energy and generates considerable GHG emissions in the form of CO_2, nitrous oxide (N_2O) and methane. Therefore, producing more fertilizer through conventional technology for use in algal culture may be counterproductive (Chisti, 2013). Hence, recycling and reusing the excess nutrients in the culture medium should be encouraged to improve the life cycle energy balance of microalgae biofuels (Lam & Lee, 2012). The only available technology for nutrient recovery appears to be anaerobic digestion of the spent biomass (Chisti, 2008). In addition, the biogas produced from the anaerobic digestion process can be used to generate onsite electrical power or thermal heat to offset biomass processing and extraction processes.

Due to the severe impact of chemical fertilizers towards the overall energy balance in microalgae cultivation, there is an urgent need to search for alternative and low cost nutrient sources to ensure long-term sustainability (Lam & Lee, 2012). In this case, using wastewater to culture microalgae appears as an attractive and economical alternative. Normally, secondary and tertiary wastewaters contain significant amounts of nitrate and ortho-phosphate

which are not removed during primary treatment. These nutrients can be used to culture microalgae and at the same time, microalgae play an important role as reagent to purify the wastewater. Dassey *et al.* (2014) showed that the energy imbalance could be improved using an algal system to treat wastewater for total N and P (Figure 1.7 left) . They also found that a further improvement could be obtained by combining nutrient supply through wastewater treatment with the use of residual biomass for methane production (Fig. 1.7 right).

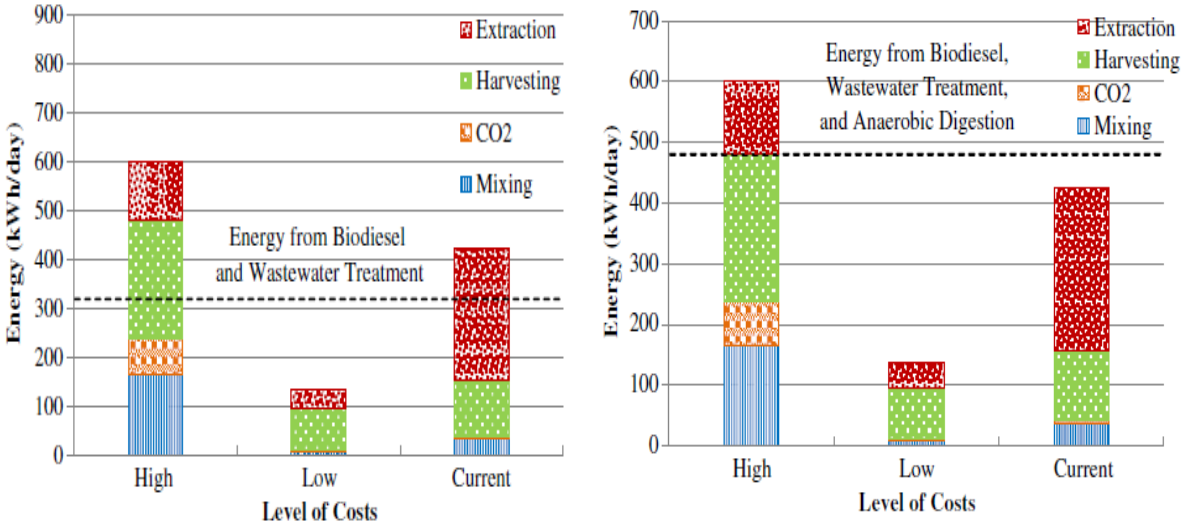

Figure 1.7 - ***Comparison of high, low, and current energy estimates for algal biodiesel production and the energy extracted as biodiesel plus supplemental value for wastewater treatment (left) or plus supplemental values for wastewater treatment and anaerobic digestion (right) (Dassey et al., 2014).***

1.4.3 Harvesting of microalgal biomass

The energy consumed in harvesting and drying of microalgae biomass should not be ignored as it may bring significant adverse effect towards the overall energy balance in producing microalgae biofuels (Lam & Lee, 2012). An efficient algal harvesting process should be applicable for all kinds of algal species, yield a product with a high dry weight percentage, and require minimum investment, energy, and maintenance (Dassey *et al*., 2014).

Up to now, centrifugation and filtration are still not energy-feasible methods to harvest microalgae in commercial scale; in fact these methods involve extensive energy consumption, and high capital and maintenance costs resulting to unsustainable practice for long-term operation (Lam & Lee, 2012). On the other hand, flocculation offers a relatively low energy way to harvest microalgae. However, conventional flocculation method is also characterized by several disadvantages: (1) high dosage of multivalent salt is required to achieve satisfactory result, (2) it produces large quantity of sludge that increases the difficulty to dehydrate the biomass , (3) flocculation efficiency is highly dependent on pH level, (4) flocculant toxicity should not be ignored especially if health related products are to be

extracted out from microalgae biomass before being used for subsequent biofuel production (Lam & Lee, 2012).

A suitable harvesting strategy may involve one or more steps and be achieved in several physical, chemical, or biological ways, in order to perform the desired solid-liquid separation (Martins *et al*., 2010). Most harvesting systems will employ a 2-stage dewatering process, where stage 1 increases the algae concentration from 0.01-0.1% mass to 1–2% mass and stage 2 increases the final concentration to ~20% biomass (Dassey *et al*., 2014) (Table 1.5).

Table 1.5 - ***A comparison of potential harvesting techniques and costs for algal biomass (DAF stands for dissolved air flotation)*** **(Dassey *et al*., 2014).**

Harvest method	Efficiency (%)	Initial C_o (g/L)	Final C (g/L)	Energy (kWh/kg algae)	kWh/day
Centrifugation	100	1.0	200	0.338	186.3
Settle → centrifuge	65[a]	0.8	120	0.292	198.4
Settle → centrifugation	65	0.5	50	0.235	100.1
Flocculation/pH → settling → belt press	90	0.5	200	0.458	139.9
Not listed	100[a]	0.5	200	0.879	241.6
Flocculation → DAF → centrifugation	70	0.1	200	1.440	112.9
Flocculation → DAF → belt press	70	0.1	200	1.086	85.1
Electrocoagulation → DAF → centrifugation	76	0.14	200	1.133	114.5

[a] Values were not listed so they were assumed.

In parallel, membrane filtration (e.g., microfiltration (MF) and ultrafiltration (UF)) has received increased attention due to its high separation efficiency and easy operation (Zhang et al., 2010). Zhang *et al*. (2010) used a UF process to harvest and dewater algal cells, where cross-flow filtration and air-assisted backwash were used to maintain a high water flux. Unfortunately, these pressure-driven MF and UF membrane processes are prone to fouling and are relatively energy intensive (Zou *et al*., 2011). Recently, forward osmosis (FO) has emerged as a promising alternative separation technology. FO membranes could provide an initial dewatering step for harvesting microalgae (Buckwalter *et al*., 2013). Driving by the concentration difference across a solute-rejecting dense membrane, FO does not require an external applied pressure. A pure water flux is established spontaneously across the FO membrane from a low concentration feed water to a high concentration draw solution under the chemical potential gradient. Compared to pressure-driven MF and UF processes, FO offers many advantages including (1) better separation efficiency thanks to its nonporous rejection layer and (2) potentially lower power consumption (e.g., in the case where a high osmotic pressure, such as seawater, is naturally available) (Zou *et al*., 2011).

1.4.4 Lipid extraction

Lipid extraction from microalgal biomass has not received sufficient attention and represents one of the many bottlenecks hindering economic industrial-scale production of microalgal biodiesel (Halim *et al*., 2011). An ideal lipid extraction technology for microalgal biodiesel production should be lipid specific, in order to minimize the co-extraction of non-lipid contaminants (such as protein and carbohydrates), efficient (both in terms of time and energy), non reactive with the lipids, relatively cheap (both in terms of capital cost and operating cost) and safe (Halim *et al*., 2011).

Each current technology has its merits and limitations. Despite having low reactivity with lipids and being directly applicable to relatively wet feedstock, organic solvent extraction is slow and uses a large amount of expensive/toxic solvents. On the other hand, supercritical carbon dioxide extraction is a promising green technology that can potentially be used for large-scale microalgal lipid extraction. It is rapid, non-toxic, has high selectivity towards acylglycerols, and produces solvent-free lipids; however, Its main disadvantages are associated with the high capital cost and the high energy requirement for supercritical fluid compression.

As previously mentioned, dewatering the microalgal biomass can be energetically prohibitive; for this reason, it would be economically beneficial if the selected lipid extraction technology can be directly applied to relatively wet feedstock (Halim *et al*., 2011). However he showed that the extraction from wet paste resulted in decreasing lipid yields.

1.5 Light supply

Microalgae can absorb only a portion of the total radiation coming from the sun, and this part corresponds to the kind of photons photosynthesis can use. It is represented by the solar spectrum limited by wavelength of 400 and 700 nm. Photosynthetically active radiation (PAR) represents 46% of total irradiance.

Light spectrum and intensity are factors that directly affect the performance of phototrophic microalgal growth, both indoors and outdoors. In outdoors cultures, sunlight is the major energy source, whereas innovations in artificial lighting, such as light-emitting diodes (LED) and optical fibers, are interesting for indoor cultivation systems. In this case, the big challenge is the high cost of artificial lighting (Amaro *et al*., 2011).

The light provides all the energy required to support algal metabolism, but, if present in excess, it can damage cells, leading to oxidative stress and photoinhibition and thus lower photosynthetic efficiency (Gris *et al*., 2014).

In PBRs, algal cultures reach high optical densities, which cause inhomogeneity in light distribution. Consequentially , the cells on the surface, directly exposed to light, absorb most

of the available radiation, but must also activate mechanisms of energy dissipation, to avoid oxidative damage (Gris *et al*., 2014). Instead, the cells in the dark zone of the PBR receive only a small part of the radiation, which is limiting for their growth. The consequence of the light distribution is a reduced efficiency in using available energy along the depth of PBR. A reduction of light path could be beneficial, but thin reactors are unlikely to be economically sustainable on a large-scale. In addition, in thin reactors, problems of photosaturation and inhibition are enhanced.

A further source for complexity to be considered is that in PBRs cells are actively mixed and move between the dark and light regions. Such dark/light cycles have been suggested to increase the photosynthetic efficiency in several cases (Grobbelaar, 2010; Kimbet *et al*., 2006; Nedbal *et al., 1996*).

In the work of Gris *et al.* (2014) the effect of different illumination on *S. obliquus* was investigated in a flate plate PBR. They found that at low light intensities, ranging from 10 to 150 μmol m^{-2} s^{-1}, the specific growth rate and cell concentration increased linearly with light intensity, with a peak at 150 μmol m^{-2} s^{-1} , and showed that, in this range, light is limiting for cell growth. Over this limit, the increase of light intensity did not result in any enhancement of the growth rate nor increased final cell concentration, suggesting that the saturation point of photosynthesis was reached (Figs. 1.6 (a), (b) and (c)). It is also worth mentioning that other species grown in thin flat panels similarly showed photosaturation at irradiances over 150 μmol photons m^{-2} s^{-1} (E. Sforza *et al*., 2012).

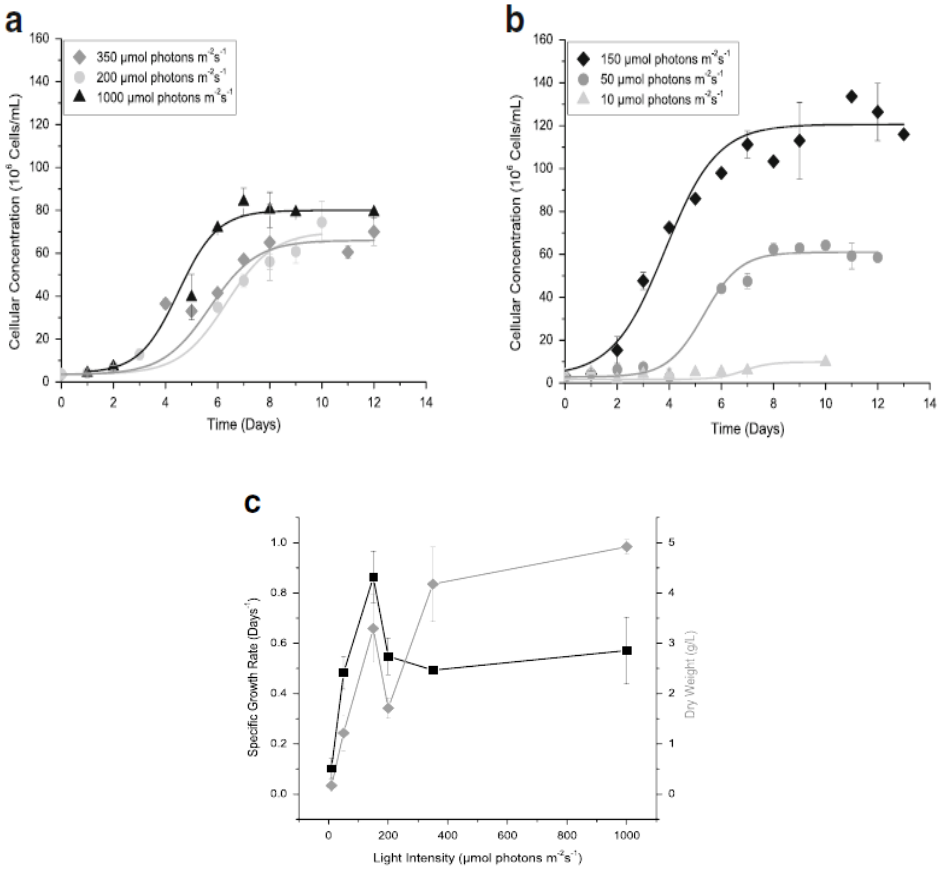

Figure 1.6 – ***(a) Cellular concentration of algae exposed to low light intensities ranging from 10 to 150 µmol m^{-2} s^{-1}, (b) cellular concentrations at high light intensities, ranging from 200 to 1000 µmol m^{-2} s^{-1}, (c) growth parameters determined from curves reported in (a) and (b), specific growth rate (squares) and biomass concentration (rhombus) (Gris et al., 2014)*.**

1.5.1 Growth modeling as a function of light

In literature several models of photosynthetic biomass growth have been developed. They can be divided in two main groups, that is static and dynamic models (Luo et al., 2004). Static models are the simplest and the most used for photobioreactor performance determination and reactor design; they are based on empirical or semi-empirical data but they lack generality, ignoring the dynamic nature of represented phenomena. Dynamic models attempt to describe physiological phenomena such as photoinibition and photolimitation and the relation between growth rate and irradiance is based on cell physiology and not on experimental data. These models are extremely complex, detailed and involve a large amount of variables and parameters.

Cornet model (Cornet et al., 1995) and generalized by Pruvost (Pruvost et al., 2011) belongs to the first category and in literature it was frequently used to model photosynthetic growth. Cornet model refers to an isotropic radiative field and the scattered part of light is considered to be parallel to the main radiation direction (Cornet et al., 1995). The method refers to artificial light but it was expanded in order to consider the dynamic nature of solar radiation,

such as incident angle variation and the daily direct or diffuse light distribution (Pruvost et al., 2011). The model provides a formulation for the biomass duplication rate as a function of irradiance at each point of the reactor depth:

$$r_{x,z} = \rho_m \frac{K}{K+I(z)} \varphi E_a I(z) C_x - \mu_e C_x \quad (1.1)$$

where $r_{x,z}$ is the biomass duplication rate at distance z from the panel (kg m^{-3} s^{-1}), ρ_m the maximum energetic yield for photon conversion (-), K the half saturation constant for photosynthetis (μmol photons m^{-2} s^{-1}), φ the mass quantum yield for Z-scheme of photosynthetis (kg μmol $photons^{-1}$) and μ_e the maintenance term, including both respiration and death of cells (s^{-1}).

In Eq. 1.1 the contributions of both biomass growth and maintenance due to the cells respiration and death are considered.

Particularly, in the work of Domenicali (2013) a sensitivity analysis was performed in order to understand the influence of μ_e on the Cornet model. Results in Fig. X. show that the steady state biomass concentration is strongly influenced by the maintenance parameter . The same results were found for the biomass productivity.

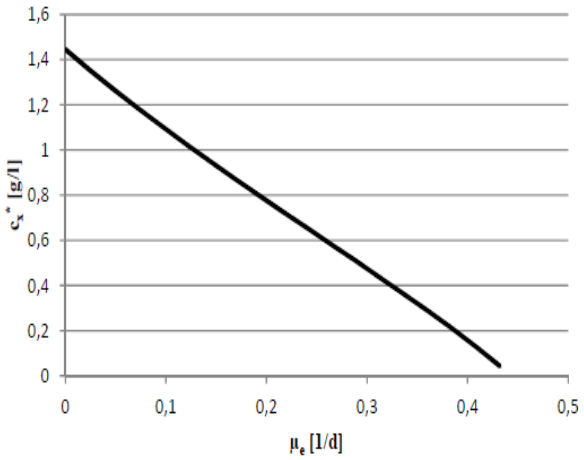

Figure 1.7 - ***Trends of the stationary biomass concentration by varying μ_e(Domenicali, 2013).***

It can be concluded that μ_e is the parameter to tune in order to reproduce well the experimental results, as also found in the work of Bertucco *et al.* (2014). The maintenance is a key parameter of most mathematical growth models (Bernardi *et al.*, 2014; Wu & Merchuk, 2001), including those used for large scale PBR design (Quinn et al., 2011).

1.5.2 Energy requirements for photoautotrophic growth and maintenance

As previously mentioned, the maintenance process has to be taken into account when quantifying a kinetic growth, because it limits somehow the duplication rate, diverting part of light energy from production of new cell material to cell physiological functions, which include (van Bodegom, 2007):

1. shifts in metabolic pathways;
2. energy spilling reactions
3. cell motility;
4. changes in stored polymeric carbon;
5. osmoregulation;
6. extracellular losses of compounds not involved in osmoregulation;
7. proofreading, synthesis and turnover of enzymes and other macromolecular compounds such as enzymes and RNA;
8. defencence against O_2 stress.

However, its quantification is a subject of continuous debate, which is caused by the existence of partly overlapping concepts and the evolution of the variables describing the maintenance.

Several models were applied to measure and characterize the energy requirement of microbial growth as a function of substrate concentration (Minkevich *et al*., 2000; Pirt, 1965; van Bodegom, 2007). Particularly Minkevich *et al*. (Minkevich et al., 2000) found that, in the case of inhibiting substrate, inhibition may result in increased maintenance energy demand, so showing how growth rate and yield depend on growth conditions.

On the other hand, little is known about the experimental quantification of algal maintenance requirement. Only few authors tried to apply the same concepts to the photosynthetic organisms, considering the light as a limiting substrate (Gons & Mur, 1980; Kliphuis *et al*., 2012). However, the effect of saturating light on energy parameters for photosynthetic organisms has not been investigated yet. Instead, this is fundamental in order to understand the possible energy loss in an actual outdoor PBR, where algae are inevitably exposed to variable incident light due to diurnal and seasonal differences in irradiation, which can strongly influence the efficiency of energetic pathways and, eventually, the overall biomass productivity.

1.6 Aim of the thesis

In this work, the effect of light intensity and irradiation regime on maintenance rate was assessed, by growing *S.obliquus* in a continuous laboratory-scale flat-plate PBR at different residence times, thus studying different growth rates. Particularly, the maintenance

parameters were calculated according the approach of Pirt (1965) and van Bodegom (2007). In addition, at non limiting nutrients (N and P) conditions, the effect of different light intensity and irradiation regimes on microalgae growth, photosynthetic efficiency, lipid and pigment content and nutrient uptake was investigated.

Chapter 2

Maintenance: an overview on its quantification

2.1 Material balance of a continuous system

The PBR can be modeled as a continuous stirred tank reactor (CSTR) for the particular mixing, as demonstrated by tracer experiments carried out previously by Facca (2013). So the material balance with respect to the biomass, with the assumption of a constant volumetric flow rate $\dot{V}$, is expressed by:

$$\frac{dC_{x,u}}{dt} = \dot{V} \cdot C_{x,in} - \dot{V} \cdot C_{x,u} + V_{PBR} \cdot r_{x,u} \quad (2.1)$$

where V_{PBR} is the reactor volume (L), $C_{x,in}$ and $C_{x,u}$ the biomass concentrations in and out of the reactor ($g_x\ L^{-1}$), $\dot{V}$ the constant volumetric flow rate ($L\ d^{-1}$) and $r_{x,u}$ the biomass production rate, defined as $(\mu \cdot C_{x,u})$ ($g\ L^{-1}\ d^{-1}$). Particularly, μ is the specific growth rate (d^{-1}). If it is assumed that only nutrients (i.e. no microalgae) are fed to the reactor, at steady state conditions Eq. 2.1 is reduced to:

$$0 = -\dot{V} \cdot C_{x,u} + V_R \cdot \mu \cdot C_{x,u} \quad (2.2)$$

From which the following can be derived:

$$\mu = \frac{1}{\tau} = D \quad (2.3)$$

where τ is the residence time in the reactor (d) defined as:

$$\tau = \frac{V_{PBR}}{\dot{V}} \quad (2.4)$$

and D is the dilution rate (d^{-1}).

Thus, according to Eq. 2.3, it results that the growth rate at steady state is equal to the dilution rate D. Consequently, by setting different dilution rates, different growth rates can be studied. Moreover, the volumetric biomass productivity of the PBR (P_v, $g\ L^{-1}d^{-1}$), defined as the rate of change of biomass density, is equal to the biomass production rate:

$$P_v = \frac{C_{x,u}}{\tau} = \mu \cdot C_{x,u} \quad (2.5)$$

On the other hand, the areal biomass productivity of the PBR (P_a, g d-1m-2), defined as the biomass productivity per unit irradiated area, can be expressed as:

$$P_a = \frac{\dot{V} \cdot C_{x,out}}{A_{PBR}} \quad (2.6)$$

where $\boldsymbol{A_{PBR}}$ is the illuminated surface of the PBR (m^2).

2.2 Microbial model for maintenance

Microbial maintenance is defined as "the energy consumed for functions other than productions of new cell material" (Pirt, 1965). In the past several authors tried to measure the maintenance energy requirements of heterotrophic microorganisms and most of the proposed models are based on the work of Pirt.

2.2.1 Pirt model

Pirt (1965) stated that the decreasing growth yields at decreasing growth rate should be explained by a requirement of energy for cell maintenance. Accordingly, a model was proposed to correlate the maintenance requirement, the growth yield and the growth rate. Other authors optimized the model of Pirt by adding terms accounting for more complex phenomena, such as the effect of inhibiting substrate on cell maintenance (Chenl & Johns, 1996; Minkevich *et al*., 2000)

The main parameters used to describe microbial maintenance and correlate it to growth, are the yield coefficient and the maintenance coefficient.

Based on studies on continuous flow cultures, Herbert (1956) was the earliest microbiologist to consider the maintenance requirement as a negative growth or "endogenous metabolism", later termed "specific maintenance rate" by Pirt (1965), to account for yield variation with growth rates. Accordingly, the following equation was proposed:

$$\frac{dC_x}{dt} = \mu \cdot C_x - a \cdot C_x \quad (2.7)$$

where C_x is the microbial biomass ($g_x\ m^{-3}$), $\boldsymbol{\mu}$ the true specific growth rate (d^{-1}) and $\boldsymbol{a}$ the specific maintenance rate (d^{-1}). The death term is not considered in this equation, because it is referred to exponential phase of growth.

On the other hand, Schulze & Lipe (Schulze & Lipe, 1964) formulated the maintenance energy in terms of the substrate energy consumed to maintain cells, later termed "maintenance coefficient" by Pirt (1965). Eventually, Pirt proposed a relationship between the maintenance coefficient and the growth rate, according to:

$$q = -\frac{1}{x} \cdot \frac{dC_s}{dt} = m_E + \frac{\mu}{Y_G} \tag{2.8}$$

$$-\frac{dC_S}{dt} \cdot Y_{APP} = \frac{dC_x}{dt} \tag{2.9}$$

where q is the specific substrate consumption rate ($g_s\ g_x^{-1}\ d^{-1}$) used for growth and maintenance, m_E the maintenance coefficient ($g_s\ g_x^{-1}\ d^{-1}$), C_s the concentration of the energy supplying substrate ($g_s\ L$), Y_G the "true" growth yield coefficient ($g_x\ g_s^{-1}$) and Y_{APP} the apparent or observed yield coefficient ($g_x\ g_s^{-1}$).

As defined by Pirt (1965), Y_{APP} considered that, in the production of a certain amount of biomass, a portion of energy substrate was consumed in new cell synthesis, another part in maintenance of the cells, while Y_G included consumption of substrate only for net growth purposes.

From Eq. (2.8) it follows that, if Y_G and m_E are both constant, a linear relationship between q and μ should be obtained. The slope of the curve will be the inverse of Y_G and the intercept on the Y-axis will be m_E.

Moreover, Pirt derived a relation between a and m_E, according to:

$$m_E = \frac{a}{Y_G} \tag{2.10}$$

2.2.2 Relation between Y and m: Van Bodegom Model

Van Bodegom (van Bodegom, 2007) revised the work of Pirt to calculate *a*, in contrast with the relationship found by Pirt (1965), i.e. Eq. (2.10), that considered $\boldsymbol{a}$ as constant for all growth rates. From Eq. (2.8), in combination with the definitions of $\boldsymbol{Y_G}$ and $\boldsymbol{Y_{APP}}$, the author found that:

$$\frac{1}{Y_{APP}} = \frac{1}{Y_G} + \frac{m_E}{\mu} \tag{2.11}$$

Similarly to Eq. (2.8), if Y_G and m_E are both constant, the plot of $1/Y_{APP}$ against $1/\mu$ should be a straight line with slope m_E and intercept on the ordinate $1/Y_G$.
From the Eqs. (2.7) and (2.9), in combination with the definitions of Y_G and Y_{APP}, it followed that:

$$\frac{1}{Y_{APP}} = \frac{\mu}{\mu - a} \cdot \frac{1}{Y_G} \tag{2.12}$$

By substituting $1/Y_G$ in either Eqs. (2.11) and (2.12), he derived that:

$$m_E = \frac{a}{Y_{APP}} \tag{2.13}$$

which is equal to Pirt equation only if $Y_G = Y_{APP}$.
So, according to Van Bodegom's approach, there isn't a constant relationship between m_E and a, because the apparent growth yield depends on μ if maintenance occurs. In addition, the difference between Eq. (2.13) and Eq. (2.10) could be substantial if maintenance is large, as can be seen in Fig. 2.1.

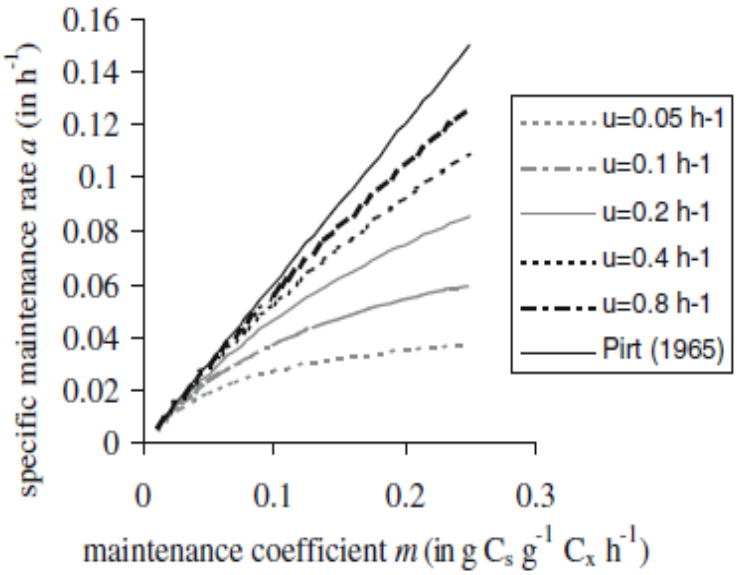

Figure 2.2 - ***Comparison between Van Bodegom (Eq. 2.13) and Pirt model (Eq. 2.10) for various μ values with $Y_G = 0,6\ g_x\ g_s^{-1}$ (van Bodegom, 2007).***

2.3 Effect of inhibiting substrate on maintenance in heterotrophic culture

As reviewed by Van Bodegom (2007), Y_G and m_E are constant and can be applied to calculate the basal maintenance. On the other hand, for heterotrophic microorganisms, it was demonstrated that Y_{APP} and μ could be represented by the Pirt model (Eqs. 2.8 and 2.11) with a constant value of m_E, only when no substrate inhibition of cell growth was observed. Particularly, Chen & Johns (1996) investigated the relationship between substrate inhibition and maintenance energy of *Chlamydomonas reinhardtii*, grown heterotrophically on acetate. They demonstrated that substrate inhibition may result in increased maintenance demand. In fact, for chemostat cultures, it was shown that a linear relationship between $1/Y_{APP}$ and $1/\mu$ was possible only for low acetate concentrations. On the opposite, when the acetate concentration in the culture broth was greater, inhibition on cell growth occurred and a linear relationship between $1/Y_{APP}$ and $1/\mu$ could not be attained (Fig. 2.2). So it resulted that m_E, depends on the substrate concentration and increases at higher inhibition.

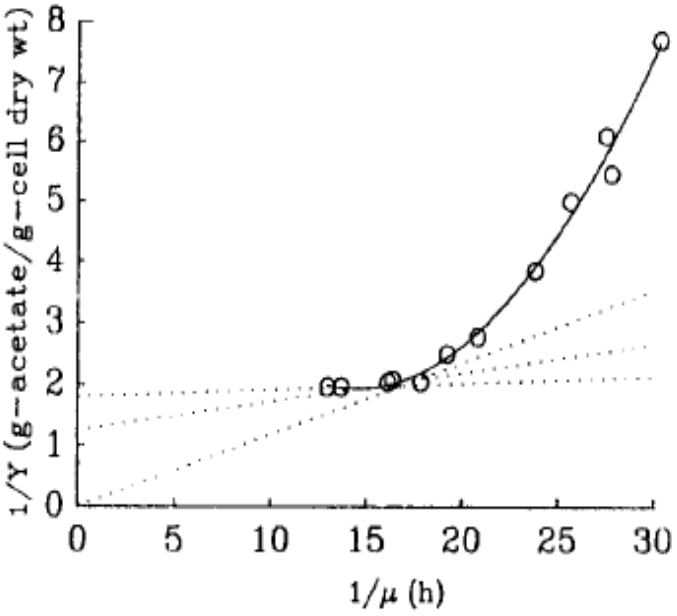

Figure 2.2 - ***Relationship between $1/Y_{APP}$ and $1/\mu$ of C. reinhardtii grown heterotrophically at various initial acetate concentrations (Chenl & Johns, 1996).***

The same trend was observed also by Minkevich et al. (2000), who studied the effect on the specific growth rate and cell biomass yield of ethanol and zinc, during cultivation of the yeast Candida valida. He found two different relations between Y_{APP} and μ in the case of low substrate concentration and inhibiting substrate concentration, respectively (Fig. 2.3). In the region at low concentration of substrate, the author found that the maintenance coefficient is close to the constant term m_E and can be expressed as:

$$Y_{APP} = \frac{Y_G}{m_E \cdot Y_G + \mu} \tag{2.14}$$

On the other hand, at higher substrate concentration, a different dependence of Y_{APP} on μ was obtained, due to the increased maintenance resulting in a general lower Y_{APP} than under non inhibiting conditions.

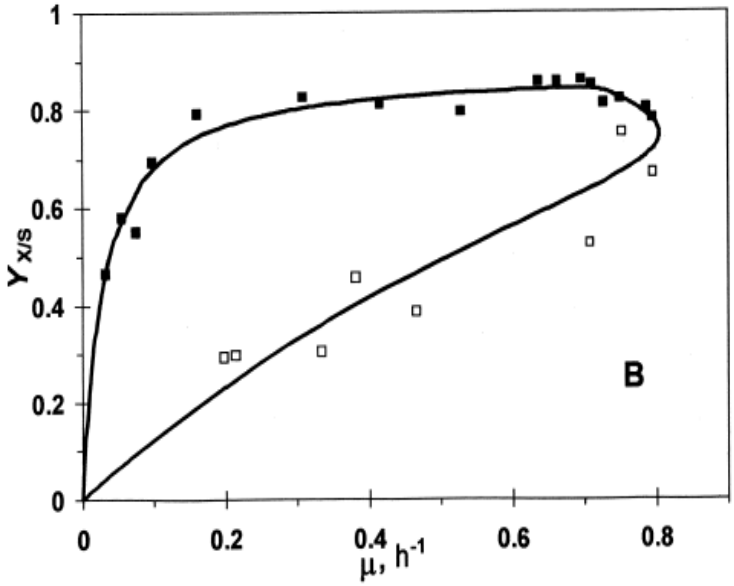

Figure 2.3 - ***The biomass yield of C. valida from ethanol vs the specific growth rate in the experiments with ethanol concentration varied. Closed symbols: ethanol limited growth ; Open symbols: ethanol inhibited growth (Minkevich et al., 2000).***

The relation under inhibiting condition was expressed by (Chen & Johns, 1994b) (Fig. 2.4), which proposed a simple mathematical model based on a mass balance on cell growth, to predict the actual maintenance energy coefficient and to account for the loss of biomass in the inhibited cultures:

$$Y_{APP} = \alpha \cdot \mu - \beta \tag{2.15}$$

where μ represents the "true" specific rate substrate utilization and α and β are fitting constants.

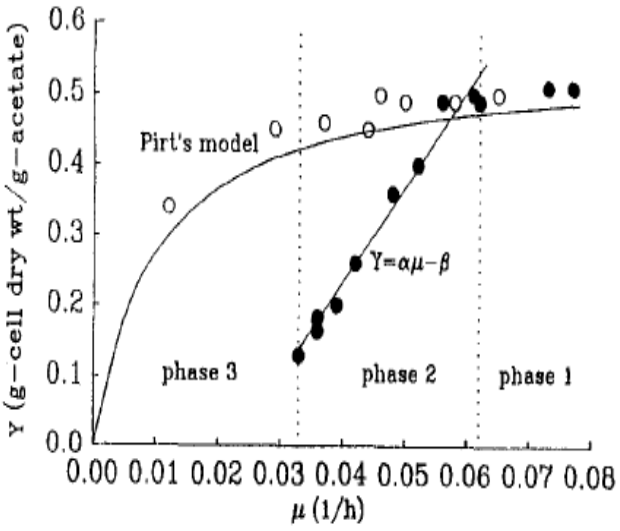

Figure 2.4 - ***Comparison of the inhibition model (Eq. 2.15) with the Pirt model (Chenl & Johns, 1996).***

2.4 Application of microbial models to photosynthetic organisms

Little is known about the energy requirement for maintenance in photosynthetic organisms, where the energy for all metabolic pathways is provided by light. Thus, its quantification for these kind of organisms is more complex than for heterotrophic ones, due to the complex relation between light availability, light excess and uptake system on growth.

2.4.1 Gons & Mur model

Gons & Mur (1980) stated that, for algae, as well as for heterotrophic microorganisms in energy-limiting conditions, growth yields decreased at low growth rates as a result of a requirement of energy for maintenance. So they demonstrated that the Pirt model (Pirt, 1965) could be applied to light-limited cultures, where light energy is considered as a limiting substrate. Based on the energy balance around the reactor, the growth rate resulted proportional to the energy absorbed, except for the energy required for maintenance:

$$\mu = \left(\frac{dE}{dt} \cdot \frac{1}{X}\right) \cdot c - \mu_e \tag{2.16}$$

where dE/dt is the light uptake rate (J d-1) of the energy X (J) stored in the culture biomass, c is the "true" efficiency of light energy conversion into the chemical energy that is stored in biomass (dimensionless) and μ_e is the specific maintenance rate constant (d-1).
The term $(\mu \cdot X)$ represents the energy part used in biomass synthesis and $(\mu_e \cdot X)$ the energy part diverted from growth, as a result of maintenance processes.

The specific light uptake rate $dE/dt \cdot 1/X$ (d^{-1}), that is the amount of energy consumed per unit of biomass over time, was calculated as:

$$\frac{dE}{dt} \cdot \frac{1}{X} = \frac{PFD_{abs} \cdot E_P \cdot A_{PBR}}{C_x \cdot LHW \cdot V_{PBR}} \tag{2.17}$$

where PFD_{abs} is the light absorbed by the culture (mmol photons m^{-2} d^{-1}), E_P the energy of photons (kJ mmol photons $^{-1}$) LHW is the low heat value of biomass (kJ g^{-1}).

Gons & Mur (1980) applied the model to the light-limited growth of *Scenedesmus protuberans*, in continuous cultures growing with light-dark cycles of 16 and 8 h and temperatures of 20 °C and 28 °C. All experiments were carried out with cultures of 1 L in standard, pyrex glass, double walled cylindrical vessels, illuminated by one or three circular white fluorescent lamps, corresponding to an average value of incident light of 12 and 38 W m^{-2}, respectively. PFD_{abs} was calculated by photodiode measurements of the light distribution in culture suspensions.

According to the approach proposed by the authors, μ is proportional to $dE/dt \cdot 1/X$ (Fig. 2.5). By the linearization of μ as function of $dE/dt \cdot 1/X$, the negative intercept with the ordinate represents μ_e, while c is the slope of the line.

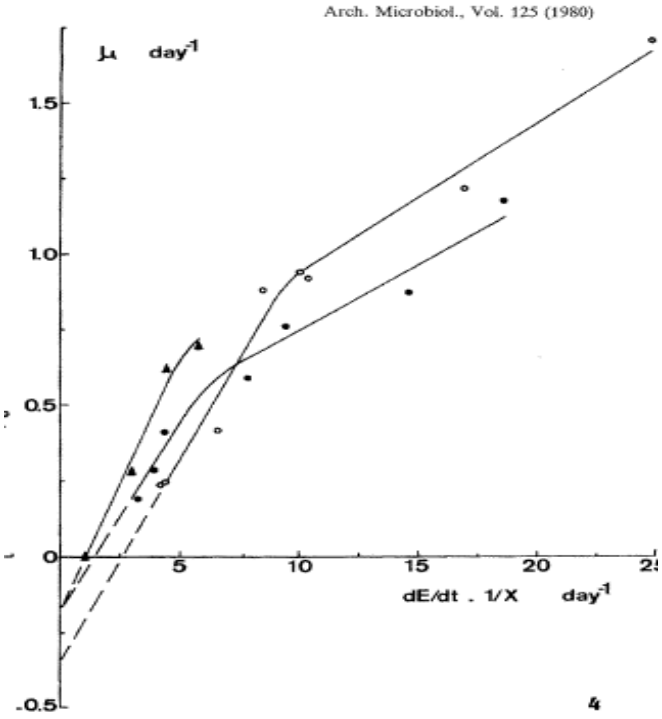

Figura 3.5 - ***The relationship between specific growth rate and specific light uptake rate at 20 °C (1 lamp; triangles, and 3 lamps; dots) and at 28 °C (3 lamps; circles) (Gons & Mur, 1980).***

The obtained values of μ_e and c are shown in Table 2.1. Gons and Mur concluded that μ_e wasn't affected by used irradiances, but only by temperature; on the contrary c depended on incident light, but did not change with temperature.

Table 2.1 - μ_e and c values determined by Gons and Mur (Gons & Mur, 1980).

	μ_e (d^{-1})		c (-)	
	Irradiance		**Irradiance**	
	12 W m^{-2}	38 W m^{-2}	12 (W m^{-2})	38 (W m^{-2})
Temperature 20 °C	0.14-0.19	0.14-0.19	0.14-0.16	0.11-0.13
Temperature 28 °C	-	0.3-0.4	-	0.11-0.13

2.4.2. Kliphuis et al. model

Kliphuis *et al.* (2012) recently applied the continuous PBR approach to measure the energy requirements for maintenance and biomass formation in *C.reinhardtii*, under an average irradiance lower than 100 μmol photons m^{-2} s^{-1}. Experiments were carried out in a continuous pre-sterilized flat panel PBR at different dilution rates ranging between 0.018 and 0.064 h^{-1}. The system consisted of two transparent polycarbonate sheets, held together by stainless steel frame, and was characterized by a working volume of 0.4 L, a light path of 25 mm and an illuminated area of 195 cm^2 (10 x 19.5 cm) (Fig. 2.6). Temperature was maintained at 25 °C by an external water bath and the continuous illumination was provided by a red LED panel of 20 x20 cm placed on one side of the PBR.

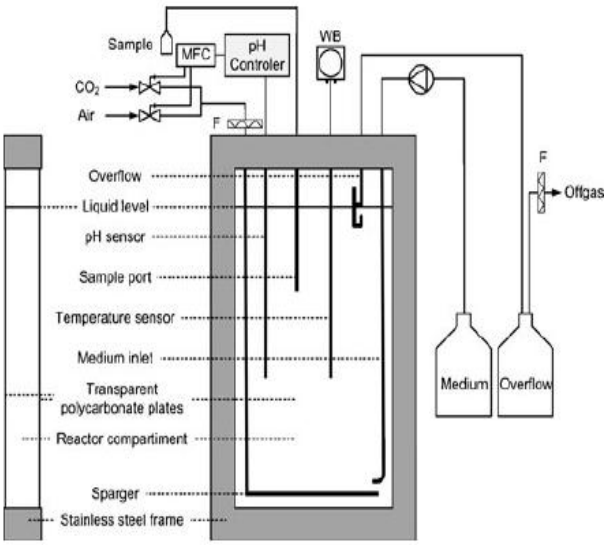

Figure 2.6 - *Schematic front and side view of the PBR setup used by Kliphuis et al. (2012) for the continuous experiments. MFC: mass flow controller for both air and CO2, WB: water bath, F: air filter.*

The relationship proposed to describe the correlation between the specific light supply r_{Ex} (mmol photons g^{-1} d^{-1}) and μ (d^{-1}) was based on the model of Pirt (1965), as previously proposed by Zijffers *et al.* (2010):

$$r_{Ex} = \frac{\mu}{Y_G} + m_E \tag{2.18}$$

where,

$$r_{Ex} = \frac{PFD_{abs} \cdot A_{PBR}}{C_x \cdot V_{PBR}} \tag{2.19}$$

PFD_{abs} was found by subtracting the light falling through the culture at steady state from the amount of light falling through the reactor filled with medium only, according to:

$$PFD_{abs} = I_{in} - BI - I_0 \tag{2.20}$$

where I_{in} is the incident light (mmol photons m^{-2} d^{-1}), BI the back irradiance (mmol photons m^{-2} d^{-1}) and I_0 the light absorbed by the sole medium and panel (mmol photons m^{-2} d^{-1}).
In addition, the calculated light supply rate was corrected to account for the inefficiency of light use:

$$r_{Ex,\mu} = r_{Ex} \cdot \varphi_{Pmax} \tag{2.21}$$

Where $r_{Ex,\mu}$ is the specific light utilization rate (mmol photons g^{-1} d^{-1}) and $\varphi_{Pmax}$the maximum photochemical quantum yield (dimensionless), assumed to be equal to 0.8.
The values of C_x and PFD_{abs}, found for each steady state by Kliphuis *et al.*, are summarized in Table 2.2., as a function of the growth rate.

Table 2.2 - C_x, PFD_{abs} and μ determined for each chemostat experiment (Kliphuis et al., 2012).

Growth rate[a] μ (h^{-1})	Residence time[a] (h)	Biomass density C_x[b] (g L^{-1})	Photon flux density absorbed PFD_{abs} (μmol photons m^{-2} s^{-1})	Specific light utilization rate $r_{Ex,\mu}$ (mmol photons g^{-1} h^{-1})
0.018±0.000	55.1±0.5	0.78±0.04	88	15.8±0.8
0.019±0.000	52.8±1.2	0.84±0.08	87	16.7±1.5
0.031±0.001	32.3±1.0	0.41±0.02	80	25.7±1.4
0.034±0.001	29.7±1.1	0.39±0.02	73	26.8±1.6
0.052±0.001	19.3±0.5	0.21±0.01	51	36.1±1.7
0.061±0.003	16.5±0.7	0.11±0.01	36	45.5±3.7
0.064±0.001	15.6±0.0	0.10±0.01	31	44.8±3.7

A plot of these points (Fig. 2.7) shows that the amount of light used by the algae increased proportionally to the growth rate while a fixed amount of maintenance light energy was necessary to keep the algae in a healthy state. By the linearization of r_{Ex} as function of μ, the positive intercept on Y-axis and the inverse of the slope give a value of m_E and Y_G of 5.63 mmol photons g^{-1} h^{-1} and 1.26 g mol photons^{-1}, respectively.

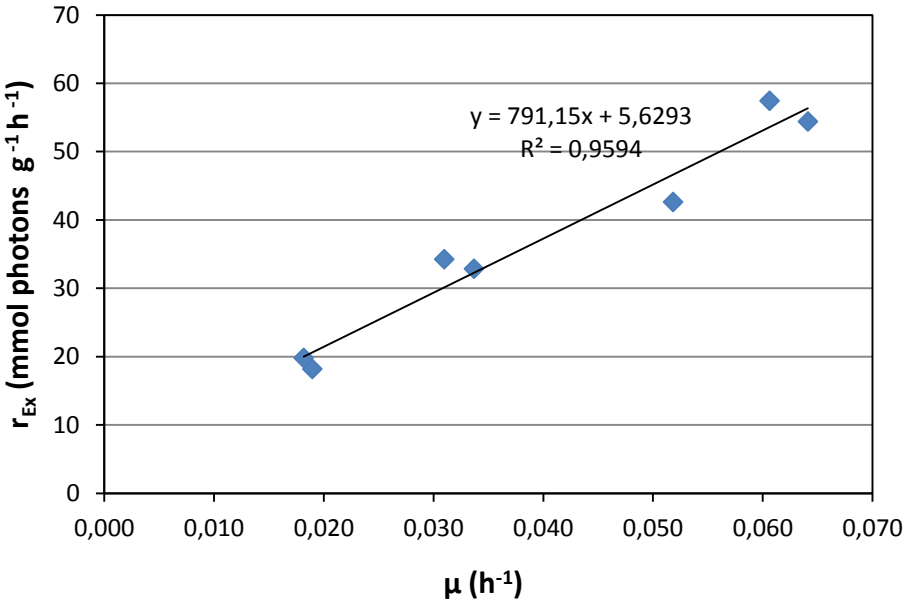

Figure 2.7 - *Relationship between r_{Ex} and μ, obtained plotting Kliphuis data.*

They observed that the value of Y_G was high compared to biomass yields found for other green microalgae. In fact, several authors obtained yields ranging from 0.5 to 1 g mol photons^{-1} for other green microalgae, but at high irradiances of 1000 μmol photons m^{-2} s^{-1} or more (Table 2.3). They concluded that the differences between the yields at high and low irradiances reflected the fact that a large part of the light was "wasted" at higher irradiances, because in these conditions the antenna complexes in the algal photosystems became saturated and the remainder of the absorbed light was dissipated as heat and fluorescence.

Table 2.3 – ***Comparison of biomass yields on light energy and the used irradiances for different microalgae from literature (Kliphuis et al., 2012).***

Organism	Y_{xE} or Y_{xE}^{obs} (g mol^{-1})	Light intensity (µmol photons m^{-2} s^{-1})	Reference
Chlamydomonas reinhardtii	1.25±0.06[a,d]	80	This paper
Dunaliella tertiolecta	0.78[a]	930	Zijffers et al. (2010)
Chlorella sorokiniana	0.75[a]	930	Zijffers et al. (2010)
Chlorella sorokiniana	0.80[b]	1500	Kliphuis et al. (2010b)
Chlorella sorokiniana	1.0[b]	2100	Cuaresma et al. (2009)
Chlamydomonas reinhardtii	1.11[b,c]	110	Takache et al. (2010)
Chlamydomonas reinhardtii	0.73[b,c]	500	Takache et al. (2010)
Chlamydomonas reinhardtii	0.51[b,c]	1000	Takache et al. (2010)

[a] $Y_{xE}=\mu / (r_{Ex}+m_E)$, according to Eq. 7

[b] $Y_{xE}^{obs}=\mu/r_{Ex}$ (the observed yield was not corrected for maintenance requirements)

[c] Recalculated from data obtained in flat Torus photobioreactor by Takache et al. (2010)

[d] Calculated by linear regression ($P<0.05$)

Finally, even if these authors measured experimentally the maintenance coefficient and yield, they did not calculate the specific maintenance rate. In addition, no data are available about the influence of light intensity and regime on both maintenance coefficients and rate.

2.5 Intensity and biomass yield

The biomass yield on light energy of green algae was recently investigated by Zijffers *et al.* (2010) at saturating light intensities. Particularly, the objective of the work was to determine the effect of biomass density and light path on the biomass yield of *Dunaliella tertiolecta* and *Chlorella sorokiniana* at constant photon flux density of about 930 µmol photons m^{-2} s^{-1}. Experiments were carried out in a continuous flat panel PBR, composed of transparent polycarbonate sheets held together in a frame similar to the system used by Barbosa *et al.* (2005) and characterized by a width of 20 cm, a height of 60 cm, and a light path of 1,25 or 2,15 cm (Fig. 2.8). The temperature was maintained at 30 °C and 37 °C for *D. tertiolecta* and *C. sorokiniana*, respectively, and the system was illuminated on one side using ten compact fluorescent tubes.

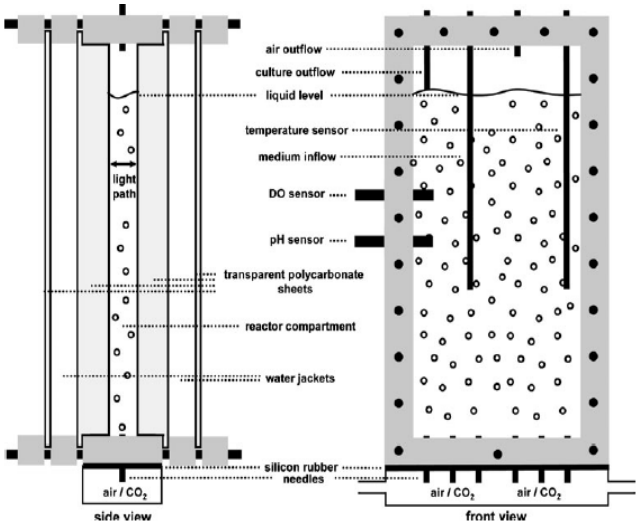

Figure 2.8 - ***Schematic front and side view of the flat panel PBR used by Zijffers et al. (2010).***

The algae were cultivated using the D-stat method as described by Paalme *et al*. (1995) and later applied by Barbosa *et al.* (2005). In general, the dilution rate was changed applying a constant deceleration rate according to:

$$D = D_0 - d \cdot t \tag{2.22}$$

where D_0 is the dilution rate at which the D-stat method starts (h^{-1}), d the deceleration rate (h^{-2}) and t the time (h).

In this way, the microalgae productivity can be determined for a wide range of dilution rates in less time compared to performing a number of chemostat cultivations. However, the continuous rate of change of the dilution rate have to be chosen such that microalgae are able to acclimate to the continuously changing conditions in the PBR (Paalme *et al.*, 1995).

Fig. (2.9) shows the dilution rate changes during the D-stat cultivations, applied to the two algae.

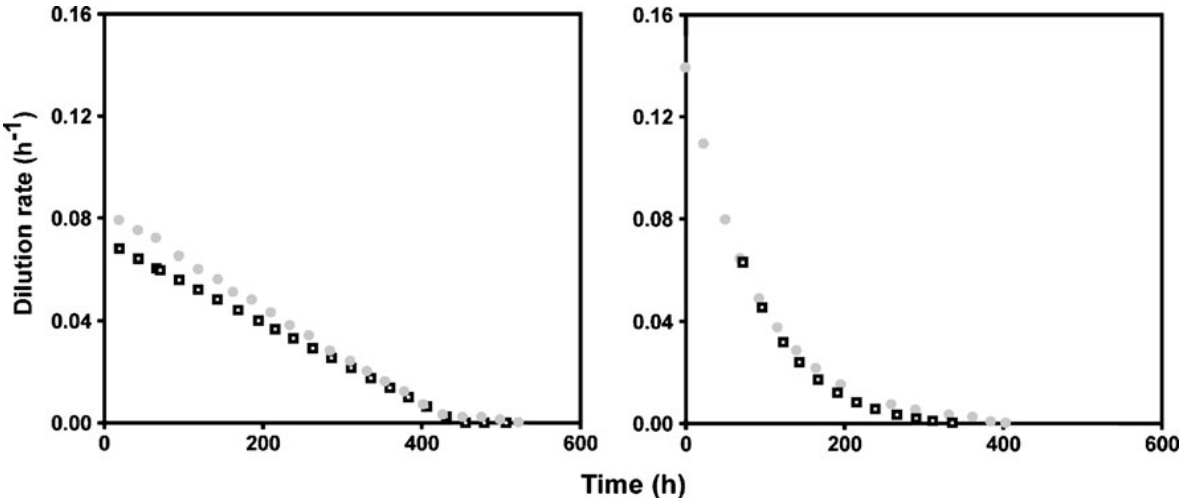

Figure 2.9 - ***Dilution rate profiles obtained by Zijffers et al. (2010) during the D-stat cultivations of D. tertiolecta (left) and for C. sorokiniana (right) cultivations (Zijffers et al., 2010).***

They plotted Y_{APP} , calculated according to Eq. 2.23, as a function of $r_{E,x}$ (Fig.2.10):

$$Y_{APP} = \frac{C_x \cdot \mu \cdot V_{PBR}}{PFD_{abs} \cdot A_{PBR}} \tag{2.23}$$

They observed that at higher photon flux densities, a relatively constant yield between 0.6 and 0.8 g mol photons^{-1} was obtained, while at lower photon flux densities, i.e., at higher biomass concentrations, the yield dropped considerably.

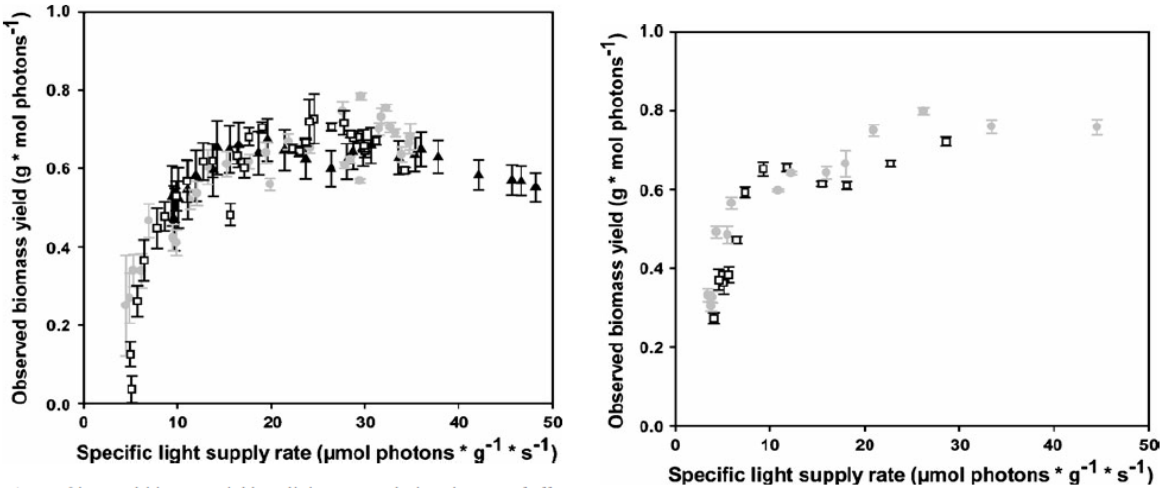

Figure 2.10 - ***Observed biomass yield on light energy during the D.tertiolecta (left) and C.sorokiniana (right) cultivations, obtained by Zijffers et al. (2010).***

Moreover, to demonstrate that maintenance requirements was the reason for the reduction of the observed yield at lower light supply rates, they fitted their data through the model of Pirt (Eq.2.8) and Kliphuis (Eq.2.18), for both *C. sorokiniana* and *D. tertiolecta*. So $r_{E,x}$ was plotted

as a function of μ (Fig. 2.11). Particularly, a "true" growth yield of 0.782 and 0.751 g mol photons^{-1} was found for *D. tertiolecta* and *C. sorokiniana*, respectively.

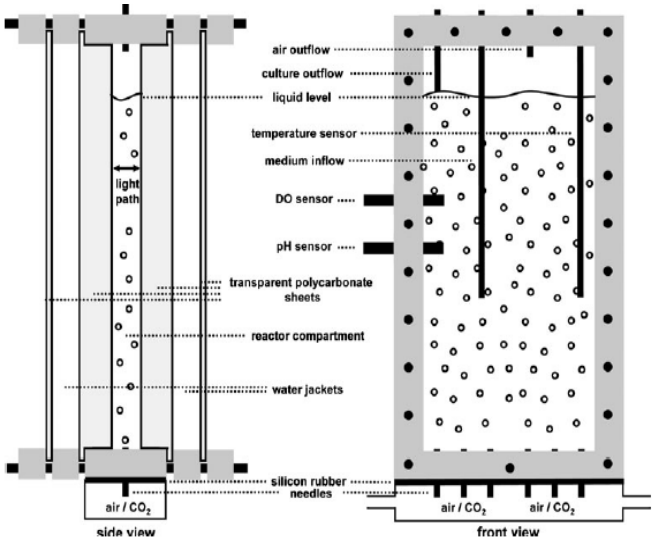

Figure 2.11 – ***Specific light supply rate as a function of μ for D. tertiolecta (left) and C.sorokiniana (right), obtained by Zijffers et al. (2010).***

The authors concluded that the constant value of Y_G shows that the steep decrease in the observed biomass yield at high biomass concentration might not to be caused by a decrease in efficiency of light use, but by an increase in maintenance energy requirement because of the increase in biomass concentration.

Chapter 3

Materials and methods

3.1 Microalga and medium composition

S.obliquus 276-7 from SAG (Culture Collection of Algae at the University of Göttingen, Germany) is the green microalga used during the laboratory activity. This is one of the most promising species as feedstock for biodiesel production, since it presents several advantages such as a fast growth, efficient CO_2 fixation, the ability to grow in wastewaters and accumulate lipids (Gris *et al.*, 2014). *S. obliquus* is a common green alga, often occurring as almost a pure culture in fresh water plankton. Usual habitates are water like clean ponds, lakes and rivers, mainly in Asia and Europe. Cells are commonly occurring in colonies as multiple of two, with four or eight cells being most common. The morphology of the colony can be varied considerably by varying the medium in which the cells are growing. In a medium with low phosphorous or salt concentration, it is induced to grow unicellular, forming around 10 μm long elliptical cells. Fig. 3.1 shows an optical microscope image of *S.obliquus* cells.

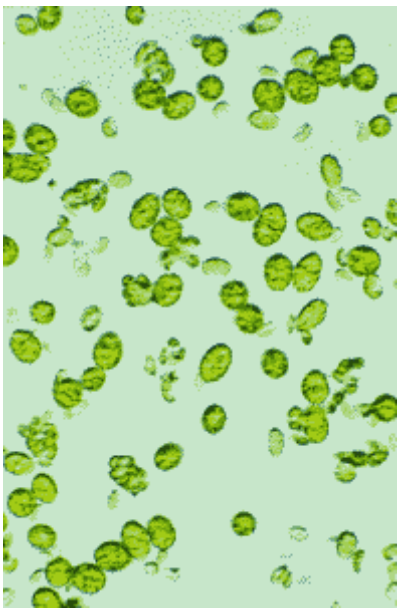

Figure 3.1 – ***Cells of S. obliquus under light microscope (http://www.uni-koeln.de***)

The microalga was maintained and cultured in BG11 medium, whose composition is reported in Table 3.1. The medium was sterilized in an autoclave for 20 min at 121°C in order to prevent any contamination. During continuous experiments, the composition of BG11-medium was modified by adding higher concentrations of $NaNO_3$ and K_2HPO_4 (3 g L^{-1} and 500 mg L^{-1}, respectively) to ensure that N and P were not limiting.

Table 3.1 – *BG11 composition*.

Component	Concentration	Unit of measure
Na_2MG EDTA	1E-03	g/L
Ferric ammonium citrate	6E-03	g/L
Citric acid . $1H_2O$	6E-03	g/L
$CaCl_2$. $2H_2O$	36E-03	g/L
$MgSO_4$. $7H_2O$	75E-03	g/L
K_2HPO_4	30.5E-03	g/L
H_3BO_3	2.86E-03	g/L
$MnCl_2$. $4H_2O$	1.81E-03	g/L
$ZnSO_4$. $7H_2O$	0.222E-03	g/L
$CuSO_4$. $5H_2O$	0.079E-03	g/L
$COCl_2$. $6H_2O$	0.050E-03	g/L
$NaMoO_4$. $2H_2O$	0.391E-03	g/L
Na_2CO_3	20E-03	g/L
$NaNO_3$	1.5	g/L
Hepes 1M pH 8	10E-03	mM/L

3.2 Reactor setup

Pre-cultures for the inoculum were grown in 250 mL glass bottles under a continuous enriched CO_2 feed flow and constant light intensity of 150 μmol photons m^{-2} s^{-1}. Continuous experiments were carried out in a vertical flat panel PBR (Fig. 3.2), with a working value of 250 ml and sterilized in autoclave. *S.obliquus* was inoculated into the reactor with culture medium. In order to prevent the occurring of washout, the reactor operation was first started in a batch mode. The depth of the reactor (1,2 cm) is shallow in order to reduce the cells self-shading and to allow a maximum utilization of light. The surface exposed to light is 208 cm^2. Previous studies (M. Facca, 2013) permitted to assess that this reactor can be considered a

CSTR type with a good approximation, in fact the dead volume was estimated to be 10% of the total volume. The reactor is made of two transparent polycarbonate sheets glued to an "U" support. The support thickness affects the system volume and the light path length. The mixing in the culture was ensured by a magnetic micro-stirrer and a CO_2–air (5% v/v) flow, fed through a sieved silicone tube placed at the reactor bottom. The gas flow also supply a non limiting CO_2 content to the culture. The total gas flow rate was 1 L h^{-1} and the air entering the reactor was regulated using suitable valves and flowmeters. The fresh medium was fed at a constant rate by a peristaltic pump (Watson-Marlow sci400, flow rate range: 25-250 mL d^{-1}), and a mixture of medium and cells was withdrawn from the PBR at the same rate by an overflow tube. The outlet biomass was collected in a sterilized tank. So, the residence time in the reactor was directly controlled by the peristaltic pump, according to Eq. 2.4. Several flow rates were used, thus leading to different residence times and growth rates.
The systems were placed inside an incubator (Frigomeccanica Andreaus) whose temperature was maintained constant at 23°C (±1°C), on the basis of previous studies (B. Gris, 2012).

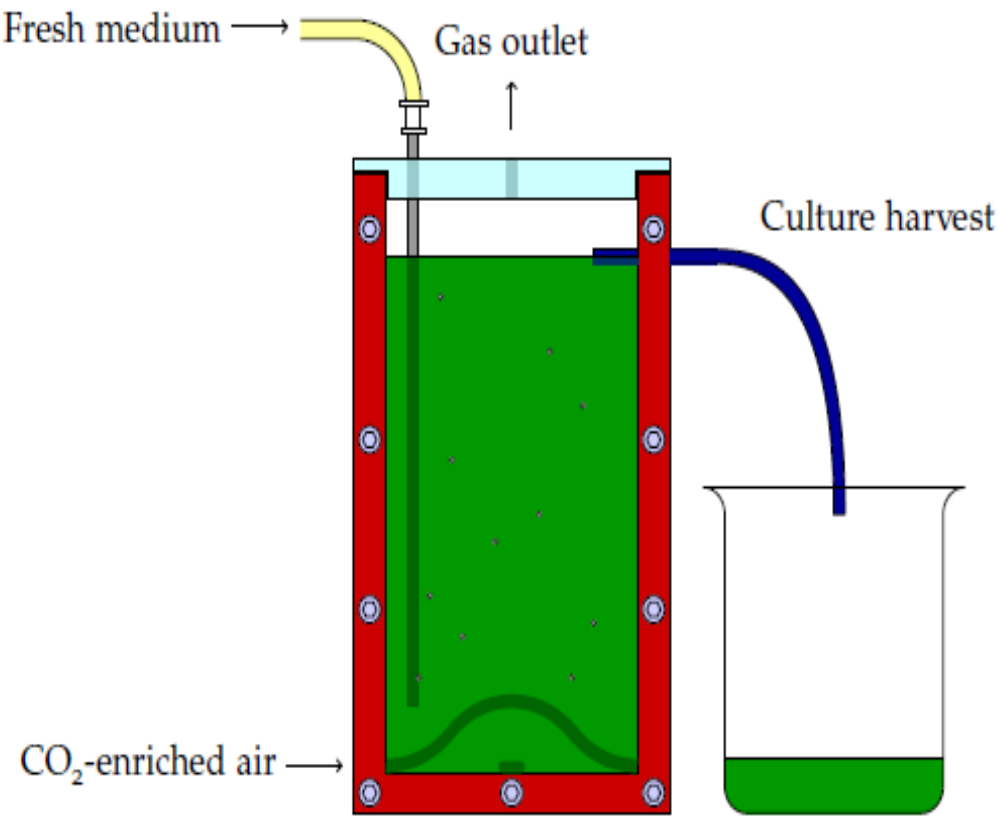

Figure 3.2 - ***Sketch of the continuous lab-scale reactor set up.***

3.3 Lamps as energy source

Light was provided by a LED lamp (Photon System Instruments, SN-SL 3500-22) both for continuous and alternated day-night cycles. The photon flux density (PFD) was measured using a photoradiometer (HD 2101.1 from Delta OHM), which quantifies the PAR in the range 400-700 nm. The measurements of the PAR photon flux density were realized on 6 points of the surface of the reactor and then averaged in order to obtain the value of irradiance needed, e.g. 150 and 650 μmol photons m^{-2} s^{-1} for the experiments at constant intensities. The same measurements were collected on 6 points of the back of reactor, when the steady state conditions were reached. The average of these value allowed to obtain the back irradiance for each residence time. It is clear that an higher concentration of biomass in the reactor causes an higher turbidity effect and the irradiance measured behind the reactor will be lower.
For experiments under day/night light conditions, the light intensity as a function of time was simulated so that to provide the PBRs with the same PAR amount of energy received under natural conditions at the selected latitude. PVGIS Solar Irradiation Data (http://re.jrc.ec.europa.eu/pvgis/) is an online available database of typical day evolution of irradiation on a given surface for any location and time of year. This software was used as the source of irradiation data for the location of Padova, Italy. An incident angle of 35° was applied, as the default setting of the database, in order to exploit the maximum solar energy. Two months were selected as representatives of each season: January for Winter and July for Summer. So the LED lamp linked to a digital controller was programmed in order to simulate the irradiation profiles from PVGIS database. Measurements of PAR photon flux density were performed to verify the correspondence between experimental and simulated day-night irradiation curves (Fig. 3.3).

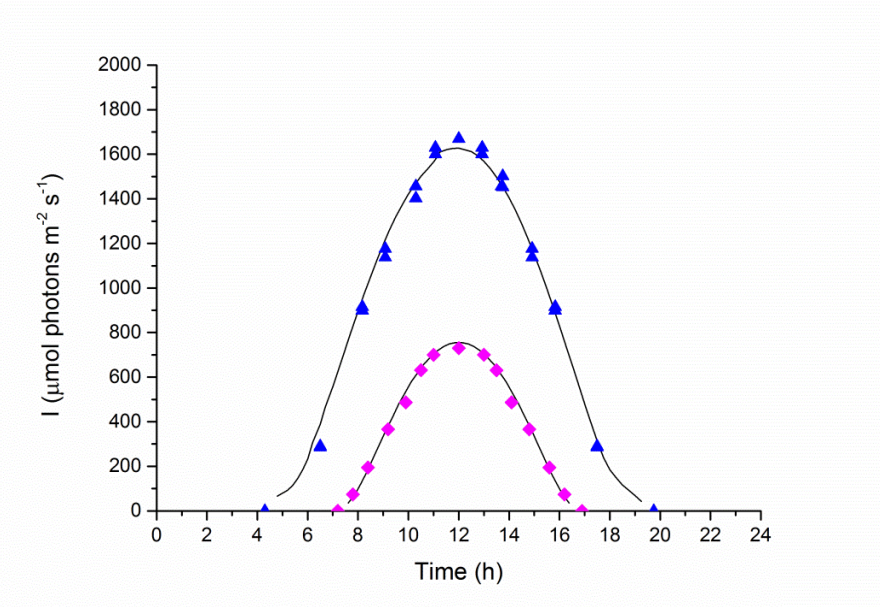

Figure 3.3 - ***Irradiation profiles (lines) from PVGIS database and measures of light impinging experimental PBR of the two representative months: January data for Winter (rhombus), July for Summer (triangles).***

A typical Winter day in Padova is characterized by 9 h of light and 12 h of darkness and the incident light reaches a maximum value of about 730 µmol photons m^{-2} s^{-1} at midday. On the other hand, the Summer irradiation curve is characterized by a light period of 15 hours and a dark period of 9 hours and the maximum value at midday is about 1700 µmol photons m^{-2} s^{-1}. The average value of the global daily irradiation (GI) supplied to the culture in the Summer and Winter regime was calculated as:

$$GI = \frac{\int_0^{24} punctual\ irradiance}{24\ hours} = \frac{\int_0^{24} I(t)dt}{24\ hours}\left[\frac{W}{m^2}\right] \qquad (3.1)$$

The values of GI obtained for the Summer and the Winter regime were 548.69 and 149.08 µmol photons m^{-2} s^{-1}, respectively.

At least 5 residence time were set for each light condition. After each change of residence time, a transient period of operation was observed and the steady state operation was reached and maintained at least for 5 days.

3.4 Analytical Methods

In this section the standardized procedures used to measure the biomass concentration, N and P concentration and the lipid and pigment content are described.

3.4.1 Measurements of biomass concentration

Microalgal concentration was monitored by three different procedures:

1. optical density (OD) or absorbance;
2. cell concentration;
3. dry weight (DW).

Usually, cells concentration and OD measures were performed on the same sample, with different dilution factors.

3.4.1.1 Optical Density

OD, measured in a spectrophotometer, was determined daily according to the following standardized procedure:

1. a sample (1.5-2 ml) of microalgal solution is taken using BD Falcon™ Express™ Pipet-Aid®;
2. the absorbance of the sample at $\boldsymbol{\lambda}$ = 750 nm, placed in a cuvette with $\boldsymbol{l = 1\ cm}$, is measured using Spectronic Unicam UV-500 UV-visible double beam spectrophotometer. At this wavelength chlorophyll does not absorb photons and light attenuation is uniquely due to scattering phenomena, i.e., to cells and suspended solids concentration. As this equipment works in the absorbance range of 0.1 - 1, the sample is diluted with the culture medium when the upper limit is exceeded.

Single beam and double beam are the two major classes of spectrophotometers. The first uses a reference standard to standardize or blank the instrument before taking measurements and the second splits the beam of light into two different paths, one of which passes through the sample while the other passes through a reference standard. Double beam spectrophotometers measure the ratio of light intensities and, therefore, are not as sensitive to fluctuations in the light source or detector.

3.4.1.2 Cell concentration

Cell concentration was measured using a Bürker Counting Chamber (HBG, Germany) (Fig. 3.4 left). It is a glass slide 7.5x3.5 cm wide and 4 mm deep. The chamber is composed of two areas of 0.1 mm of depth, each of them contains a network of 9 large squares of 1mm side and divided by a triple line. Each large square represents a volume of 0.1 μL and contains 16 smaller squares, divided by double lines (Figure 3.4 right).

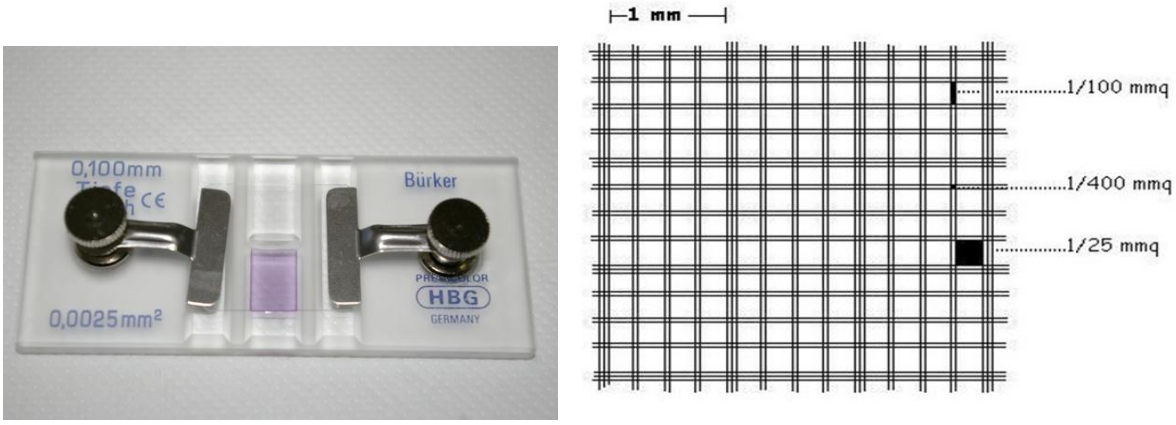

***Figure 3.4* – Burker Counting Chamber (left); Burker Counting Chamber network (right).**

Cell count was determined daily using a standardized procedure:

1. the culture sample is diluted with distilled water with a dilution factor ranging from 20 to 200, depending on concentration;
2. once fixed the cover slip to the chamber, both chambers are loaded with the diluted cell suspension using a micropipette and tip; the space is filled by capillary action. Approximately 20 µL are required per side;
3. cell counting is performed by a microscope; only 3 of the 9 squares are counted, and then an average value was calculated.

The total cell number was calculated as follows:

$$\frac{cells}{mL} = \left(\frac{\sum cells\ counted\ in\ 3\ squares}{3}\right) \cdot dilution\ factor \cdot 10^4 \qquad (3.2)$$

where 10^4 is the volume factor; in fact, as previously mentioned each large square is characterized by a volume of 0.1 µL, that equates to 1/0.0001 mL (10^4).

3.4.1.3 Dry weight

The DW of microalgal biomass represents the amount of dried microalgae per unit of volume and it was determined daily only when the steady state conditions were reached. A standardized procedure was followed:

1. a sample of 5 ml of microalgal suspension is collected using BD Falcon™ Express™ Pipet-Aid®;
2. a biomass filter (Sartorius Stedim Biotech cellulose nitrate filter pore size 0,2 µm) is placed in the oven at 80 °C for 10 minutes to remove the absorbed humidity and then weighted with Atilon Acculab Sartorius Group microbalance with instrument sensitivity of 10^{-4} g. This value represents the tare;

3. the biomass filter is placed in a apposite filtering vacuum flask and the known volume of sample is spilled on the filter. The liquid fraction flows through while microalgal biomass is retained;
4. the filter is placed in the oven at 80° C for 2-4 hours to remove inter- and intra-cellular water;
5. the filter is weighted. This value represents the gross weight.

The dry weight was calculated according to:

$$DW = \frac{gross\ weight - tare}{sample\ volume}\ \left[\frac{g}{L}\right] \tag{3.3}$$

As previously mentioned at least 5 dilution rates were studied for each light condition. For each resident time, steady state operation was confirmed by checking constant OD_{750}, cell concentration and *DW* for at least 3-5 days. So steady state concentrations were averaged on three to five points and the residence time was changed. Thus for each dilution rate it was possible to calculate the average cell density and the photosynthetic efficiency (%PAR), according to Eqs. 3.4 and 3.5, respectively:

$$Average\ cell\ weight = \frac{DW}{Cells/mL} \tag{3.4}$$

$$\%PAR = \frac{C_x \cdot \dot{V} \cdot LHW}{PFD_{abs} \cdot E_p \cdot A_{PBR}} \tag{3.5}$$

3.4.2 Measurements of nutrients concentration

The nutrients analyzed were nitrates (N-NO_3) and phosphates (P-PO_4), assessed at least twice at each steady state, in order to verify the hypothesis of non-limiting nutrients operating conditions. Samples of culture were filtered through a 0.2 μm filter in order to measure only dissolved nutrients. Nutrient concentration were measured at the inlet and outlet reactor and the nutrient/biomass yields were calculated as:

$$Y_{i/X} = \frac{C_{i_{IN}} - C_{i_{OUT}}}{C_x} \tag{3.6}$$

where the subscript i indicates N or P; $C_{i_{IN}}$ and $C_{i_{OUT}}$ are the concentration of i at inlet and outlet of the reactor, respectively (mg_i) and $Y_{i/X}$ is the Nitrogen (or Phosphorous)-Biomass yield ($mg_i\ mg_x{}^{-1}$).

3.4.2.1 Nitrates

$N\text{-}NO_3$ concentration was measured by an analytical test kit provided by St. Carlo Erba Reagenti, Italy (code 0800.05482). The assay is based on reduction of nitrates to nitrites that react with sulfanilic acid producing diazonium ion. By the reaction with gentisc acid (2,5 dihydroxibenzonic acid) a dying molecule is produced and detected spectrophotometrically at $\lambda = 445\, nm$. The calibration line (Figure 3.5) was evaluated by means of known nitrate concentration standard solutions prepared with sodium nitrate ($NaNO_3$). Equation associated to calibration line is:

$$A_{445} = 0{,}0112\ \text{ppm} + 0{,}0373; \quad R^2 = 0{,}968 \tag{3.7}$$

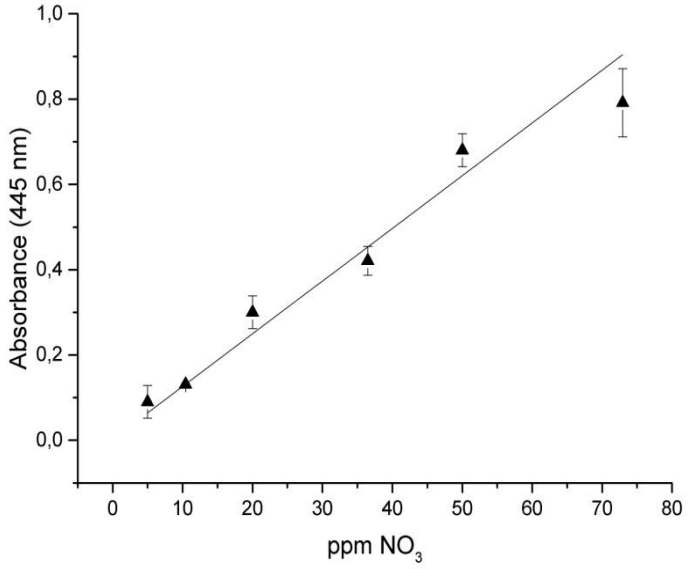

Figure 3.5 - ***Nitrates kit calibration curve***.

3.4.2.2 Ortophosphates

$P\text{-}PO_4$ concentration was measured by a modified analytical method described in APHA-AWWA-WEF, 1992. The mixed reagent was prepared immediately before the analysis (since it become unstable in 3-4 hours), mixing predetermined quantities of stock solutions and ascorbic acid solution. The latter must be prepared the same day of the analysis, as it become unstable in 24 hours, while stock solutions can be stored for months. The composition of each solution is:

- sulphuric acid 5N: prepared diluting 35 ml of 96%p/p of sulphuric acid in 250 ml of milliQ water;

- potassium antimonyl tartrate: 0.34 g of potassium antimonyl tartrate was dissolved in 250 ml of milliQ water;
- ammonium molybdate: 7.5 g of ammonium molybdate tetrahydrate was dissolved in 250 ml of milliQ water;
- ascorbic acid: 1.35 g of ascorbic acid was dissolved in 25 ml of milliQ water.

The final composition of the mixed reagent is reported in Table 3.2.

Table 3.2 - ***Mixed reagent final composition***.

Solution	Volume (mL)
Sulphuric acid 5N	25
Potassium antimonyl tartrate	5
Ammonium molybdate	10
Ascorbic acid	10

250 µl of this mixture were used for 2,5 ml of sample. The absorbance of the sample due to the colorimetric reaction was measured spectrophotometrically after 5 minutes at $\lambda = 705\ nm$. The calibration line was evaluated by means of known orthophosphates standard solutions prepared with potassium dihydrogen phosphate (KH_2PO4) (Fig. 3.6). Equation associated to calibration line is:

$$A_{705} = 0{,}1211\ ppm + 0{,}0257;\ \ R^2 = 0{,}992 \qquad (3.8)$$

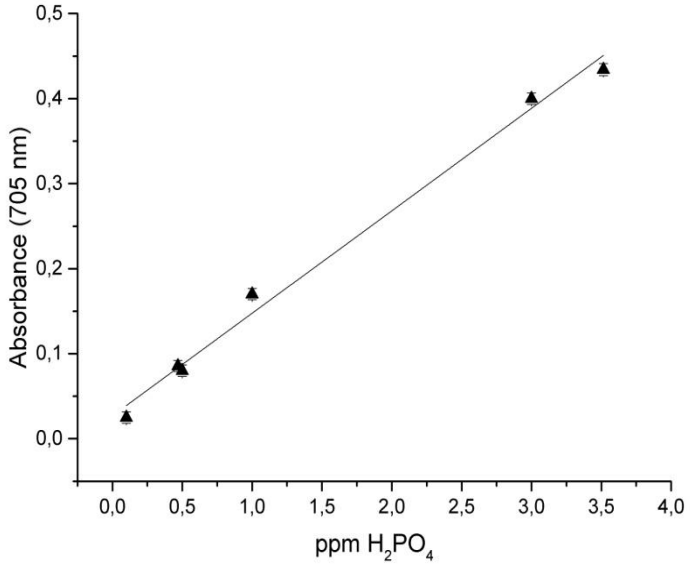

Figure 3.6 - ***Phosphates calibration curve.***

3.4.3 Soxhlet extraction of total lipids

Total lipids were extracted from dried cells using methanol-chloroform (2:1 vol/vol) as solvent mixture in a Soxhlet apparatus (Fig. 3.7)

The algal culture is centrifuged at 5000 rpm for 10 minutes, at room temperature. After centrifugation the supernatant is discarded and the biomass is dried and ground into a fine powder in a mortar pestle. Before Soxhlet extraction, the powder is placed in the oven for 2 hours at 80 °C to remove residual humidity and then weighted. The powder is then placed inside a thimble made of filter paper (0.22 μm of porosity), which is loaded into the main chamber of the Soxhlet extractor. The Soxhlet extractor is placed onto a flask containing the extraction solvent. The solvent is heated, so that the solvent vapour travels up a distillation arm, and floods into the chamber housing the thimble of dried biomass. A condenser ensures that solvent vapour turns into liquid and drips back down into the chamber housing the solid material. The chamber containing the biomass is slowly filled with warm solvent. Total lipids will then dissolve in the warm solvent. When the Soxhlet chamber is almost full, it is automatically emptied by a siphon side arm, with the solvent running back down to the distillation flask. This solvent recirculation was repeated for about 24 hours. During each cycle, a portion of the non-volatile compound dissolves in the solvent. After many cycles the desired compound is concentrated in the distillation flask. The advantage of this system is that instead of many portions of warm solvent being passed through the sample, just one batch of solvent is recycled. After extraction the solvent is removed, by a rotary evaporator, yielding the extracted compounds.

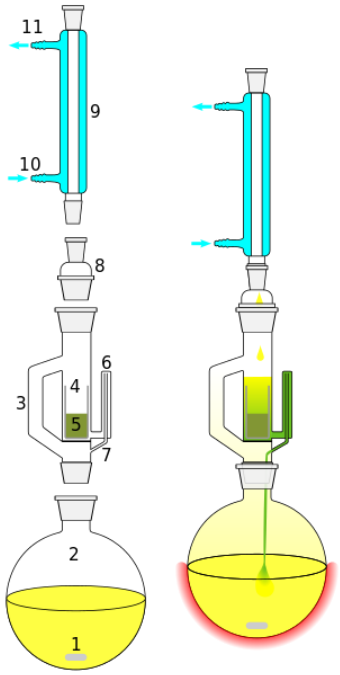

Figure 3.7 - ***Soxhlet apparatus scheme: 1) Stirrer bar; 2) Still pot; 3) Distillation path; 4) Thimble; 5) Solid; 6) Siphon top; 7) Siphon exit; 8) Expansion adapter; 9) Condenser; 10) Cooling water in; 11) Cooling water out (http://it.wikipedia.org).***

The main components of a rotary evaporator are:

- A motor unit that rotates the evaporation flask or vial containing the user's sample;
- A vapor duct that is the axis for sample rotation, and is a vacuum-tight conduit for the vapor being drawn off of the sample;
- A vacuum system, to substantially reduce the pressure within the evaporator system;
- A heated fluid bath (generally water) to heat the sample;
- A condenser with a coil through which coolant passes;
- A condensate-collecting flask at the bottom of the condenser, to catch the condensed solvent;
- A mechanical or motorized mechanism to quickly lift the evaporation flask from the heating bath.

The solvent is heated via the heating bath. A thin film of solvent forms on the inner surface of the rotating evaporating flask, resulting in a higher rate of evaporation. Rotation ensures homogenous mixing of the sample and prevents overheating inside the flask. The solvent vapor flows at high speed into the condensation part of the system. At this point the energy inside the solvent vapor is transferred to the cooling medium and the solvent condenses. The condensed solvent flows by force of gravity into the receiving flask. Vacuum is used to lower the boiling temperature and hence raise the efficiency of the distillation process. The

temperature of the heating bath depends on the type of solvent used ; in our case environmental temperature was used.
The lipid content was calculated by this formula:

$$\%\ lipids = \frac{mass\ of\ (flask + extracted\ lipids) - mass\ of\ empty\ flask}{mass\ of\ powder} * 100\ \left[\frac{g_{lipids}}{g_{biomass}}\right] \quad (3.9)$$

3.4.4 Pigments extraction

Pigment content determination was performed according to the procedure optimized in a previous work (B. Gris, 2012). The extraction was generally realized on a fresh pelleted sample of microalgal culture containing $10*10^6$ cells and the entire process was repeated until the extraction was complete. After centrifugation the supernatant was discharged and a spatula tip of quartz powder was added in the sample. The powder, through a micro pestle, allows the breaking of the cells and then the solubilization of pigments. The solvent used for pigments extraction was dimethyl sulfoxide (DMSO) (generally 500 µL for each extraction cycle). The pestle action was always realized with 100 µL of solvent. Subsequently the other 400 µL of DMSO were added and the sample was incubated at 60 °C for 15 min. After incubation, the sample was centrifuged at maximum speed for 10 minutes and the solvent containing the pigments was recovered. Then the color of cellular pellet was observed in order to evaluate if the extraction was complete. However, this evaluation does not allow to determine with certainty whether the extraction has been completed. After solvent addition it's important to work in the dark to avoid the degradation of extracted pigments. The quantification was performed spectrophotometrically by analyzing the spectrum from 350 to 750 nm (bandwidth 1 nm) and using quartz cuvettes. As this device works in the absorbance range of 0.1 - 1, the sample was diluted with DMSO when the upper limit is exceeded. The solvent was used as blank along the entire wavelength range. The software Vision 32 software allows to collect and save data in .txt files. Therefore pigment concentration is measured by applying the Lambert-Beer law:

$$A_\lambda = \varepsilon \cdot c \cdot l \quad (3.10)$$

where A_λ (dimensionless) is the sample absorbance at wavelength λ (nm), l is the path length (cm), ε is the extinction coefficient (mL cell^{-1} cm^{-1}) and c is the analyte concentration (cell mL^{-1}) .
The relation between A and the transmittance T (dimensionless), which is a measure of the fraction of light that passes through the sample, is:

$$A_\lambda = \log\frac{I}{I_0} = \log T \quad (3.11)$$

where I_0 is the intensity of light which strikes the sample and *I* is the intensity of light after passing through the sample.

The equation to determine concentrations of chlorophyll *a* (*Chl a*) and *b* (*Chl b*) as well as total caretenoids (*Carot*) in µg mL^{-1} in the solvent were taken from the work of Wellburn (1994):

$$Chl\ a = 12{,}19\ A_{665} - 3{,}45\ A_{649} \tag{3.12}$$

$$Chl\ b = 21{,}99\ \mathrm{A}_{649} - 5{,}32\ \mathrm{A}_{665} \tag{3.13}$$

$$Carot = (1000\ \mathrm{A}_{480} - 2{,}14 Chl\ a - 70{,}16 Chl\ b)/220 \tag{3.14}$$

Subsequently, taking into account the cell number of the culture sample it's possible to determine the pigment content in terms of pg $cell^{-1}$.

3.5 Error propagation

For sums, differences, products, and quotients, propagation of errors was calculated as follows (http://www.astro.unipd.it/ciroi/spfis1/sperI_cap9.pdf):

1. Sum and difference: when two quantities A and B are added (or subtracted), their determinate errors add (or subtract).

$$R = A + B;\quad \Delta R = \Delta A + \Delta B \tag{3.15}$$

$$R = A + B;\quad \Delta R = \Delta A + \Delta B \tag{3.16}$$

where ΔA and ΔB represent the errors in *A* and *B* respectively, while ΔR is the error in R;

2. Product or division: when two quantities *A* and *B* are multiplied or divided, their relative determinate errors add.

$$R = A \cdot B\ or\ \frac{A}{B};\ \frac{\Delta R}{R} = \frac{\Delta A}{A} + \frac{\Delta B}{B} \tag{3.17}$$

where $\Delta A/A$ and $\Delta B/B$ are the relative errors in *A* and *B* respectively, while *R* is the relative error in *R*;

Chapter 4

Continuous flow experiments

During the experimental activity several continuous-flow experiments were carried out in the flat plate PBR, described in section 3.2, at two constant intensities (150 and 650 μmol photons m^{-2} s^{-1}) and two seasonal irradiation regimes, representing the Winter and Summer in Padova. Light was provided by the LED lamp, described in section 3.3, both for continuous and alternated day-night cycles.

At least 5 dilution rates were studied for each light condition. Two panels were used for each experiment, working simultaneously at different residence times. After every step change of either conditions (residence time or irradiation mode) a transient was observed, whose duration depended on the condition. Steady state operation was confirmed by checking constant OD_{750}, cell concentration and biomass concentration for at least 3-5 days.

Moreover, for each steady state the N and P consumption was measured, in order to verify the hypothesis of non-limiting nutrients operating conditions.

4.1 Constant light intensity

In this section, results of continuous light irradiation are reported: two different light intensities were chosen, based on the work of Gris et al. (2014). 150 μmol photons m^{-2} s^{-1} is the optimum light for *S. obliquus* growth in batch runs, while 650 μmol photons m^{-2} s^{-1} is over the photosaturation limit. Accordingly, in this thesis, cell growth was studied both under limiting and saturating condition.

4.1.1 150 μmol photons m^{-2} s^{-}

In the first experiment, the PBRs were exposed to a constant illumination of 150 μmol photons m^{-2} s^{-1}, setting dilution rates in a range of 0.187 to 0.99 d^{-1} were used. At the beginning of each run, the systems were operated in a batch mode, in order to achieve higher cell concentrations from an initial diluted cultures. On the 6^{th} day, the peristaltic pump was turned on and the flow rates were set to 115.15 ml d^{-1} for the first panel and 62.08 ml d^{-1} for the second one, resulting in residence times of 2.17 d and 4.027 d, respectively. In both PBRs, after 10 days of transient operation, a steady state was eventually reached. Subsequently, other residence times were investigated by changing the peristaltic pump speed and,

consequently, the flow rates. In this case, the steady state conditions were achieved in few days, suggesting that cell have been acclimated to the light condition, and need less time to reach a constant concentration.

The data collected from both panels are shown in Figs. 4.1 and 4.2 in terms of cell concentration and, in Figs. 4.3 and 4.4, in terms of DW.

The biomass concentration profile was calculated by the experimental correlation between dry weight and cell concentration, obtained by correlating the daily cellular counts and the dry weights measured occasionally and always at steady state. This correlation line change for each experimental run, due to a different cell size at different light condition, as already reported by Gris *et al.*, (2014). Thus, the correlation was determined for each of them.

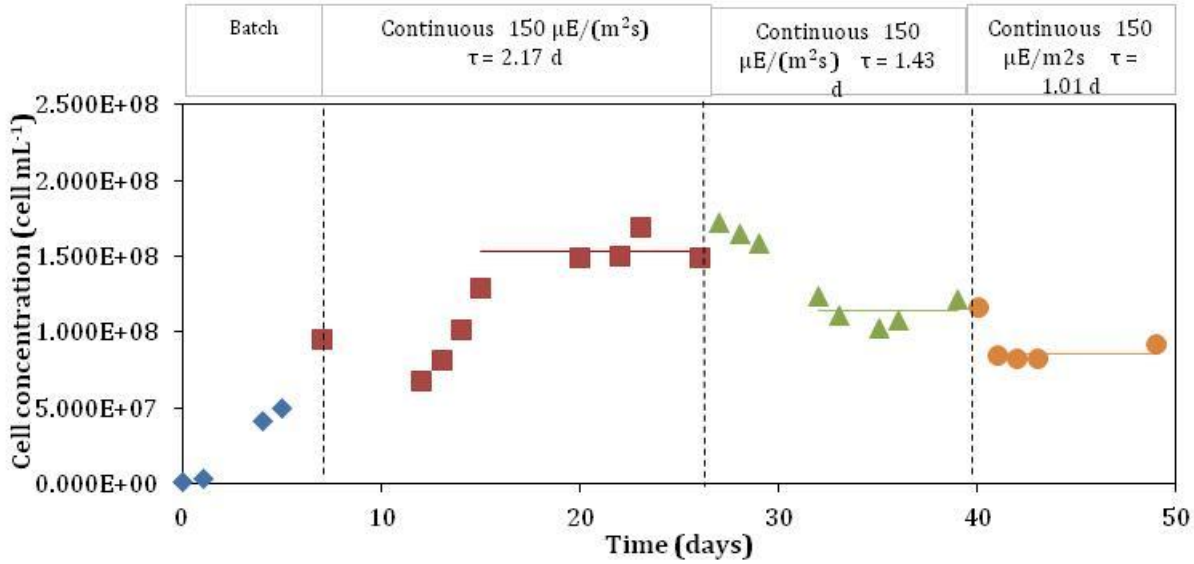

Figure 4.1 – Cell concentration of S. obliquus during the continuous experiment at constant light intensity of 150 µmol photons m^{-2} s^{-1}. Solid lines indicate the average value of stationary cell concentration for each residence time.

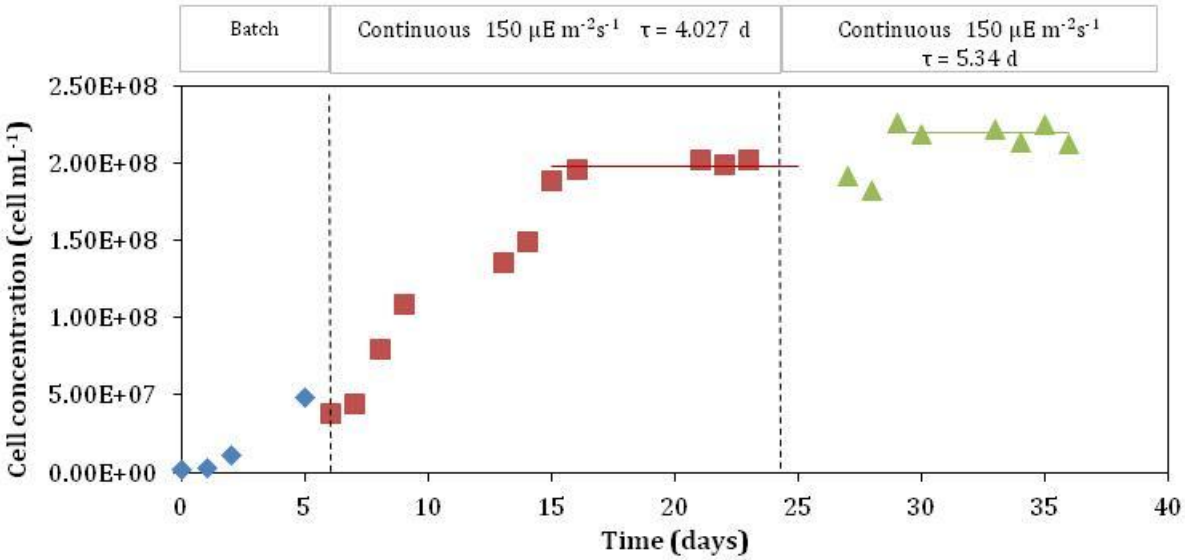

Figure 4.2 – ***Cell concentration of S. obliquus during the continuous experiment at constant light intensity of 150 µmol photons m^{-2} s^{-1}. Solid lines indicate the average value of stationary cell concentration for each residence time.***

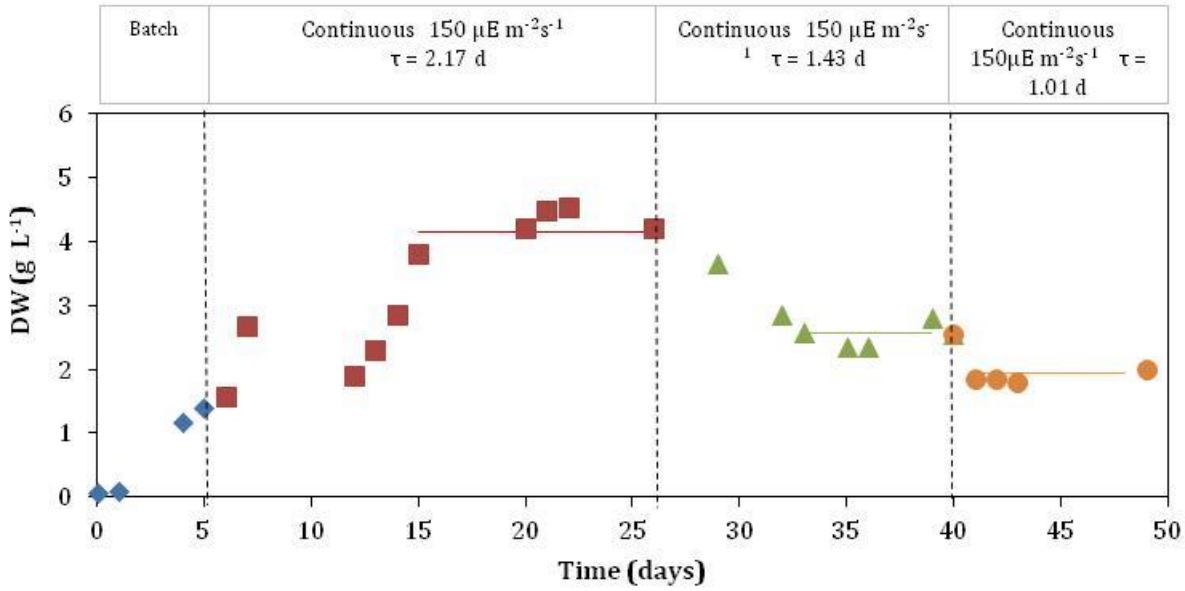

Figure 4.3 – ***DW of S. obliquus during the continuous experiment at constant light intensity of 150 µmol photons m^{-2} s^{-1}. Solid lines indicate the average value of stationary DW for each residence time.***

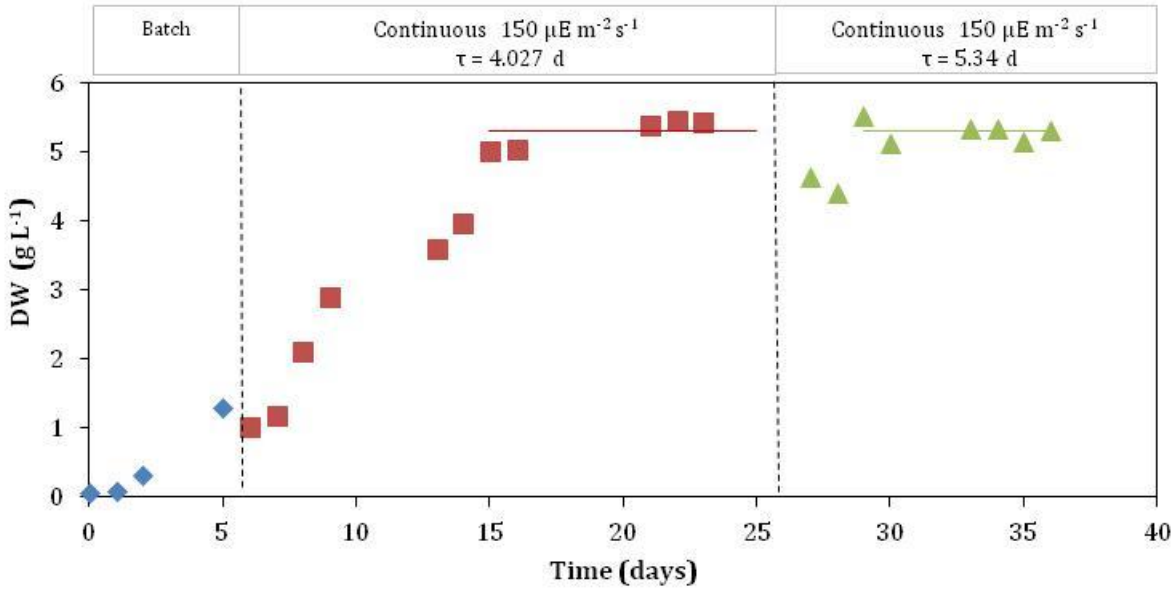

Figure 4.4 – ***DW of S. obliquus during the continuous experiment at constant light intensity of 150 µmol photons m^{-2} s^{-1}. Solid lines indicate the average value of stationary DW for each residence time.***

Operating variables and results for each residence time are summarized in Table 4.1.
The steady state values of DW and cell concentration were calculated as an average of daily measures at steady state operation. So the volumetric and areal productivity were calculated for each residence time, according to Eqs. (2.5) and (2.6).

Table 4.1 - ***Operating variables and results related to the continuous experiments at constant illumination of 150 µmol photons m^{-2} s^{-1}.***

Residence time (d)	**Specific growth rate** (d^{-1})	**Inlet flowrate** (ml d^{-1})	**Stationary biomass concentration** (g L^{-1})	**Stationary cell concentration** (*10^6 cell mL^{-1})	**Volumetric biomass productivity** (g L^{-1} d^{-1})	Areal biomass productivity (g m^{-2} d^{-1})
2.17	0.461	115.21	4.14 ± 0,29	153 ± 9.84	1.91 ± 0.14	22.93 ± 1.62
4.03	0.248	62.08	5.29 ± 0.22	198.28 ± 5.71	1.31 ± 0.05	15.79 ± 0.66
5.34	0.187	46.82	5.30 ± 0,15	220.38 ± 5.94	0.99 ± 0.03	11.93 ± 0,33
1.01	0.990	247.52	1.94 ± 0,03	86.12 ± 4.62	1.92 ± 0.03	23.09 ± 0.37
1.43	0.699	174.82	2.55 ± 0,21	113.8 ± 9.11	1.78 ± 0.03	21.43 ± 1,805

4.1.2 650 µmol photons m^{-2} s^{-1}

The second experiment was carried out under a constant saturating intensity of 650 µmol photons m^{-2} s^{-1}. Dilution rates in a range of 0.187 to 1.282 d^{-1} were investigated. Moreover. the second experiment started from the previous one. instead of interrupting operation and restarting from a batch mode. So only the value of light intensity was changed. A longer transient was observed. as a consequence of the need of the cells to acclimate to the new light condition. In the subsequent changes of residence times. only few days were needed to reach the new steady state concentration. confirming that cells were adapted to the saturating light.
The data collected for each residence time are shown in Figs. 4.5 and 4.6 in terms of cell concentration and 4.7 and 4.8 in terms of DW.

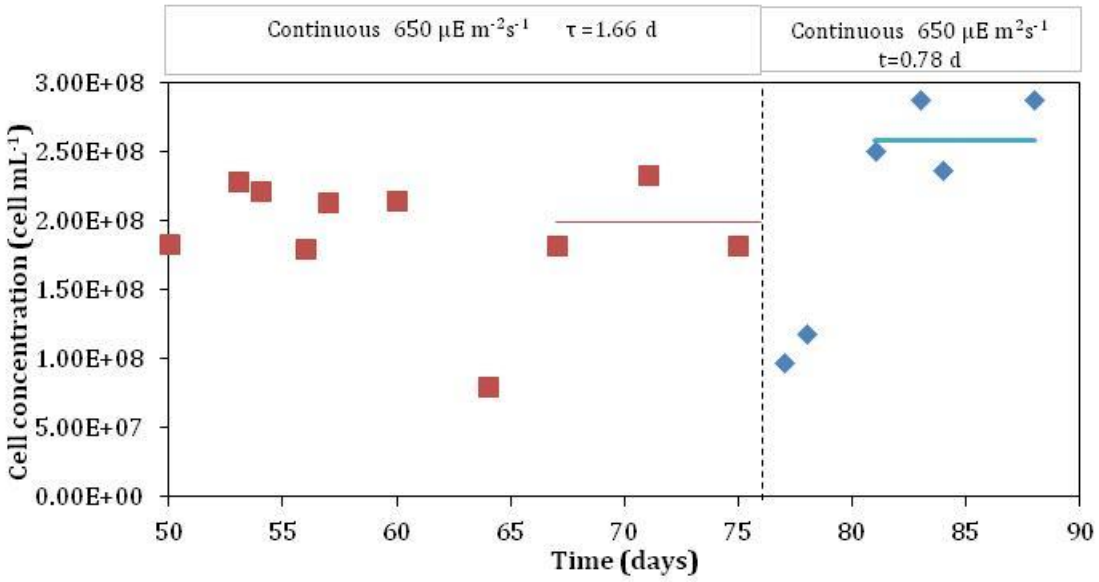

Figure 4.5 – ***Cell concentration of S. obliquus during the continuous experiment at constant light intensity of 650 µmol photons m^{-2} s^{-1}. Solid lines indicate the average value of stationary cell concentration for each residence time.***

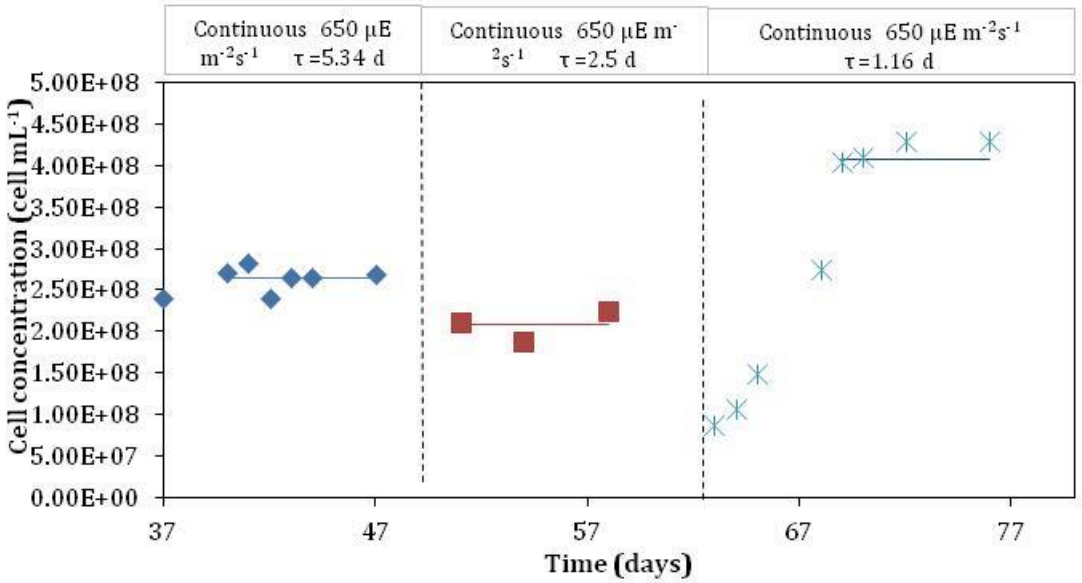

Figure 4.6 – ***Cell concentration of S. obliquus during the continuous experiment at constant light intensity of 650 µmol photons m^{-2} s^{-1}. Solid lines indicate the average value of stationary cell concentration for each residence time.***

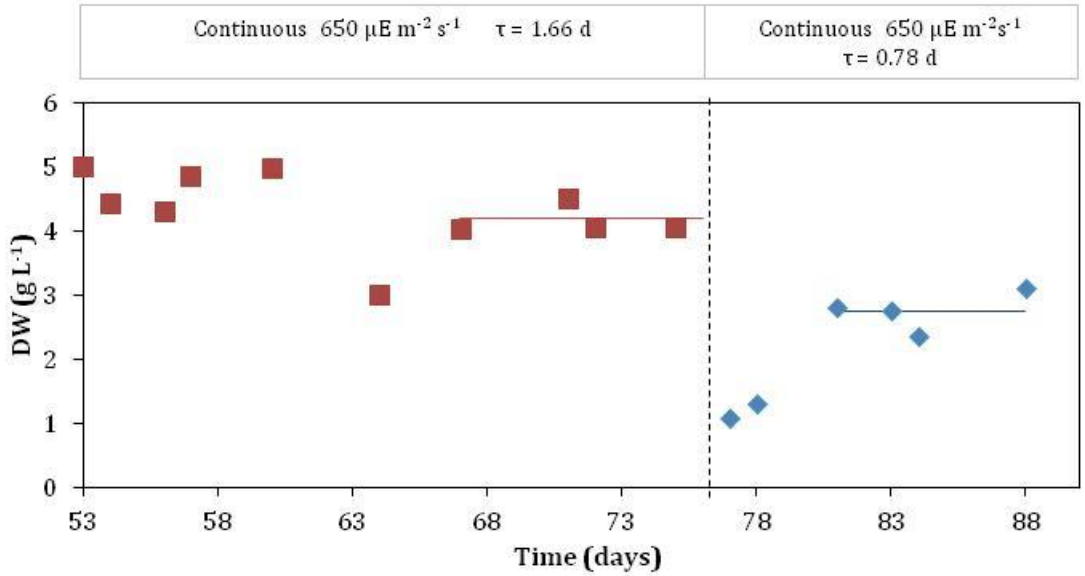

Figure 4.7 - ***DW of S. obliquus during the continuous experiment at constant light intensity of 650 µmol photons m^{-2} s^{-1}. Solid lines indicate the average value of stationary DW for each residence time.***

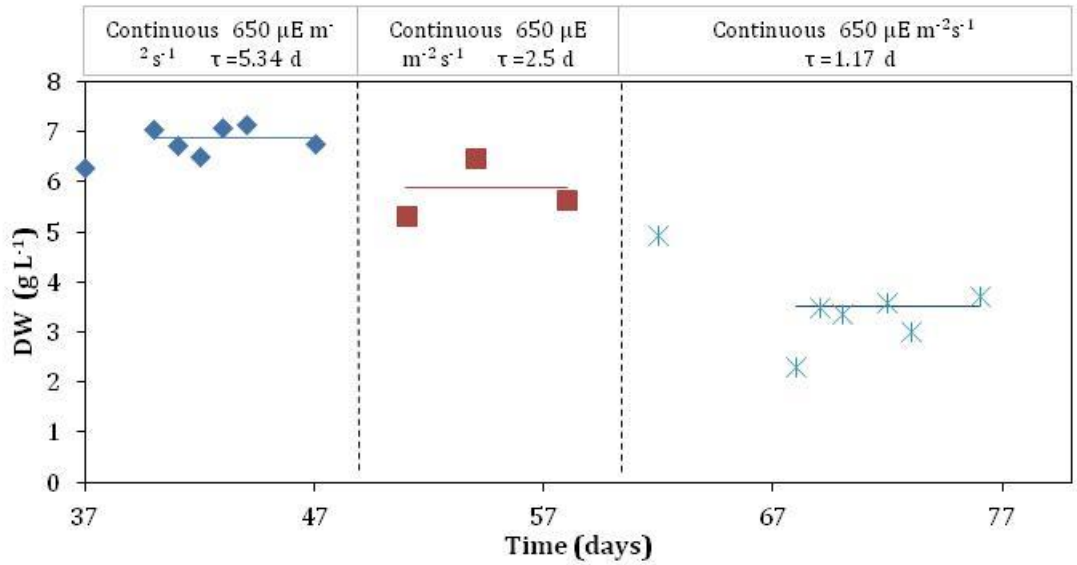

Figure 4.8 - ***DW of S. obliquus during the continuous experiment at constant light intensity of 650 µmol photons m^{-2} s^{-1}. Solid lines indicate the average value of stationary DW for each residence time***

Operating variables and results for each residence time are summarized in Table 4.2. Stationary values and volumetric and areal productivity were calculated similarly to the first experiment.

Table 4.2 - ***Operating variables and results related to the continuous experiments at constant illumination of 650 µmol photons m^{-2} s^{-1}.***

Residence time (d)	Specific growth rate (d^{-1})	Inlet flowrate (ml d^{-1})	Stationary biomass concentration (g L^{-1})	Stationary cell concentration (*10^6 cell mL^{-1})	Volumetric biomass productivity (g L^{-1} d^{-1})	Areal biomass productivity (g d^{-1} m^{-2})
5.34	0.187	46.82	6.88 ± 0.25	265.21 ± 14.01	1.29 ± 0.05	15.49 ± 0.57
1.66	0.602	150.60	4.25 ± 0.22	199 ± 29.44	2.56 ± 0.13	30.77 ± 1.62
2.5	0.400	100	5.90 ± 0.66	207.90 ± 18.37	2.36 ± 0.26	28.36 ± 3.16
0.78	1.282	320.51	2.75 ± 0.3	258 ± 26.60	3.53± 0.38	42.45 ± 4.62
1.17	0.857	214.22	3.53 ± 0.27	407.83 ± 4.01	3.02 ± 0.23	36.32 ± 2.81

4.2 Day/Night light conditions

In this section, results related to the two seasonal irradiation regimes are reported. Day/night light conditions were tested in order to investigate *S.obliquus* behavior in a more realistic environment. Reactor samples were always collected at 9 am with respect to the simulated day/night cycle.

4.2.1 Summer: July

In this third experiment the PBRs were exposed to an irradiation regime typical of the Summer season in Padova, as explained in section 3.3. Dilution rates were set between of 0.197 and 1.563 d^{-1} .

For the lowest residence time (τ = 0.78 d) the experiment started from the steady-state of the previous one, so there was no initial batch phase (Figs 4.9 and 4.10). Afterwards, it was always necessary to restart from a batch mode, at a constant light intensity of 150 μmol photons m^{-2} s^{-1} because of the excessive reactor fouling. The data collected for the other residence times are shown in Figs. 4.11 and 4.12, in terms of cell concentration, and 4.13 and 4.14 in terms of DW.

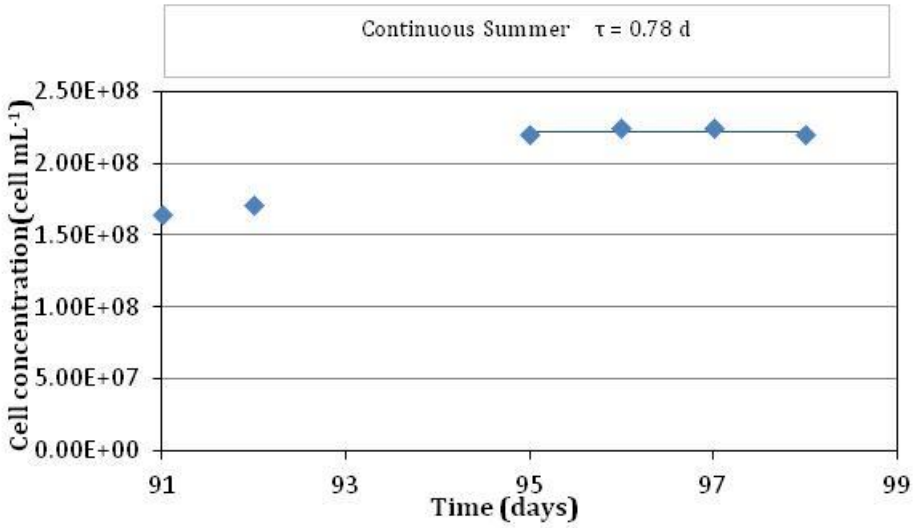

Figure 4.9 - ***Cell concentration of S. obliquus during the continuous experiment and under the Summer irradiation regime. Solid line indicate the average value of stationary cell concentration for τ = 0.78 d.***

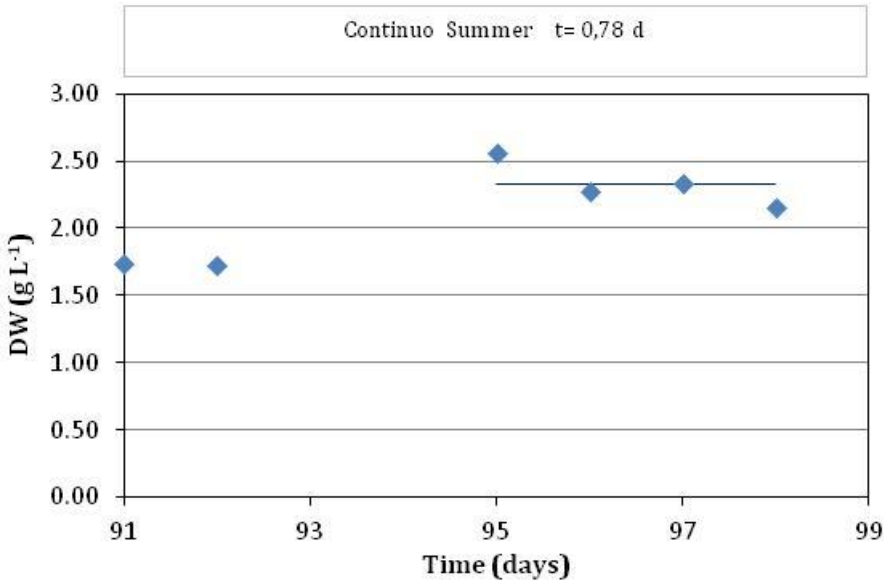

Figure 4.10 - *DW of S. obliquus during the continuous experiment and under the Summer irradiation regime. Solid line indicate the average value of stationary DW for τ = 0.78 d*

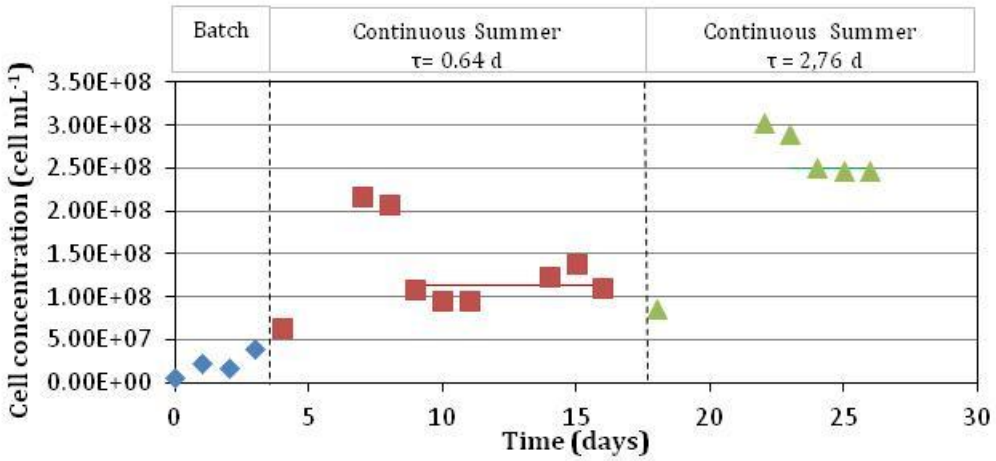

Figure 4.11 - *Cell concentration of S.obliquus during the continuous experiment and under the Summer irradiation regime. Solid lines indicate the average value of stationary cell concentration for each residence time.*

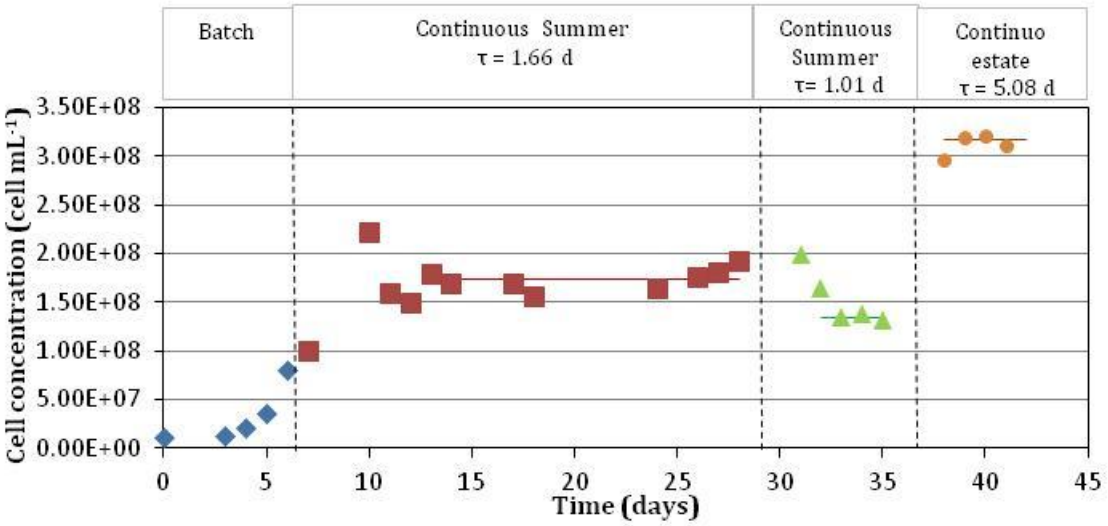

Figure 4.12 - ***Cell concentration of S.obliquus during the continuous experiment and under the Summer irradiation regime. Solid lines indicate the average value of stationary cell concentration for each residence time.***

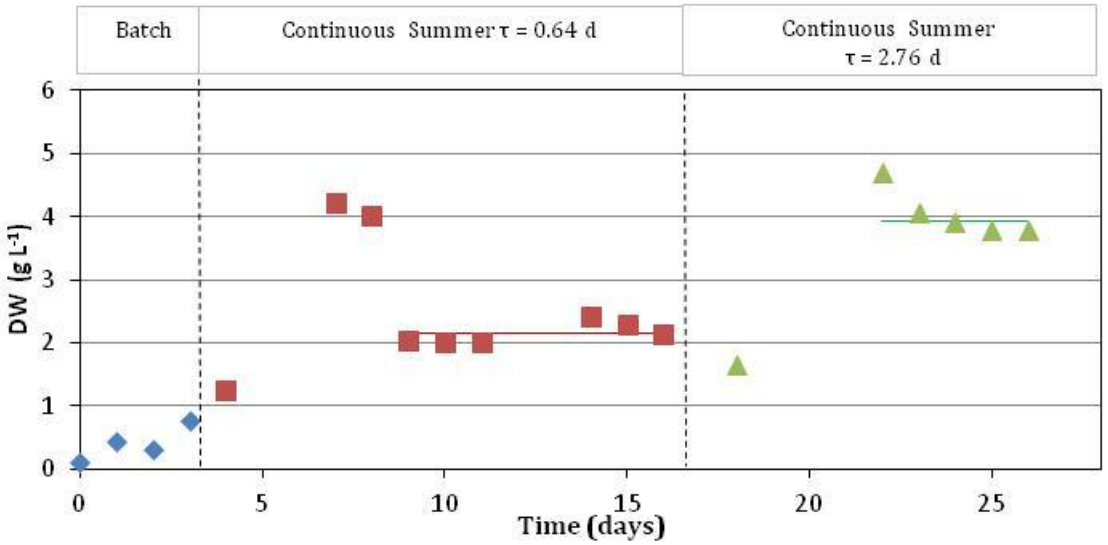

Figure 4.13 - ***DW of S.obliquus during the continuous experiment and under the Summer irradiation regime. Solid lines indicate the average value of stationary DW for each residence time.***

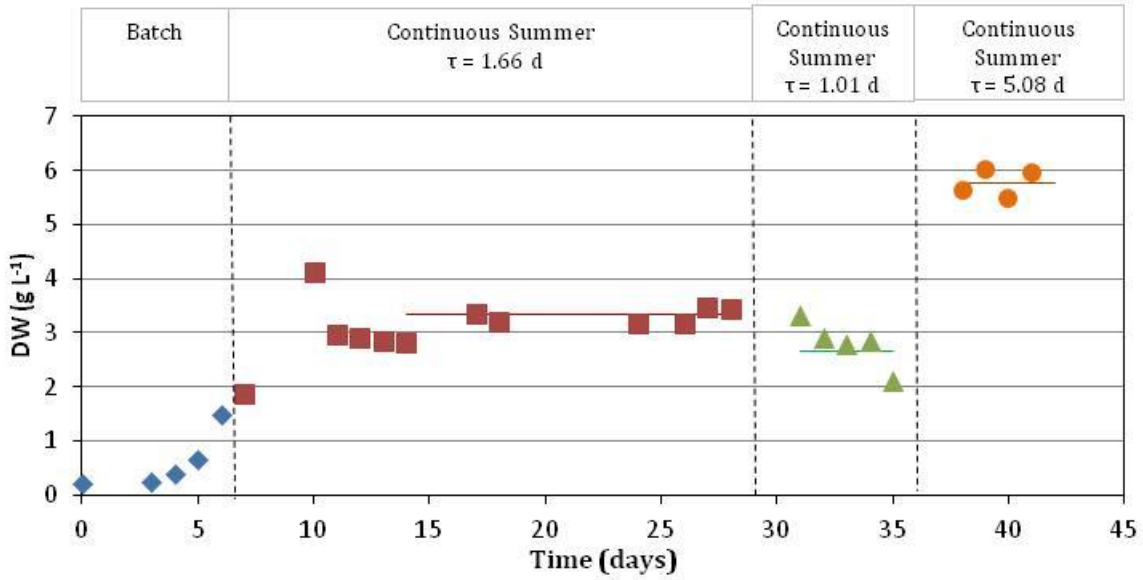

Figure 4.14 - ***DW of S. obliquus during the continuous experiment and under the Summer irradiation regime. Solid lines indicate the average value of stationary DW for each residence time.***

Operating variables and results for each residence time are summarized in Table 4.3. Steady state values and volumetric and areal productivity were calculated similarly to the previous experiments.

Table 4.3 - ***Operating variables and results related to the continuous experiments under the Summer irradiation regime.***

Residence time (d)	Specific growth rate (d^{-1})	Inlet flowrate (ml d^{-1})	Stationary biomass concentration (g L^{-1})	Stationary cell concentration (*10^6 cell mL^{-1})	Volumetric biomass productivity (g L^{-1} d^{-1})	Areal biomass productivity (g d^{-1} m^{-2})
0.779	1.282	320.51	2.33 ± 2.05E-01	221.60 ± 2.68	2.99 ± 0.26	35.90 ± 3.16
2.76	0.362	90.58	3.99 ± 9.89E-02	249.50 ± 2.12	1.45 ± 0.04	17.38 ± 0.44
0.639	1.563	390.63	2.15 ± 0.19	112.53 ± 19.02	3.36 ± 0.31	40.38 ± 3.76
1.66	0.602	150.60	3.34 ± 0.14	173.55 ± 16.57	2.05 ± 0.08	24.62 ± 1.01
1.01	0.990	247.52	2.67 ± 4.05E-01	134.33 ± 3.51	2.64 ± 0.40	31.77 ± 4.76
5.08	0.197	49.19	5.77 ± 0.26	317.27 ± 5.52	1.14 ± 0.05	13.66 ± 0.61

4.2.2 Winter: January

In the fourth experiment the PBRs were exposed to an irradiation regime typical of the Winter season in Padova, as explained in section 3.3. Dilution rates in the range between of 0.197 to 1.283 d^{-1} were set. The experiments started from the steady-state of the previous ones, so there was no a batch phase for both panels. Cell concentration and DW profiles for each residence time are shown in Figs. 4.15. 4.16. 4.17. 4.18. It can be observed that at residence time of 0.78 d washout occurred.

In the fourth experiment the PBRs were exposed to an irradiation regime typical of the Winter season in Padova, as explained in section 3.3 . Dilution rates in the range between of 0.197 to 1.283 d^{-1} were set. The experiments started from the steady-state of the previous ones, so there was no a batch phase for both panels. Cell concentration and DW profiles for each residence time are shown in Figs. 4.15. 4.16. 4.17. 4.18. It can be observed that at residence time of 0.78 d washout occurred.

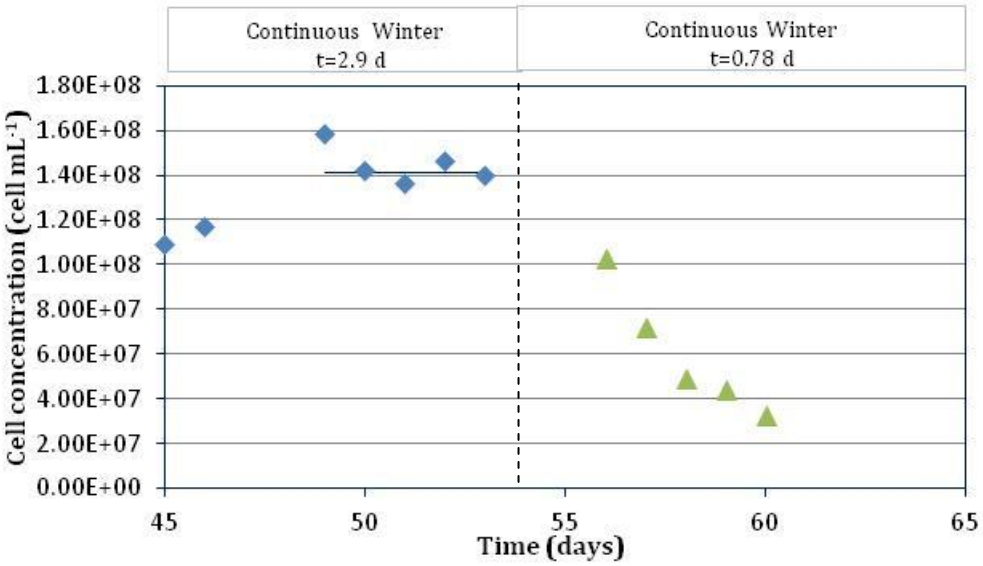

Figure 4.15 – Cell *concentration of S. obliquus during the continuous experiment under the Winter irradiation regime. Solid line indicate the average value of stationary cell concentration for τ = 2.9 d.*

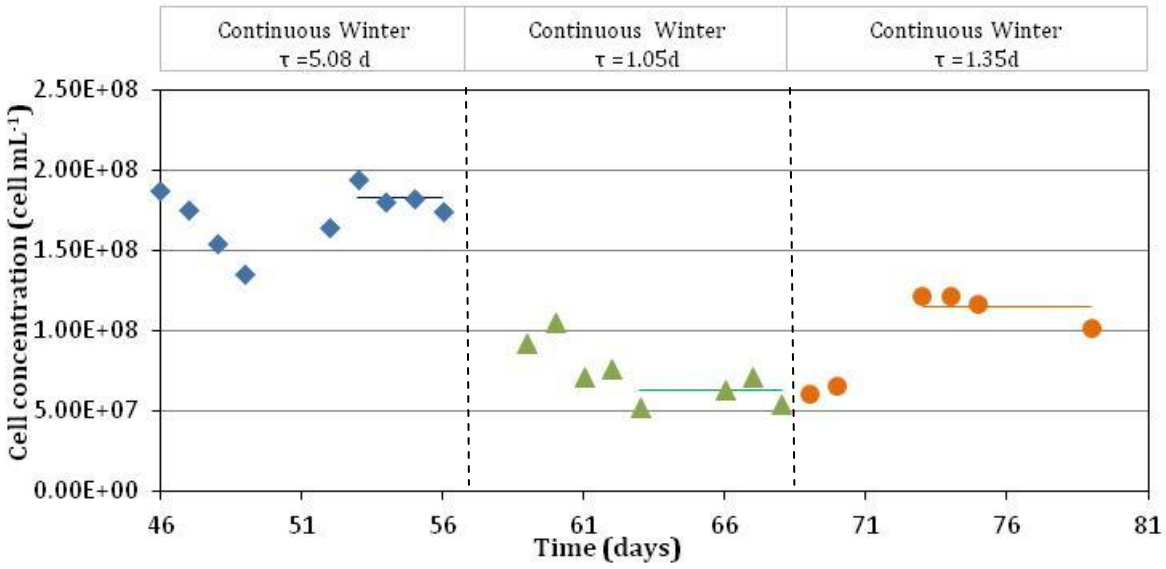

Figure 4.16 – ***Cell concentration of S. obliquus during the continuous experiment under the Winter irradiation regime. Solid line indicate the average value of stationary cell concentration for each residence time.***

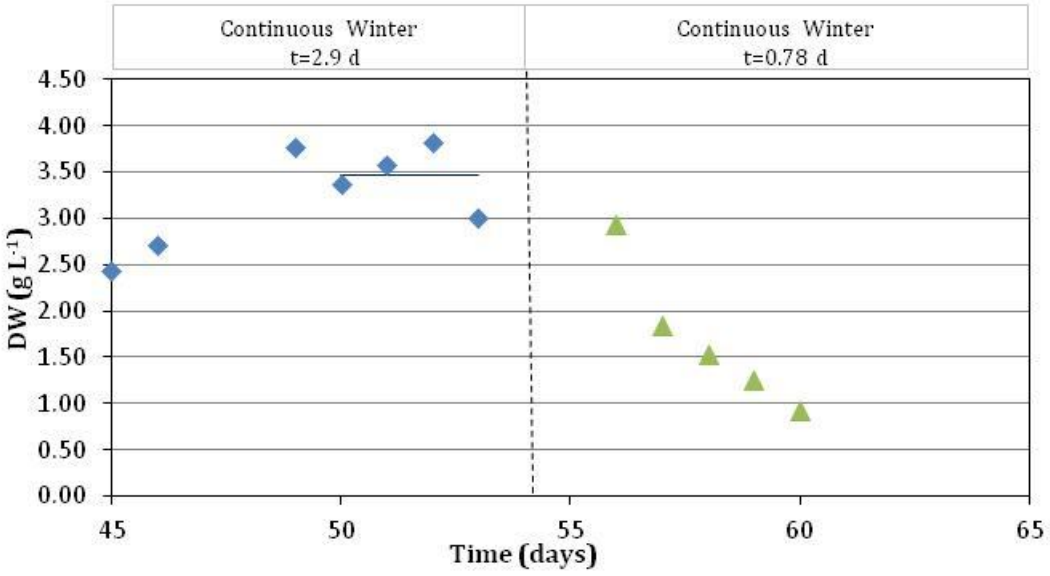

Figure 4.17 - ***DW of S.obliquus during the continuous experiment under the Winter irradiation regime. Solid line indicate the average value of stationary DW for τ = 2.9 d.***

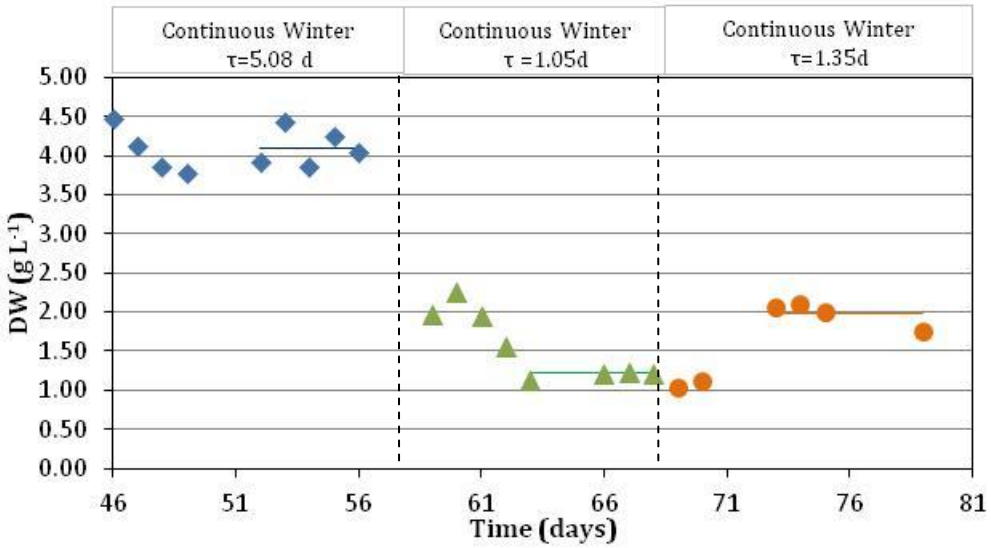

Figure 4.18 - ***DW of S. obliquus during the continuous experiment under the Winter irradiation regime. Solid line indicate the average value of stationary DW for each residence time.***

Operating variables and results for each residence time are summarized in Table 4.4. Steady state values and volumetric and areal productivity were calculated similarly to the previous experiments.

Table 4.4 - ***Operating variables and results related to the continuous experiments under the Winter irradiation regime.***

Residence time (days)	Specific growth rate (d^{-1})	Inlet flowrate (ml d^{-1})	Stationary biomass concentration (g L^{-1})	Stationary cell concentration (*10^6 cell mL^{-1})	Volumetric biomass productivity (g L^{-1} d^{-1})	Areal biomass productivity (g d^{-1} m^{-2})
5.08	0.197	49.21	4.1 ± 0.24	182.80 ± 8.70	0.81 ± 0.05	9.70 ± 0.57
2.89	0.345	132.76	3.47 ± 0.42	141.16 ± 5.03	1.20 ± 0.14	22.15 ± 2.68
1.05	0.952	238.10	1.25 ± 0.02	62.67 ± 8.50	1.19 ± 0.02	14.31 ± 0,23
1.35	0.741	185.19	1.97 ± 0.03	114.79 ± 9.38	1.46 ± 0.02	17.54 ± 0.27

4.3 Results and discussion

Continuous flow experiments with a vertical flat panel PBR were performed both at constant illumination (150 μmol photons m^{-2} s^{-1} and 650 μmol photons m^{-2} s^{-1}) and under simulated day/night cycles (Summer and Winter irradiation regime). At least 5 dilution rates were set for each light condition. So the influence of light intensity on the growth of *S.obliquus* was analyzed at different rates of dilution, under limited as well as saturating intensities of illumination. For each steady state it was found that nutrients (N and P) were not limiting. Stationary data were elaborated in order to study the effect of different light conditions on microalgae growth, photosynthetic efficiency, lipid and pigment content and nutrient uptake. Data related to the residence time $\tau = 1.76$ were taken from a previous work (Bertucco *et al*., 2014). The obtained results are presented and discussed in this section.

4.3.1 Biomass concentration

The steady state biomass concentrations under the four different illumination conditions as a function of residence time are represented in Fig. 4.19. The general trend showed a biomass concentration increase with the residence time. as already reported by Martinez *et al.* (1999) for *S. obliquus*, Barbosa *et al*. (2005), Zijffers *et al.* (2010) and Tercero *et al.* (2013) for other species.

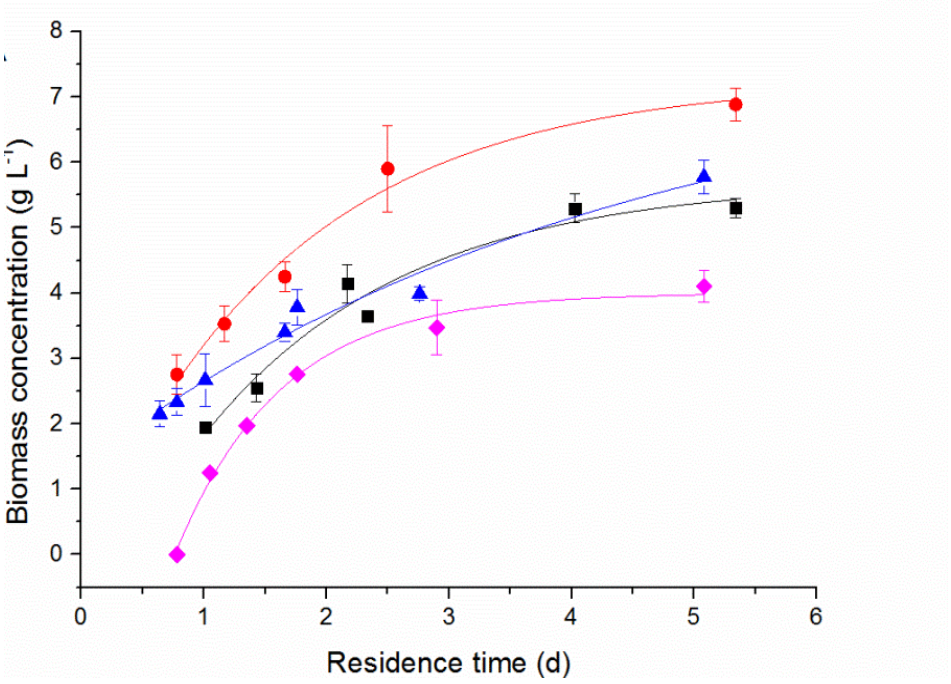

Figure 4.19 - ***Data of biomass concentration against residence time at different light conditions (square for 150 µmol photons m^{-2} s^{-1}, circles for 650 µmol photons m^{-2} s^{-1}, triangles for Summer and rhombus for Winter). Solid lines are eye guides only.***

The slope of the curve decreases at higher residence times, as a result of the self-shading effect, which becomes relevant even if the depth of the reactor is small. The highest biomass concentration was found under 650 µmol photons m^{-2} s^{-1} of continuous irradiation, while generally the day-night regime corresponded to lower concentration, obviously due to the biomass removal from the reactor during the night. A similar effect of light irradiation was observed on biomass productivity (Fig. 4.13), which was higher for higher constant irradiations and decreased under day-night conditions.

4.3.2 Biomass productivity

The results obtained in this work suggest that biomass productivity is inversely related to the residence time, except in the case of Winter season (Fig. 4.20).

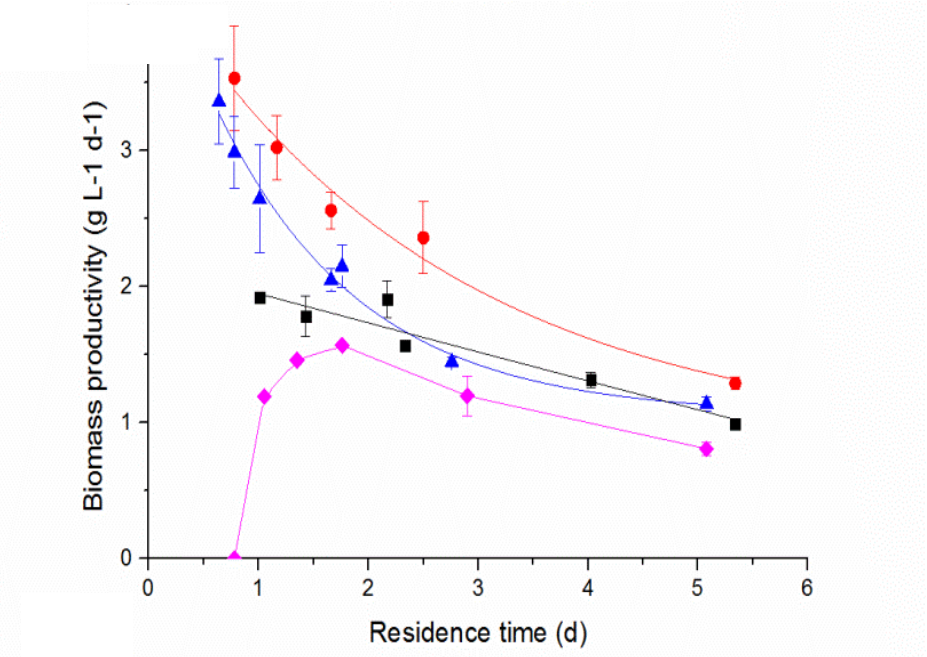

Figure 4.20 - ***Data of biomass productivity against residence time at different light conditions (square for 150 µmol photons m^{-2} s^{-1}, circles for 650 µmol photons m^{-2} s^{-1}, triangles for Summer and rhombus for Winter). Solid lines are eye guides only.***

The decrease with residence time, in the case of 150, 650 µmol photons m^{-2} s^{-1} and Summer, can be explained by looking at the Fig. 4.21, where data of energy conversion for each experiment are reported. For all these conditions, a decrease of efficiency can be observed with the increase of residence time, suggesting that, when biomass concentration increased, the actual light available for cell growth diminished as a result of self-shading effect.

A different trend in biomass productivity was observed in the case of the Winter season, where a maximum was found, as already reported by Martinez *et al.* (1999) and Ruiz *et al.* (2013), that reported a decreased productivity at residence times lower than a threshold value which is species dependent. This is probably due to the values of residence time that are closer to the wash out condition.

In our experiments we observed a maximum at 1.35 d under Winter condition only, because at residence time of 0.78 d the washout occurred. In this case, it is interesting to apply the washout model to estimate the maximum specific growth rate (Molin, 1983) which can be calculated between 0.952 and 1.2 d^{-1} as result of the inverse of residence times 1.05 and 0.78 d, according to Eq. 2.3.

Ruiz *et al.* (2013) proposed a model, based on the work of Verhulst, for the determination of the maximum productivity θ_P, which gives:

$$\theta_P = 2\,\mu_{max}^{-1} \qquad (4.1)$$

In our experiments, by considering a maximum specific growth rate for Winter season between 0.952 and 1.2 d^{-1}, a maximum of productivity of 1.6-2.10 d is calculated by applying the eq. 4.1, which is consistent to the data reported in Fig. 4.20.
In the other cases of irradiation considered, no maximum in productivity was observed. Thus it is possible to only state that the maximum specific growth rate is higher than Winter season, according to the availability of light and its effect on growth rate.

4.3.3 Energy conversion

The calculated photosynthetic efficiencies, from Eq. 3.5, for the experiments performed are depicted in Fig 4.21. The theoretical limit is represented by the horizontal dashed line. A high energy conversion efficiency in both Winter regime and constant irradiation of 150 µmol m^{-2} s^{-1} was observed, especially with the lower residence times which are close to the maximum theoretical photosynthetic efficiency. On the other hand, under Summer irradiation regime and constant irradiation 650 µmol m^{-2} s^{-1}, cultures resulted strongly photo-inhibited with reduced photoconversion efficiencies.

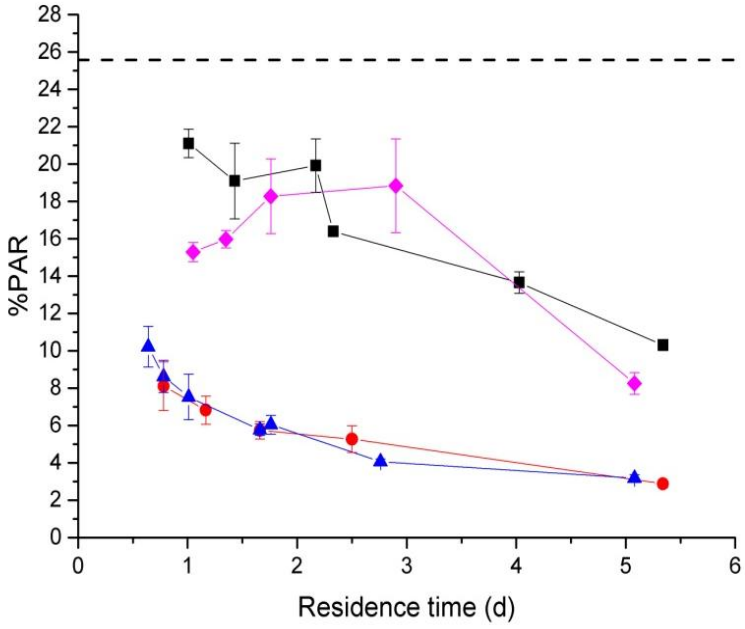

Figure 4.21 - ***Data of photo-conversion (%PAR) against residence time at different light conditions (square for 150 µmol photons m^{-2} s^{-1}, circles for 650 µmol photons m^{-2} s^{-1}, triangles for Summer and rhombus for Winter). Solid lines are eye guides only.***

4.3.4 Nutrient yields

As stated previously, the N and P concentrations were measured during each stationary phase in order to ascertain the hypothesis of non limiting nutrient conditions. By plotting the nutrient/biomass yield, calculated according to Eq. 3.6, as function of the residence time, a similar trend was observed for both N and P (Fig. 4.22 A and B).

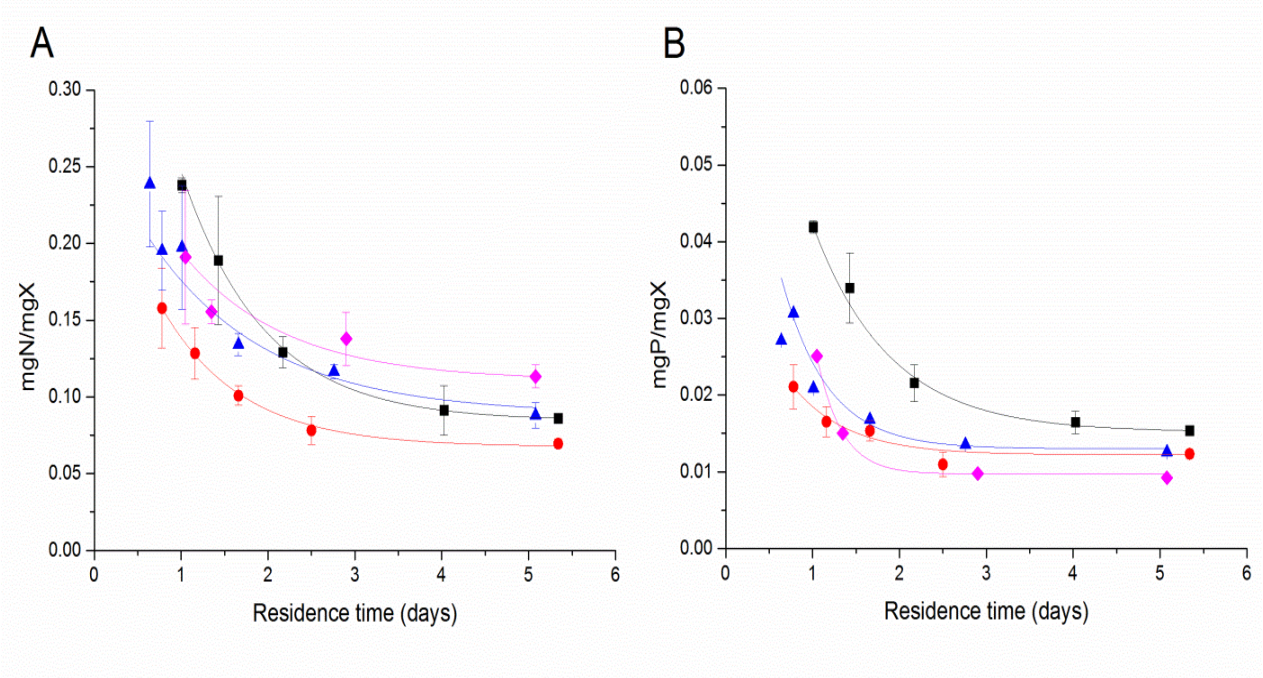

Figure 4.22 – ***Nitrogen (A) and phosphorous (B) / biomass yields as a function of residence time at different irradiations (square for 150 µmol photons m^{-2} s^{-1}, circles for 650 µmol photons m^{-2} s^{-1}, triangles for Summer and rhombus for Winter).***

The nutrient consumption under day-night cycle can be described as quite complex, because a part of the nutrients is removed from reactor at night while some accumulation occurs within microalgal cells under dark, that can then be exploited under light period. Therefore, only data under continuous irradiation were considered (Fig. 4.23 A and B).

Martinez *et al.*, (1999) observed for *S.obliquus* an increased P ratio on biomass at higher growth rates, suggesting an higher internal P content as a result of increasing cellular nucleic acids and compounds of high energy content under high-growth-rate conditions. This is in agreement with our data reported in Fig. 4.23 B. where a linear correlation was highlighted between $Y_{P/X}$ and μ. The same trend was found also in the case of $Y_{N/X}$ (Fig. 4.23 A). suggesting that there is an accumulation of N at higher growth rates. This is in agreement with data reported by Quigg & Beardall (2003). In fact. for *D. tertiolecta* they found an increase of protein turnover and pool at higher growth rates, which is associated to the raise of respiration rate and maintenance requirement.

More complex is the effect of high light on nutrient/biomass yields, which were found generally lower for both N and P. Even if there is not a deep knowledge of the relation between light and nutrient uptake, some authors suggest that light inhibition can affect the elemental composition of microalgae. For example Quigg & Beardall (2003) reported a relation between the reduction of cellular N quote (in terms of pg cell^{-1}) with the increase of photon flux.

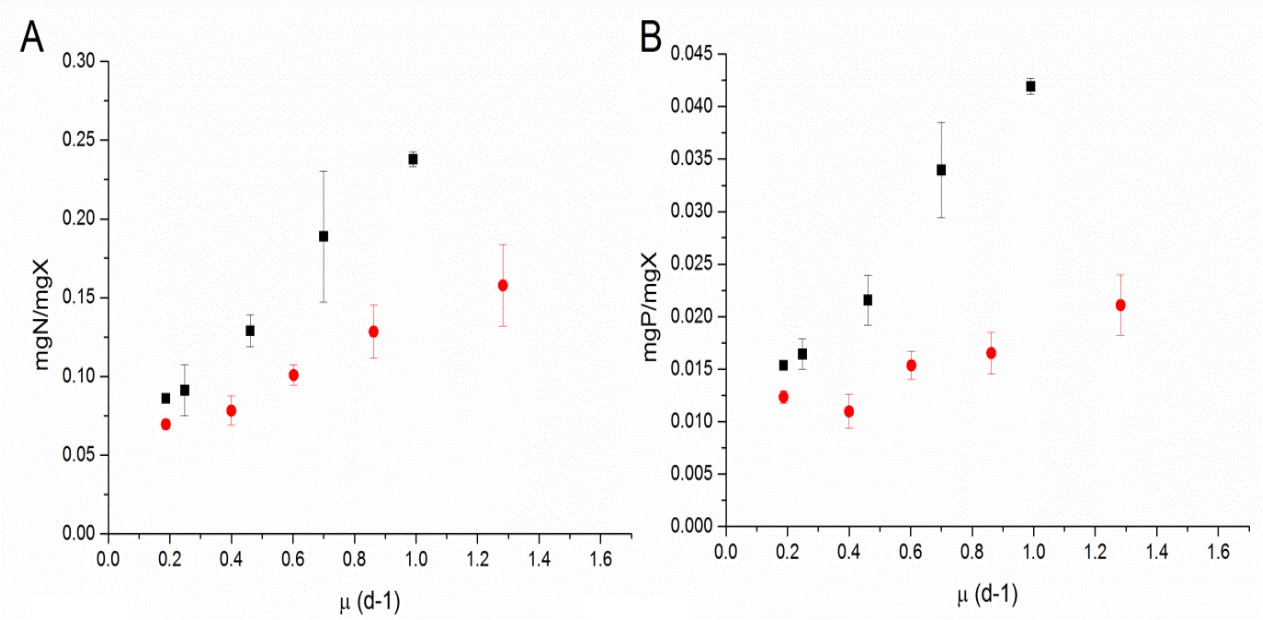

Fig. 4.23 – ***Nitrogen (A) and phosphorous (B) / biomass yields as function μ at different irradiations (square for 150 μmol photons m^{-2} s^{-1}, circles for 650 μmol photons m^{-2} s^{-1}).***

4.3.5 Average cell density

A different cell size was observed at the optical microscope, suggesting that it is affected by residence time and light. Accordingly, the average cell density was calculated and the data were plotted as a function of growth rate (Fig. 4.24). Results suggest that the average cell density, calculated by using Eq. 3.4. decreases at higher growth rates, corresponding to lower biomass concentrations. This is probably due to a faster cellular division under high-growth rates conditions.

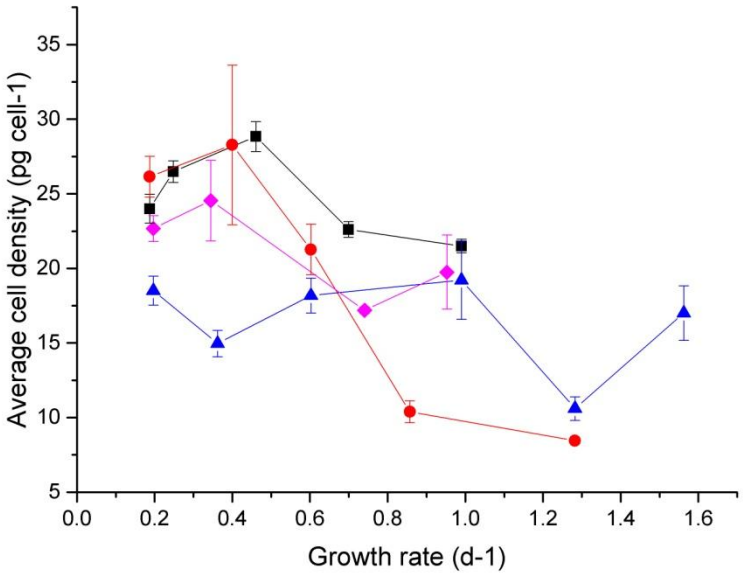

Figure 4.24 - ***Data of the average cell density against growth rate at different light conditions (square for 150 µmol photons m^{-2} s^{-1}, circles for 650 µmol photons m^{-2} s^{-1}, triangles for Summer and rhombus for Winter). Solid lines are eye guides only.***

4.3.5 Lipids

Fig. 4.25 shows that the lipid percentage in biomass. calculated by using Eq. 3.9, decreases at increasing growth rates. Martinez *et al*. (1999) reported higher content of P in the biomass at higher dilution rates, as a result of increasing cellular nucleic acids and compounds of high energy content in these conditions. On the other hand, Quigg & Beardall (2003) found an increase of protein turnover and pool at higher growth rates, which is associated to higher maintenance metabolic costs. These results suggest that high-growth-rates conditions can result in a lower lipid fraction in the cells.

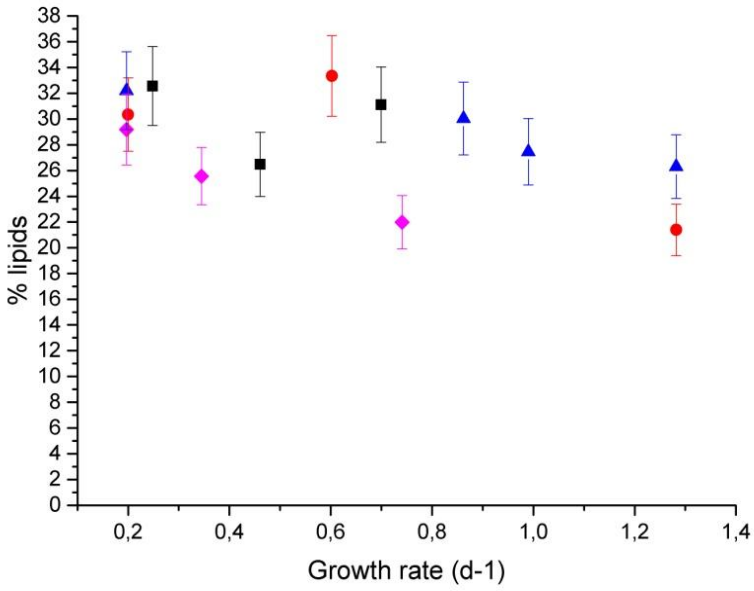

Figure 4.25 - Data of lipids percentage in biomass against growth rate at different light conditions (square for 150 µmol photons m^{-2} s^{-1}, circles for 650 µmol photons m^{-2} s^{-1}, triangles for Summer and rhombus for Winter).

4.3.6 Pigments

Data represented in Fig. 4.26 (A) show that the pigment content, expressed as the sum of *Chl a* and *Chl b* and calculated as described in section 3.4.4, decreased at increasing growth rates. This effect can be explained by the fact that the amount of light per cell increases at decreasing residence times, because the culture becomes more diluted, as also found by Kliphuis *et al*. (2012). It can be observed that the pigment content was higher at lower irradiances. suggesting that in these conditions photoinhibition occurs. In fact in high light conditions, *S.obliquus*, similar to other photosynthetic organisms, shows an acclimation response by decreasing the chlorophyll content to reduce light-harvesting ability and accumulating carotenoids which have an antioxidant activity (Gris *et al.*, 2014). Fig 4.26 (B) shows the results obtained in the work of Gris *et al.* (2014), where the effect of different light intensities on *S.obliquus* growth and biochemical composition were investigated in batch reactors. Also in this case a decrease of chlorophyll concentration at higher light intensity was observed.

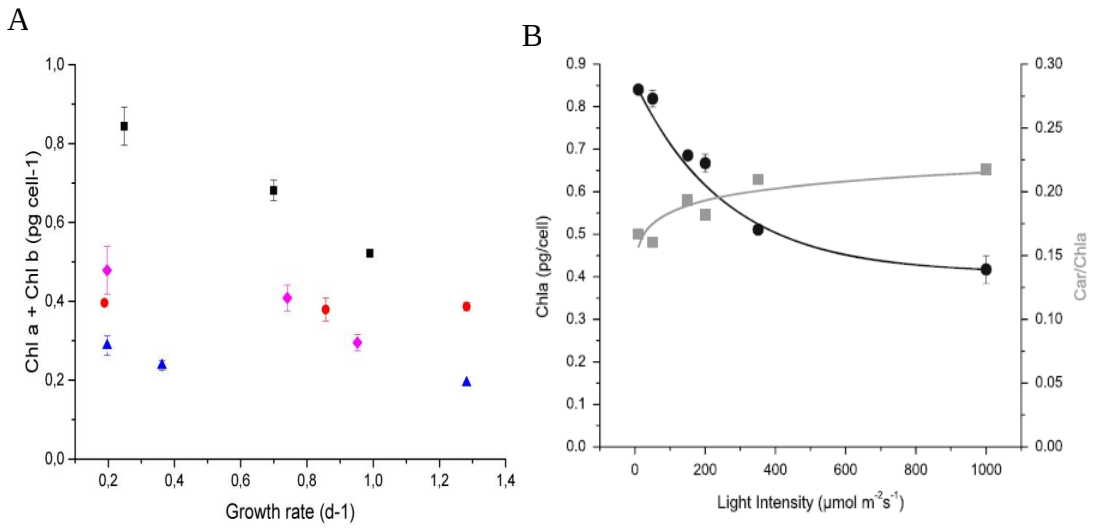

Figure 4.26 – (A) Data of lipids content, expressed as the sum of Chl a and Chl b, against residence time at different light conditions (square for 150 µmol photons m^{-2} s^{-1}, circles for 650 µmol photons m^{-2} s^{-1}, triangles for Summer and rhombus for Winter); (B) Chl a content (circles) and carotenoids/Chl ratio (squares) at various light intensities (Gris et al., 2014).

CHAPTER 5

Interpreting results by physical models

5.1 Effect of light intensity on maintenance

Data of steady state under different irradiations were elaborated to calculate the maintenance energy requirement for *S. obliquus* growth, following the approach of Gons & Mur (1980) and Kliphuis *et al*. (2012), as described previously in sections 2.4.1 and 2.4.2.

5.1.1 Gons and Mur model

In this section results related to the application of Gons and Mur model (Eq. 2.16) to our experimental data are represented in Fig.5.1. Two different series can be observed, corresponding to low (150 µmol photons m^{-2} s^{-1} and Winter regime) on the one side and high irradiances (650 µmol photons m^{-2} s^{-1} and Summer regime) on the other hand.

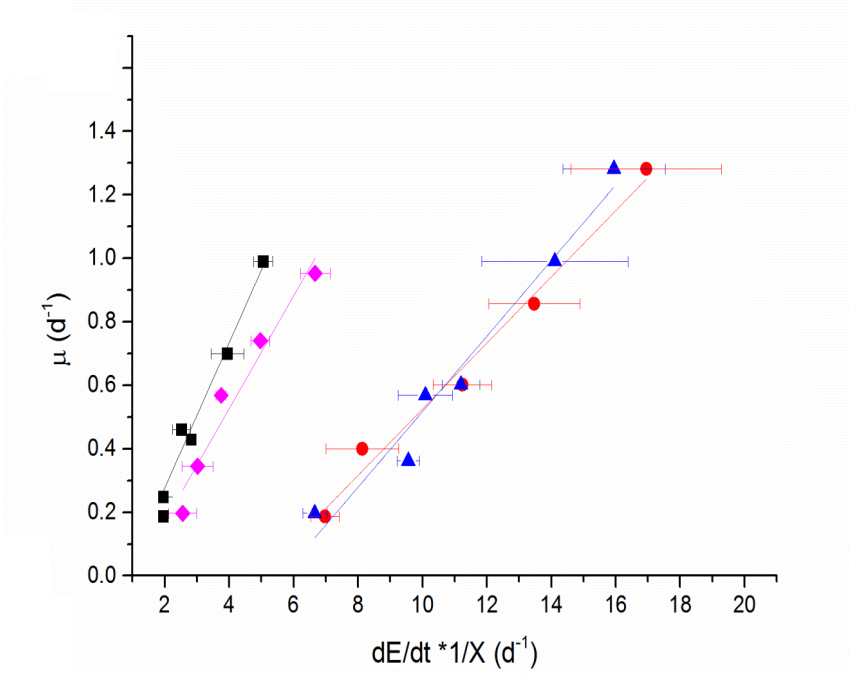

Figure 5.1- ***Linearization of specific growth rate as function of specific light uptake rate, according to Eq. 2.16 (Gons and Mur approach), at different light conditions (square for 150 µmol photons m^{-2} s^{-1}, circles for 650 µmol photons m^{-2} s^{-1}, triangles for Summer and rhombus for Winter).***

By the linearization of μ as a function of $dE/dt \cdot 1/X$, the values of μ_e and c were obtained for the four different illumination conditions. μ_e is the negative intercept on Y-axis and c is the slope of the straight line. Their values are summarized in Table 5.1.

Table 5.1 – ***Parameters of linearization of data reported in Fig.5.1, according to Eq. 2.16.***

Light regime (µmol photons m^{-2} s^{-1})	c (-)	μ_e (d^{-1})	R^2
150	0.231	0.181	0.98
650	0.178	0.185	0.99
Winter (149.08)	0.119	0.517	0.95
Summer (548.69)	0.104	0.673	0.97

These results suggest that the maintenance requirement strongly depends on the light intensity hitting the panel. In the case of 150 µmol photons m^{-2} s^{-1} and Winter regime, a close relationship was observed producing similar values of the maintenance term (around 0.18 d^{-1}). This result is comparable to that achieved by Gons & Mur (1980) for light-limited cultures (Table 2.1). On the other hand, the value of c obtained by Gons and Mur was in the range of 0.11-0.13, while we obtained values of 0.231 for the continuous intensity 150 µmol photons m^{-2} s^{-1} and 0.119 for Winter regime, suggesting that our experimental system allowed a more efficient conversion of light in biomass, as a result of the thin depth of the reactor, leading to a better exploitation of light.

On the opposite, under higher irradiances, i.e. 650 µmol photons m^{-2} s^{-1} and Summer regime, the maintenance term was much higher, resulting in values of 0.517 d^{-1} and 0.673 d^{-1} respectively. Therefore, it suggests that in these conditions photosaturation and photoinhibition occured and the energy diverted from growth to cell repair is higher than under non saturating irradiances. Accordingly, lower c values were calculated, ranging from 0.178 to 0.104, which corresponds to a lower conversion efficiency of light.

Gons & Mur (1980) found that μ_e was not affected by used irradiances, while it appeared that c depended on incident light. On the contrary our results suggest that irradiation affects both μ_e and c. This can be explained by considering that Gons & Mur worked in all cases at irradiances below the inhibiting value.

In addition, it is quite surprising that no difference in Winter regime and 150 µmol photons m^{-2} s^{-1} were detected, even if under Winter condition cells are exposed to light/ dark cycles.

In summary, by applying this approach, it is possible to observe the overall effect of light intensity on the maintenance rate, which is strongly increased under inhibiting irradiation.

Nonetheless, this approach based on Pirt model (Pirt, 1965), considers a constant biomass/light yield (Y_G), while Van Bodegom (2007) demonstrated that a Y_{APP} can be calculated, which is function of growth rate, as reported in section 2.2.2. Thus, the approach

of Kliphuis *et al*. (2012), who derived separately Y_G and the m_E parameters, appears more accurate.

5.1.2 Kliphuis approach

The maintenance energy requirement for S.obliquus at different irradiations was found also by elaborating steady state data following Kliphuis model (Eq. 2.18). The results of the application of such a method are reported in Fig. 5.2 and Table 5.2. By the linearization of $r_{E,x}$ as function of μ, it was possible to find the values of m_E and Y_G for the four different illumination conditions. In fact, m_E is the positive intercept on X-axis and Y_G represents the inverse of the slope.

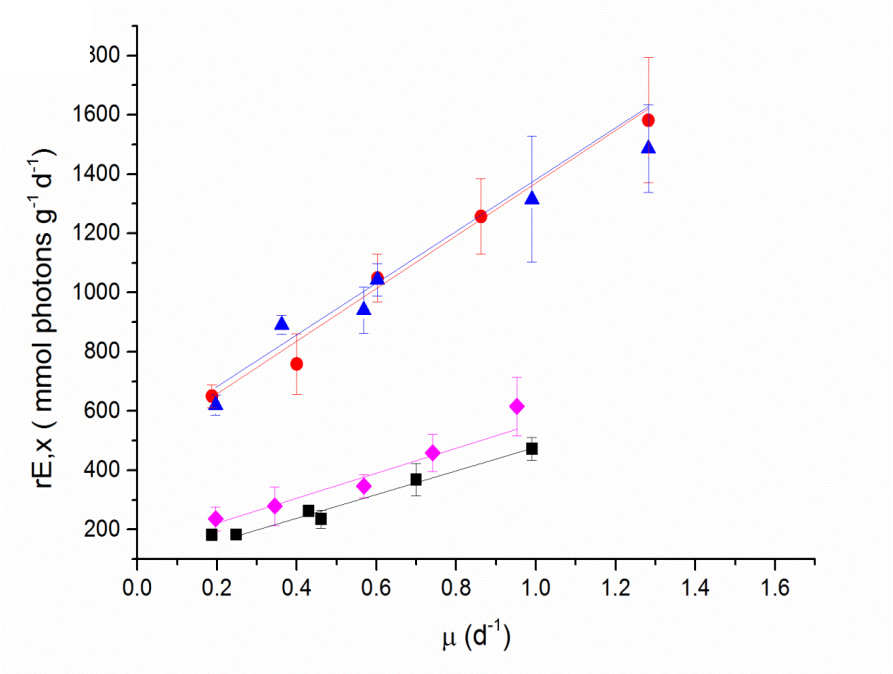

Figure 5.2*: Linearization of specific light supply rate as function of specific growth rate. according to Kliphuis approach (Eq. 2.18). at different light conditions (square for 150 μmol photons m^{-2} s^{-1}, circles for 650 μmol photons m^{-2} s^{-1}, triangles for Summer and rhombus for Winter).*

Table 5.2 – ***Parameters of linearization of data reported in Fig. 5.2. according to eq. 2.18.***

Light regime (μmol photons m^{-2} s^{-1})	m_E (mmol photons g^{-1} d^{-1})	Y_G (g mmol photons^{-1})	R^2
150	7.81E+01	2.52E-03	0.98
650	4.71E+02	1.13E-03	0.99
Winter (149.08)	1.11E+02	2.00E-03	0.95
Summer (548.69)	5.43E+02	1.32E-03	0.97

Data show a m_E which is higher for day-night regimes (111 mmol photons g^{-1} d^{-1} for Winter and 543 mmol photons g^{-1} d^{-1} for Summer) and for higher irradiances (471 mmol photons g^{-1} d^{-1} for 650 μmol photons m^{-2} s^{-1}), while Y_G is similar between irradiations at similar values of overall intensity (2.00E-03 and 2.52E-03 g mmol photons^{-1} for Winter and 150 μmol photons m^{-2} ; 1.32E-03 and 1.13E-03 mmol photons^{-1} for Summer and 650 μmol photons m^{-2}). Thus, higher irradiances corresponded to an increased m_E and lower biomass/light yield.
Data shown a m_E which is higher for day-night regimes (111 mmol photons g^{-1} d^{-1} for winter and 543 for Summer) and for higher irradiances (543 mmol photons g^{-1} d^{-1} for 650 μmol photons m^{-2} s^{-1}), while the Y_G is similar between irradiations at similar values of overall intensity. Thus, higher irradiances corresponded to an increased m_E and lower biomass/light yields. While no information are available on the effect of light on m_E, the effect on Y_G was observed also by Kliphuis *et al.* (2012), who obtained a value of Y_G of 1.26 g mol photons^{-1}, higher than those measured for other green microalgae by Cuaresma *et al.* (2009) and Zijffers *et al*. (2010), as previously mentioned in section 2.4.2. In fact. they found yields ranging from 0.5 to 1.0 g mol photons^{-1}, but working at very high irradiances of 1000 μmol photons $m^{-2}s^{-1}$).
In conclusion the approach of Kliphuis allows to clearly show the difference between the effect of light on m_E and Y_G, but no information are available to estimate the specific maintenance rate.

5.3 Van Bodegom model

As reported in section 2.2.2, Van Bodegom (2007) stated that the calculation of the specific maintenance rate a is more complex than the approach proposed by Pirt (Eq. 2.10). He showed that the relation between a and m_E was not constant, because the observed biomass/light yield Y_{APP} depends on μ (Eqs. 2.11 and 2.13).
Thus, by applying Eq.2.13, a was calculated for each μ value. Results are depicted in Fig. 5.3, suggesting that a increases with μ, as recently reported also by other authors (Michels *et al.*, 2014), who stated that higher maintenance costs can be associated with higher growth rates. On the other hand, by considering the trend of a at 650 μmol photons m^{-2} and Summer, it's clear the effect of saturating light on maintenance requirements, which is higher at higher irradiances.

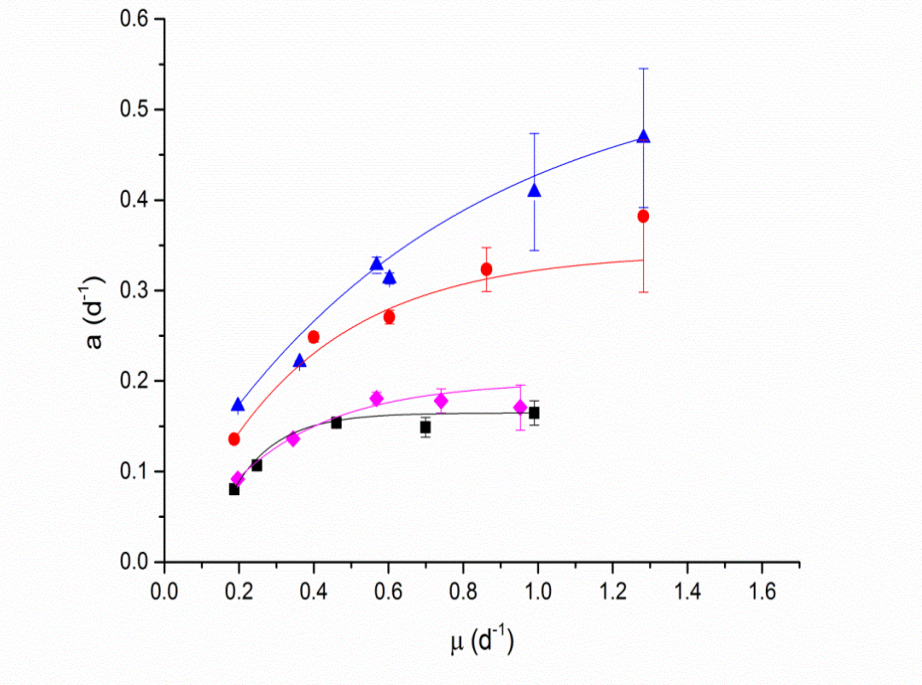

Figure 5.3 - ***Trends of specific maintenance rate as a function of μ, calculated according to Eq. 2.13. at different irradiances (square for 150 μmol m^{-2} s^{-1}, circles for 650 μmol m^{-2} s^{-1}, triangles for Summer and rhombus for Winter).***

By comparing the specific maintenance rates calculated following Pirt and Van Bodegom models, it seems that the last one is more accurate. In fact Pirt approach considers the specific maintenance rate as constant for all growth rates. Thus, Pirt values of maintenance rate are quite high, in particular at low growth rates.

In the case of photosynthetic organisms a includes not only the non growth components, such as turnover of cellular components in the normal metabolism, chemical gradients across membranes, metabolic processes involved in acclimation and the cell repair under stress, but also light dissipation

5.4 Excess of light as inhibiting substrate

As shown in the previous section, the maintenance parameter values are higher under higher irradiances, probably due to the cell repair needed as a consequence of photoinhibition and saturation. Thus, by using a similar approach to that used for heterotrophic organisms, we tried to represent the photo-inhibition with a substrate inhibition model.

As reported in section 2.3, Minkevich *et al*. (2000) and Chen & Johns (1996) demonstrated that, under inhibiting concentration, Y_{APP} as function of μ departs from the prediction of the Pirt model, which investigated lower substrate concentrations only.

In Fig. 5.4 Y_{APP}, calculated according to Eq. 2.23, was plotted as a function of μ, for each illumination condition. Two different trends for 150 μmol m^{-2} s^{-1} and the Winter regime, with respect to 650 μmol m^{-2} s^{-1} and the Summer regime can be observed.

By applying Eq. 2.14 with the Y_G and the m_E values found for 150 μmol m^{-2} s^{-1}, a curve of Y_{APP} was calculated (reported as a line in the graph), which well reproduces the trend of experimental data. Similar results were obtained by comparing the Y_{APP} under Winter season with the trend calculated by applying Eq. 2.14 on Winter maintenance parameters. This can be probably explained by the presence of a dark cycle in the Winter season, which is hard to be modeled from a yield point of view. On the other hand, under saturating light conditions, a linear relation was found, according to Eq. 2.15. Thus, the substrate inhibition hypothesis can be applied also for photosynthetic organisms. From eq. 2.15., the α and β parameters resulted 4.39E-04 (g d mol^{-1}) and 2.84E-04 (g mol^{-1}) for 650 μmol m^{-2} s^{-1} and 4.98E-04 (g d mol^{-1}) and 2.54E-04 (g mol^{-1}) for Summer condition. No data are available in the literature concerning these parameters, to which compare our results. Nonetheless, it is clearly shown that the hypothesis of photoinhibition is well represented in the case of 650 μmol m^{-2} s^{-1} and Summer regime, where the light intensity reach up to 1700 μmol photons m^{-2} s^{-1}. and for the most of time the light supply is higher than 400 μmol m^{-2} s^{-1}.

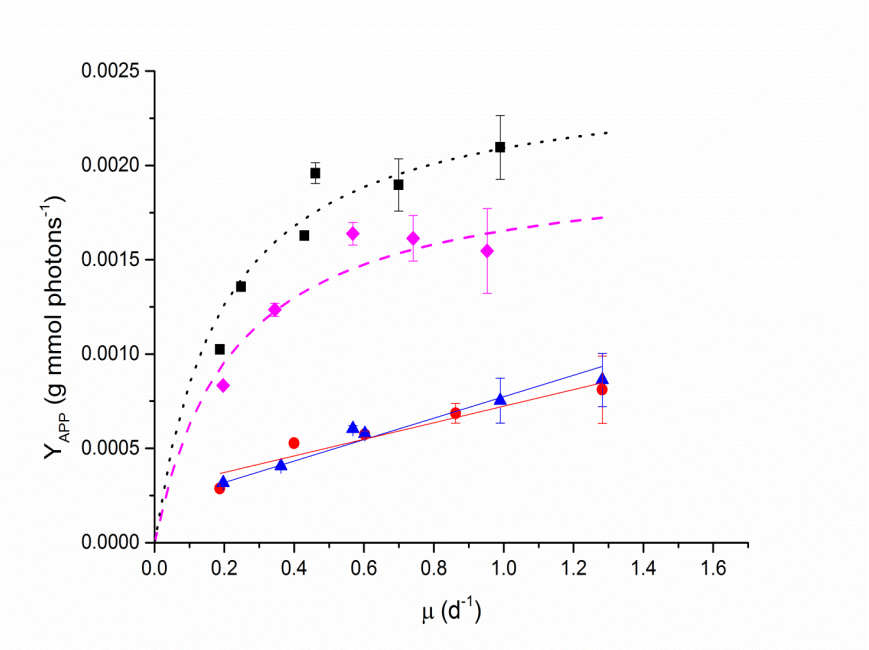

Figure 5.4 - ***Light biomass yields values as function of μ at different irradiations (square for 150 μmol m^{-2} s^{-1}, circles for 650 μmol m^{-2} s^{-1}, triangles for Summer and rhombus for Winter).***

5.5 Nutrient yields

N and P concentrations were measured during each stationary phase in order to ascertain the hypothesis of non limiting nutrient conditions. By plotting the nutrient/biomass yield, calculated according to Eq. 3.6, as function of the residence time, a similar trend was observed for both N and P (Fig. 4.23 A and B). However, as previously mentioned, the nutrient consumption under day-night cycle is quite complex to explain, so only data under continuous irradiation were considered. In Fig. 5.5 the nutrient/biomass yields , as function of the ratio between growth rate and maintenance rate, are reported. By normalizing the growth rate on maintenance rate, a linear relation was found for the nutrient/biomass yields, suggesting that part of energy wasted under saturating condition has a key role in the actual growth rate and nutrient uptake measured. This trend was never observed in the literature and the biological explanation seems quite complex.

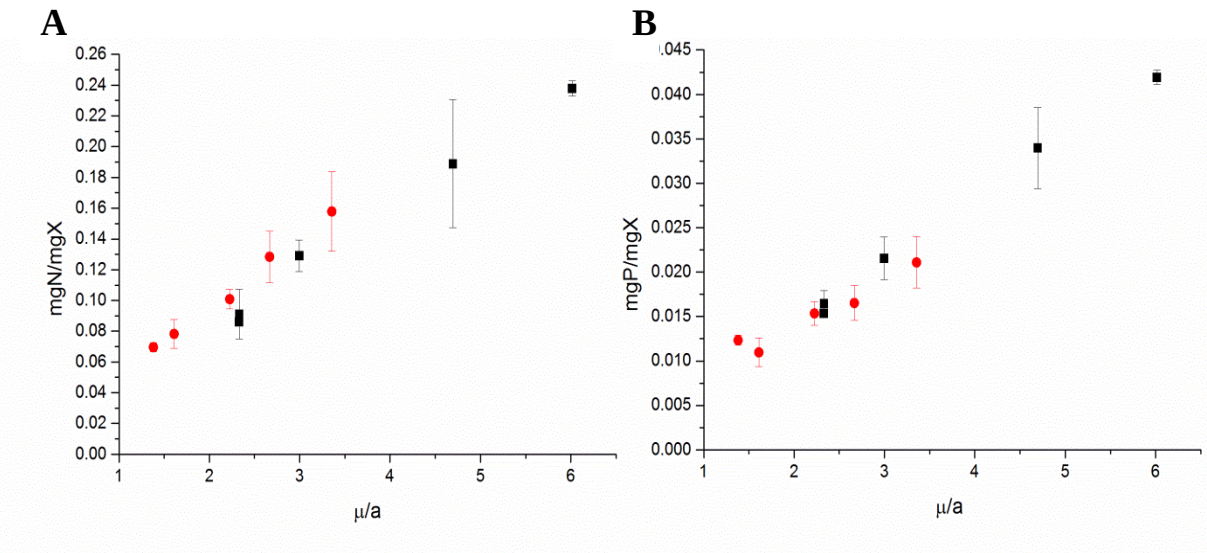

Figure 5.5 - ***N (fig 5.6A) and P (5.6B) yields as function of the ratio between growth rate and maintenance rate at different irradiations (square for 150 µmol m^{-2} s^{-1}. circles for 650 µmol m^{-2} s^{-1}).***

Conclusions

The aim of this work was to assess the effect of light intensity and irradiation regime on maintenance, by growing *S.obliquus* in a continuous laboratory-scale flate plate PBR at different residence times, thus studying different growth rates. The maintenance parameters were derived according to the models of Gons & Mur (1980) and Kliphuis *et al.* (2012) . Gons & Mur directly calculated a constant value of maintenance rate, according to Pirt model (1965), while Kliphuis derived separately m_E and Y_G. By applying these models it was found that the light influenced the maintenance, which resulted higher under higher irradiances suggesting that photosaturation and photoinhibition occurred. Kliphuis approach appeared more accurate because it clearly shows the difference between the effect of light on m_E and Y_G, however no information are available to estimate the specific maintenance rate a. Van Bodegom (2007)stated that the calculation of a from parameters m_E and Y_G was more complex than the approach proposed by Pirt (1965) and he correlated *a* to the apparent growth yield Y_{APP}, which depends on μ, instead of Y_G,which is constant. Particularly by applying Van Bodegom's approach on *S.obliquus*, it was found that *a* increased with the specific growth rate, as recently observed also by other authors (Michels *et al.*, 2014), who stated that higher maintenance costs can be associated with higher growth rates. In addition Y_{APP} resulted strongly affected by higher irradiances. In the case of photosynthetic organisms a includes not only the non growth components, such as turnover of cellular components in the normal metabolism, chemical gradients across membranes, metabolic processes involved in acclimation and the cell repair under stress, but also light dissipation. In addition, by applying the same approaches proposed for heterotrophic organisms (Chenl & Johns, 1996; Minkevich et al., 2000), the effect of saturating light on light biomass yield was modeled as a case of substrate inhibition. By applying these models it was found that the curves obtained well reproduced the trend of experimental data of Y_{APP} as a function of irradiation and growth rate. It was found that the lipid and pigment content and the average cell density depend both on growth rate and irradiance, as well as the nutrient uptake. Particularly, it was found that the nutrient uptake was strongly linked to the energetic losses due to the maintenance.

Our results are interesting to better understand the energy requirements for cell growth because the maintenance term is also a key parameter of most mathematical growth models (Bernardi et al., 2014; Wu et al., 2001), including those used for large scale PBR design (Quinn et al., 2011).

Bibliography

Abishek, M. P., Patel, J., & Rajan, A. P. (2014). Algae Oil : A Sustainable Renewable Fuel of Future, *2014*.

Amaro, H. M., Guedes, a. C., & Malcata, F. X. (2011). Advances and perspectives in using microalgae to produce biodiesel. *Applied Energy*, *88*(10), 3402–3410. doi:10.1016/j.apenergy.2010.12.014

Bahadar, A., & Bilal Khan, M. (2013). Progress in energy from microalgae: A review. *Renewable and Sustainable Energy Reviews*, *27*, 128–148. doi:10.1016/j.rser.2013.06.029

Barbosa, M. J., Zijffers, J. W., Nisworo, A., Vaes, W., van Schoonhoven, J., & Wijffels, R. H. (2005). Optimization of biomass, vitamins, and carotenoid yield on light energy in a flat-panel reactor using the A-stat technique. *Biotechnology and Bioengineering*, *89*(2), 233–42. doi:10.1002/bit.20346

Bernardi, A., Perin, G., Sforza, E., Galvanin, F., Morosinotto, T., & Bezzo, F. (2014). An Identi fi able State Model To Describe Light Intensity In fl uence on Microalgae Growth.

Bertucco, A., Beraldi, M., & Sforza, E. (2014). Continuous microalgal cultivation in a laboratory-scale photobioreactor under seasonal day-night irradiation: experiments and simulation. *Bioprocess and Biosystems Engineering*, pp. 1–8. doi:10.1007/s00449-014-1125-5

Borowitzka, M. A., & Moheimani, N. R. (2010). Sustainable biofuels from algae. *Mitigation and Adaptation Strategies for Global Change*, *18*(1), 13–25. doi:10.1007/s11027-010-9271-9

Buckwalter, P., Embaye, T., Gormly, S., & Trent, J. D. (2013). Dewatering microalgae by forward osmosis. *Desalination*, *312*, 19–22. doi:10.1016/j.desal.2012.12.015

Chen, F., & Johns, M. R. (1994). Substrate inhibition of Chlamydomonas reinhardtii by acetate in heterotrophic culture. *Process Biochemistry*. doi:10.1016/0032-9592(94)80064-2

Chenl, F., & Johns, M. R. (1996). Relationship between substrate inhibition and maintenance energy of Chlamydomonas reinhardtii in heterotrophic culture, (1982), 15–19.

Chisti, Y. (2007). Biodiesel from microalgae. *Biotechnology Advances*, *25*(3), 294–306. doi:10.1016/j.biotechadv.2007.02.001

Chisti, Y. (2008). Biodiesel from microalgae beats bioethanol. *Trends in Biotechnology*, *26*, 126–131. doi:10.1016/j.tibtech.2007.12.002

Chisti, Y. (2013). Constraints to commercialization of algal fuels. *Journal of Biotechnology*, *167*(3), 201–14. doi:10.1016/j.jbiotec.2013.07.020

Cuaresma, M., Janssen, M., Vilchez, C., & Wijffels, R. H. (2009). Productivity of Chlorella sorokiniana in a short light-path (SLP) panel photobioreactor under high irradiance. *Biotechnology and Bioengineering*, *104*, 352–359. doi:10.1002/bit.22394

Dassey, A. J., Hall, S. G., & Theegala, C. S. (2014). An analysis of energy consumption for algal biodiesel production: Comparing the literature with current estimates. *Algal Research*, *4*, 89–95. doi:10.1016/j.algal.2013.12.006

Elken, R., Vanatalu, K., & Tiisma, K. (1995). ofMicrobiological Methods The computer-controlled continuous culture of Escherichia coli with smooth change of dilution rate (A-stat), *24*, 145–153.

Gons, H. J., & Mur, L. R. (1980). Nicroliology, *7*.

Gris, B., Morosinotto, T., Giacometti, G. M., Bertucco, A., & Sforza, E. (2014). Cultivation of Scenedesmus obliquus in photobioreactors: effects of light intensities and light-dark cycles on growth, productivity, and biochemical composition. *Applied Biochemistry and Biotechnology*, *172*(5), 2377–89. doi:10.1007/s12010-013-0679-z

Grobbelaar, J. U. (2010). Microalgal biomass production: challenges and realities. *Photosynthesis Research*, *106*, 135–144. doi:10.1007/s11120-010-9573-5

Halim, R., Danquah, M. K., & Webley, P. a. (2012). Extraction of oil from microalgae for biodiesel production: A review. *Biotechnology Advances*, *30*(3), 709–32. doi:10.1016/j.biotechadv.2012.01.001

Halim, R., Gladman, B., Danquah, M. K., & Webley, P. a. (2011). Oil extraction from microalgae for biodiesel production. *Bioresource Technology*, *102*(1), 178–85. doi:10.1016/j.biortech.2010.06.136

HERBERT, D., ELSWORTH, R., & TELLING, R. C. (1956). The continuous culture of bacteria; a theoretical and experimental study. *Journal of General Microbiology*, *14*, 601–622. doi:10.1099/00221287-14-3-601

Jorquera, O., Kiperstok, A., Sales, E. A., Embiruçu, M., & Ghirardi, M. L. (2010). Bioresource Technology Comparative energy life-cycle analyses of microalgal biomass production in open ponds and photobioreactors. *Bioresource Technology*, *101*(4), 1406–1413. doi:10.1016/j.biortech.2009.09.038

Kim, Z. H., Kim, S. H., Lee, H. S., & Lee, C. G. (2006). Enhanced production of astaxanthin by flashing light using Haematococcus pluvialis. *Enzyme and Microbial Technology*, *39*, 414–419. doi:10.1016/j.enzmictec.2005.11.041

Kliphuis, A. M. J., Klok, A. J., Martens, D. E., Lamers, P. P., Janssen, M., & Wijffels, R. H. (2012). Metabolic modeling of Chlamydomonas reinhardtii: energy requirements for

photoautotrophic growth and maintenance. *Journal of Applied Phycology*, *24*(2), 253–266. doi:10.1007/s10811-011-9674-3

Lam, M. K., & Lee, K. T. (2012). Microalgae biofuels : A critical review of issues , problems and the way forward. *Biotechnology Advances*, *30*(3), 673–690. doi:10.1016/j.biotechadv.2011.11.008

Martinez, M. E., Jimnez, J. M., & Yousfi, F. E. (1999). blOi BOUI (I Kll LOOY Influence of phosphorus concentration and temperature on growth and phosphorus uptake by the microalga Scenedesmus obliquus, *67*, 233–240.

Martins, A., Caetano, N. S., & Mata, T. M. (2010). Microalgae for biodiesel production and other applications : A review, *14*, 217–232. doi:10.1016/j.rser.2009.07.020

Michels, M. H. a., Slegers, P. M., Vermuë, M. H., & Wijffels, R. H. (2014). Effect of biomass concentration on the productivity of Tetraselmis suecica in a pilot-scale tubular photobioreactor using natural sunlight. *Algal Research*, *4*, 12–18. doi:10.1016/j.algal.2013.11.011

Minkevich, I. G., Andreyev, S. V, & Eroshin, V. K. (2000). The effect of two inhibiting substrates on growth kinetics and cell maintenance of the yeast Candida 6 alida, *36*, 209–217.

Molin, G. (1983). Applied Microbiology and Biotechnology Measurement of the Maximum Specific Growth Rate in Chemostat of Pseudomonas spp . with Different Abilities for Biofilm Formation, 303–307.

Nedbal, L., Tichý, V., Xiong, F., & Grobbelaar, J. U. (1996). Microscopic green algae and cyanobacteria in high-frequency intermittent light. *Journal of Applied Phycology*. doi:10.1007/BF02178575

Pirt, S. J. (1965). The maintenance energy of bacteria in growing cultures.

Quigg, A., & Beardall, J. (2003). Protein turnover in relation to maintenance metabolism at low photon flux in two marine microalgae, (1994), 693–703.

Quinn, J., de Winter, L., & Bradley, T. (2011). Microalgae bulk growth model with application to industrial scale systems. *Bioresource Technology*, *102*(8), 5083–92. doi:10.1016/j.biortech.2011.01.019

Ramos Tercero, E. A., Sforza, E., Morandini, M., & Bertucco, A. (2014). Cultivation of Chlorella protothecoides with urban wastewater in continuous photobioreactor: Biomass productivity and nutrient removal. *Applied Biochemistry and Biotechnology*, *172*, 1470–1485. doi:10.1007/s12010-013-0629-9

Rawat, I., Ranjith Kumar, R., Mutanda, T., & Bux, F. (2013). Biodiesel from microalgae: A critical evaluation from laboratory to large scale production. *Applied Energy*, *103*, 444–467. doi:10.1016/j.apenergy.2012.10.004

\Ruiz, J., Álvarez-Díaz, P. D., Arbib, Z., Garrido-Pérez, C., Barragán, J., & Perales, J. a. (2013). Performance of a flat panel reactor in the continuous culture of microalgae in urban wastewater: prediction from a batch experiment. *Bioresource Technology*, *127*, 456–63. doi:10.1016/j.biortech.2012.09.103

Schulze, K. L., & Lipe, R. S. (1964). Relationship between substrate concentration, growth rate, and respiration rate of Escherichia coli in continuous culture. *Archiv Fuer Mikrobiologie*, *48*, 1–20. doi:10.1007/BF00406595

Slade, R., & Bauen, A. (2013). Micro-algae cultivation for biofuels: Cost, energy balance, environmental impacts and future prospects. *Biomass and Bioenergy*, *53*(0), 29–38. doi:10.1016/j.biombioe.2012.12.019

Van Bodegom, P. (2007). Microbial maintenance: a critical review on its quantification. *Microbial Ecology*, *53*(4), 513–23. doi:10.1007/s00248-006-9049-5

Wellburn, A. R. (1994). The spectral determination of chlorophylls a and b, carotenoids, using various solvents with spectrophotometers of different resolution. *Journal of Plant Physiology*, *144*, 307–313. doi:http://dx.doi.org/10.1016/S0176-1617(11)81192-2

Wu, X., & Merchuk, J. C. (2001). A model integrating uid dynamics in photosynthesis and photoinhibition processes, *56*, 3527–3538.

Xu, L., & Xiong, X. (2009). Microalgal bioreactors : Challenges and opportunities, (3), 178–189. doi:10.1002/elsc.200800111

Zhang, X., Hu, Q., Sommerfeld, M., Puruhito, E., & Chen, Y. (2010). Harvesting algal biomass for biofuels using ultrafiltration membranes. *Bioresource Technology*, *101*, 5297–5304. doi:10.1016/j.biortech.2010.02.007

Zijffers, J.-W. F., Schippers, K. J., Zheng, K., Janssen, M., Tramper, J., & Wijffels, R. H. (2010). Maximum photosynthetic yield of green microalgae in photobioreactors. *Marine Biotechnology (New York, N.Y.)*, *12*(6), 708–18. doi:10.1007/s10126-010-9258-2

Zou, S., Gu, Y., Xiao, D., & Tang, C. Y. (2011). The role of physical and chemical parameters on forward osmosis membrane fouling during algae separation. *Journal of Membrane Science*, *366*(1-2), 356–362. doi:10.1016/j.memsci.2010.10.030